Studies on Innate Immune Activation by HBV Infection and Its Sensing Mechanism in Hepatocytes

（HBV 感染による肝細胞における自然免疫応答とその認識機構に関する研究）

Kai Li

Graduate School of Chemical Sciences and Engineering,

Hokkaido University

March 2016

Abstract

Pattern recognition receptors (PRRs) recognize invading viruses mainly by sensing viral nucleic acid and trigger key antiviral immune responses in the innate immune system that act as a front line of host defense against viral infection. Hepatitis B virus (HBV) is a hepatotropic DNA virus that can cause both acute and chronic liver disease, and more than 240 million people worldwide are chronic HBV carriers that have a high risk for liver cirrhosis or hepatocellular carcinoma. Current approved therapies of chronic hepatitis B include administration of antivirally active interferon-α (IFN-α) and inhibitors of viral reverse transcription have severe side effects and a risk to develop of drug resistant mutations. The nucleic acid sensor(s) for HBV and the host innate immune response against HBV infection has not been identified. Thus, understanding of the nature of innate immunity induced by HBV will aid to characterize the immunopathogenesis of HBV infection and to further develop novel innate immune-based antiviral approaches for HBV infection or optimize the current therapy regimens of HBV. Therefore, this study tried to elucidate the innate immune activation upon HBV infection and clarify the mechanism of this activation.

The results of this study demonstrated that type III but not type I IFNs are predominantly induced in human hepatocytes in response to HBV infection, through retinoic acid-inducible gene-I (RIG-I)-mediated sensing of the 5'-ε region of HBV pregenomic RNA (pgRNA), and the induced type III IFN exhibits potent physiological antiviral activities. In addition, RIG-I could also directly suppress HBV replication in an IFN signaling-independent manner that counteracts the interaction of HBV polymerase (P protein) with the 5'-ε region, which is essential for initiation of viral pgRNA encapsidation during HBV replication. Furthermore, liposome-mediated delivery and vector-based expression of this ε region-derived RNA (εRNA) in liver abolished the HBV replication in human hepatocyte-chimeric mice.

The observations of this study reveal an innate recognition mechanism by which RIG-I dually functions as an HBV sensor activating innate signaling and to counteract viral polymerase in human hepatocytes. Moreover, this study also evaluate the therapeutic potential of the εRNA for the control of HBV infection, which may provide a better approach to the strategies for development of nucleic acid medicine, and offer an attractive clinical option for the therapy against not only HBV but also possibly other

virus infections.

List of abbreviations

5’-pppRNA/3pRNA	5′-triphosphorylated RNA
Akt	serine/threonine-protein kinases
ALRs	AIM-like receptors
ASOs	antisense oligonucleotides
CARD	caspase recruitment domain
cccDNA	covalently closed circular DNA
CDNs	cyclic dinucleotides
cGAMP	cyclic GMP-AMP
cGAS	cyclic GMP-AMP synthase
CHB	chronic hepatitis B
CLRs	C-type lectin receptors
DAI	DNA-dependent activator of interferon regulatory factor
DCs	dendritic cells
DHBV	duck hepatitis B virus
dsRNA/DNA	double-stranded RNA/DNA
ε	epsilon
ELISA	enzyme-linked immunosorbent assay
ER	endoplasmic reticulum
ERK	extracellular regulated protein kinase
FRET	fluorescence resonance energy transfer
HBcAg	HBV core antigen
HBeAg	HBV e antigen
HBsAg	HBV surface antigen
HBxAg	HBV x antigen
HBV	hepatitis B virus
HCC	hepatocellular carcinoma
HCV	hepatitis C virus
HIV	human immunodeficiency virus
HSV	herpes simplex virus
IAV	influenza A virus

IFI16	interferon, gamma-inducible protein 16
IFN	interferon
IKK	inhibitor-κB kinase
IL	interleukin
IRF	interferon-regulatory factor
ISGs	IFN stimulated genes
ISRE	interferon-sensitive response element
JAK	janus tyrosine kinase
JNK	c-Jun N-terminal kinase
KO	knockout
LAM	lamivudine
LGP2	laboratory of genetics and physiology 2
LPS	lipopolysaccharide
MAPK	mitogen-activated protein kinase
MAVS	mitochondrial antiviral signaling protein
MDA5	melanoma differentiation associated protein-5
MEND	multifunctional envelope-type nanodevice
MYD88	myeloid differentiation primary-response protein 88
NAb	neutralizing antibody
NAs	nucleos(t)ide analogues
NDV	newcastle disease virus
NF-κB	nuclear factor- kappa-B
NK cells	natural killer cells
NLRs	NOD-like receptors
NOD	nucleotide-binding oligomerization domain
NTCP	sodium taurocholate cotransporting polypeptide
P protein	HBV polymerase protein
PAMPs	pathogen-associated molecular patterns
PBMCs	peripheral blood mononuclear cells
PEG	polyethylene glycol
pgRNA	pregenomic mRNA
PHH	primary human hepatocytes

PI3K	phosphatidylinositol 3-kinase
Pol III	polymerase III
poly I:C	polyriboinosinic polyribocytidylic acid
PRRs	pattern recognition receptors
PTH	primary hepatocytes from Tupaia belangeri
rcDNA	relaxed circular DNA
RIG-I	retinoic acid inducible gene 1
RIP assay	RNA-binding protein immunoprecipitation assay
RLRs	RIG-I-like receptors
RNAi	RNA interference
SCID	severe combined immunodeficiency
siRNA	small interfering RNA
ssRNA/DNA	single-stranded RNA/DNA
STAT	signal transducers and activators of transcription
STING	stimulator of interferon genes protein
STM	stem-loop mutant
TBK1	TANK-binding kinase 1
TIRAP	Toll/IL-1 receptor (TIR) domain containing adaptor protein
TLRs	Toll-like receptors
TRAM	TRIF-related adaptor molecule
TRIF	TIR domain-containing adapter protein inducing IFN-β
TRIM25	tripartite motif containing 25
VSV	vesicular stomatitis virus
WT	wild type

List of figures

List of tables

Table of contents

1. Introduction

1.1 Hepatitis B virus

The Hepatitis B virus (HBV) is a small and enveloped DNA virus, which is highly species-and liver specific. HBV replicates only in hepatocytes and belongs to the family of hepadnaviridae (hepatotrop associated DNA viruses) [1]. HBV infection can induce immune-mediated acute and chronic liver disease. Around four hundred million people worldwide are persistently infected with HBV, which is a major causative factor associated with not only inflammation but also cirrhosis and even cancer of the liver [2].

1.1.1 History of Hepatitis B

Although Hepatitis B was recognized as a disease in ancient times, its etiologic agent was largely unknown before 1965, when Dr. Baruch Blumberg discovered an enigmatic serum protein named Australia antigen in the blood of Australian aboriginal people [3], which turned out to be the antigen that caused hepatitis B [4], this antigen later known to be the Hepatitis surface antigen (HBsAg). In 1970, Dr. David Maurice Surrey Dane discovered viral particles in the sera and liver of patients infected with this antigen by electron microscopy [5], therefore, the infectious HBV virion is also called Dane particles. In the next few years, researchers indentified the viral DNA polymerase and DNA in 1973 and 1974 respectively [6, 7]. In 1978, cloning and sequencing of the HBV DNA was reported independently and almost simultaneously by three different groups [8-10], this paved the way to understand the viral life cycle, allowed development of efficient vaccines and drugs, and also improved the diagnostic approaches to HBV infection. Even the understanding about the genomic structure and protein function of HBV was getting brighter in the next several decades after the discovery of HBV, the receptor(s) for this highly species-and liver specific virus had remained a mystery until 2012, when Yan et al. identified human sodium taurocholate cotransporting polypeptide (hNTCP) as a functional receptor for HBV [11]. This finding explained the hepatotropism of HBV, provided a new target for development of HBV inhibitors, and also opened another way to develop cell culture models for HBV infection.

1.1.2 HBV structure, genomic organization and protein function

The HBV particle is a complete infectious HBV virion containing HBV genome (Figure 1.1). The core region of HBV particle contains viral DNA and DNA polymerase

that surrounded by nucleocapsid. Assembled hepatitis B core antigens (HBcAg) build nucleocapsid that is covered with a lipid envelope containing HBsAg [12,13]. The cholesterol-rich composition of the lipid envelope is required for viral infectivity. Persistence of the small HBsAg in the serum over a period of more than 6 months is usually accepted as chronic infection [14,15].

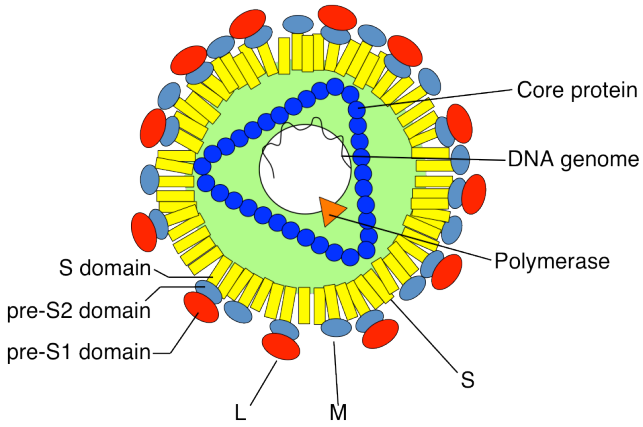

Figure 1.1 Schematic representation of HBV particle. The infectious HBV particle with a hydrodynamic diameter of about 47 nm is composed of HBV surface proteins (L-, M- and S-protein) and DNA genome (inner black circle and wavy lines), which covalently linked via the viral polymerase (orange triangle) and surrounded by nucleocapsid core protein.

The HBV genome present in virions is a 3.2 kb partially double-stranded relaxed, circular DNA (rcDNA) molecule and the smallest known full replicative mammalian viral genome (Figure 1.2). Four sets of mRNAs (3.5 kb, 2.4 kb, 2.1 kb and 0.7 kb mRNA) are transcribed from the viral minichromosomes using host cell machinery, RNA polymerase II which transcribes the four transcripts from different start site and they share the common single polyadenylation signal. The 3.5 kb pregenomic RNA (pgRNA) serve as the template for the precore/core, core and polymerase proteins in addition to being the reverse transcription substrate; the 2.4 and 2.1 kb mRNAs encode the surface proteins, and the small 0.7 kb transcript is the template for translation of HBx protein [16].

The core gene encodes the core nucleocapsid protein and pre-core protein, core protein is important in viral packaging and production of HBcAg. The pre-core protein ultimately undergoes proteolysis and becomes hepatitis B e antigen (HBeAg) in the endoplasmic reticulum (ER). The HBeAg may have an immunoregulatory role that

facilitates chronic infection within the host and is an important marker of viral replication. The surface gene encodes the pre-S1, pre-S2, and S proteins (HBsAg, comprising the large [L], middle [M], and small [S] surface proteins), which is the glycosylated envelope protein of HBV virion and the large HBsAg protein plays a key role in binding of HBV to surface receptors (NTCP) on hepatocytes [11]. The X gene encodes the X protein (HBxAg), which has transactivating properties and is thought to be involved in several functions such as cell cycle regulation, signal transduction, transcriptional activation, and DNA repair [17,18]. The polymerase gene has a large ORF (approximately 800 amino acids) and overlaps the entire length of the surface ORF. It encodes a polymerase protein with functions that are critical for packaging and DNA replication (including priming, RNA- and DNA-dependent DNA polymerase, and RNase H activities) [19].

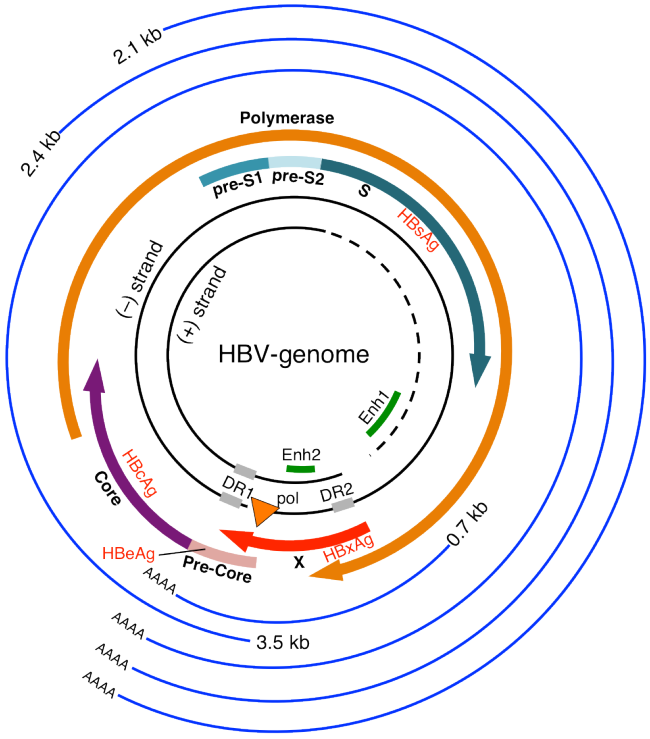

Figure 1.2 HBV genome organization. HBV contains a small, partially double-stranded (~dsDNA) genome (inner black circles) that consists of a full-length negative strand and an incomplete (dashed lines) positive strand. The colored arrows represent the four ORFs. The four major transcripts are shown as thin blue outer lines. Two enhancer regions (Enh1, Enh2, green line), two direct repeats (DR1, DR2, gray line) and viral polymerase (pol, orange triangle) are also indicated. (Adapt from [20])

1.1.3 HBV genotype and distribution

According to the molecular evolutionary analysis of HBV genomic DNA sequence, HBV strains isolated in various countries are classified into different genotypes. To date, ten genotypes (A-J) of the HBV genome have been identified by at least 8% nucleotide differences. Moreover, some HBV genotypes are further classified as sub-genotypes with a mean genetic distance of 4%-8% nucleotide differences. HBV genotype A-D and F genotypes are divided into various sub-genotypes; no sub-genotypes have been defined for E, G and H genotypes. So far, more than 30 related sub-genotypes belonging to HBV genotypes have been indentified [21]. Genotyping of HBV is essential for characterization of patient groups and for epidemiological studies. Several studies have shown that HBV genotype-specific pathogenesis may contribute to heterogeneous clinical outcomes in chronic hepatitis B (CHB) patients. For example, patients with HBV genotypes C and D infection have a lower rate of spontaneous HBeAg seroconversion. In addition, HBV genotypes C and D have a higher frequency of core promoter and pre-S mutations than genotypes A and B. Genotypes C and D also carry a higher lifetime risk of cirrhosis and hepatocellular carcinoma (HCC) development than genotypes A and B. Core promoter and pre-S mutations also correlate with an increased risk of HCC. Therapeutically, genotypes A and B patients have a better response to interferon-based therapy than genotypes C and D patients, but the response to nucleos(t)ide analogs is comparable across different HBV genotypes [22].

Genotype distribution shows variations between countries, and even between geographical regions within countries. Genotype A is widespread in sub-Saharan Africa, Northern Europe, and Western Africa; genotypes B and C are common in Asia; genotype D is dominant in Africa, Europe, Mediterranean countries, and India; genotype E is found in central and western Africa; genotype F is primarily found in Latin America and Alaska; genotype G is reported in France, Germany, and the United States; and genotype H is commonly encountered in Central and South America. Genotype I has recently been reported in Vietnam and Laos. The newest HBV genotype, genotype J, has been identified in the Ryukyu Islands in Japan (Figure 1.3). Geographic distribution of HBV genotypes may be related to route of exposure. For example, genotypes B and C are more common in high-endemic regions of perinatal or vertical exposure, which plays an important role in viral transmission. Other genotypes are

primarily observed in regions of horizontal exposure. Therefore, genotyping provides an epidemiological clue in the investigation of acquisition, because this lies in the geographical distribution of HBV [23,24].

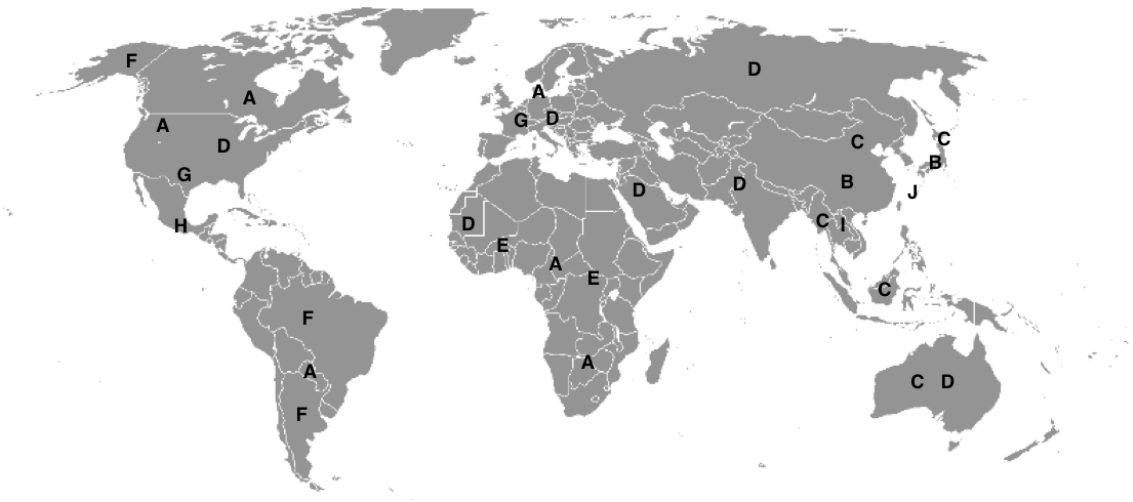

Figure 1.3 Geographic distribution of HBV genotypes worldwide. (Adapt from [23,24])

1.1.4 HBV replication

HBV infection into host hepatocytes follows a multiple step process (Figure 1.4): (1) Binding: the HBV life cycle begins with low-affinity reversible binding of the virion large surface protein (preS1) to specific receptors heparan sulphate proteoglycans (HSPGs) on hepatocytes and is followed by high-affinity irreversible binding to mediate the early entry of HBV through more specific binding of viral envelope proteins to specific receptors on hepatocytes, including the HBsAg to recently indentified functional receptor-NTCP; (2) Entry and uncoating: although the mechanisms of HBV virion into hepatocyte are not fully understood, it has been proposed that entrance ways of viruses have different mechanisms both by endocytosis and fusion into plasma membrane of virus envelope. After entrancing into hepatocytes, the virus undergoes uncoating, and the nucleocapsid of HBV containing partial double-stranded rcDNA, which is covalently bound to polymerase, is subsequently released into the cytoplasm; (3) Nuclear transport: the released nucleocapsid of HBV is transported to nuclear membrane through relationship between nuclear localization signaling (NLS) in

C-terminal of capsid protein and nuclear import receptors (importin-α and β). After nucleocapsid is trapped in nuclear pore complex (NPC) basket, the nucleocapsid is uncoated at the nuclear membrane and HBV rcDNA is released into the nucleus; (4) cccDNA synthesis: after the genome released into nucleus, the polymerase present in 5' end of the negative chain is used for positive chain synthesis to repair the rcDNA. The repaired rcDNA is converted to covalently closed circular DNA (cccDNA) through a series of processes that have not been fully elucidated. The cccDNA molecule contains histone-and nonhistone-like proteins, and it is organized in a chromatin-like structure like beads lined up on a string. They are called as minichromosome serving as the template for the transcription of all the viral mRNAs. Random integration of the HBV genome into the host chromosomes can also occur; (5) mRNA transcription: cccDNA uses all cellular transcriptional mechanisms to generation of four viral RNAs: 3.5 kb, 2.4 kb, 2.1 kb and 0.7 kb mRNAs, the transcription event is regulated by host transcription factors (CREB, STAT1, STAT2, etc.), chromatin modifying enzymes (PCAF, HDAC1, etc.), hepatocyte nuclear factors, and also viral factors such as core, regulatory X protein; (6) mRNA export: after the viral RNAs transcription in nucleus, they are transported to cytoplasm through host NFX1/p15 heterodimers like host mRNAs transportation, and the viral core protein which shuttles between nucleus and cytoplasm also play a role in viral RNAs transportation; (7) Translation: The longest 3.5 kb pgRNA is the template for precore/core, core and polymerase proteins, the 2.4 and 2.1 kb mRNAs encode the surface proteins, and regulatory HBx protein is from the small 0.7 kb transcript; (8) Encapsidation and reverse transcription: HBV nucleocapsid formation starts when the complex of the pgRNA, HBV polymerase and core protein immers has formed. When nucleocapsid assembly is completed, the conversion of the RNA into single-stranded and then into partially double-stranded rcDNA takes place through reverse transcription by the viral polymerase; (9) Recycling: After the DNA genome is synthesized, the nucleocapsid can either continue with the viral life cycle and interact with envelope proteins and get secreted as infectious virions, or they can be re-delivered to the nucleus and build up a cccDNA pool within the nucleus; (10) Enveloping: the envelopment of the mature nucleocapsid strictly depends on the presence of the viral surface proteins, especially L surface protein is required for nucleocapsid to gain its envelope. It has been reported that nucleocapsid is sent to nucleus to increase viral genome amplification if L-protein is absent. Envelope proteins

are added to ER membrane after translation, and they bud into the lumen of the ER. They are released as non-infectious spherical and filamentous particles or infectious HBV particles if they have gained envelope of DNA containing nucleocapsid by the cell; (11) Budding: after enveloping, the HBV virions bud into so-called multivesicular body (MVB); (12) Secretion: MVB then fuses with the plasma membrane for virions secretion [25,26].

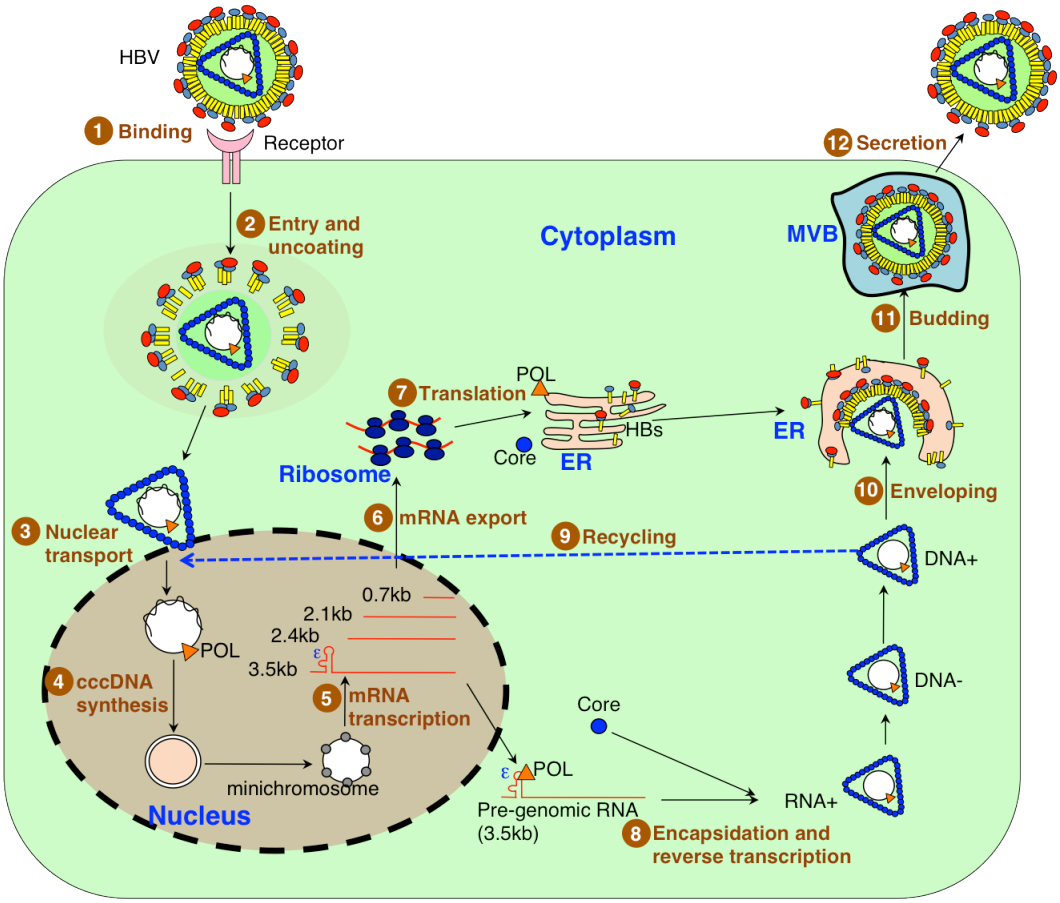

Figure 1.4 Life cycle of HBV. After entry to the cell mediated by binding virion surface protein to host receptor, uncoated HBV particle (nucleocapsids) transport the genomic HBV DNA to the nucleus, where the relaxed circular DNA is converted into covalently closed circular (ccc) DNA. The cccDNA functions as the template for the transcription of four viral RNAs (of 0.7 kb, 2.1 kb, 2.4 kb and 3.5 kb), which are exported to the cytoplasm and used as mRNAs for the translation of the HBV proteins. The longest (pre-genomic) RNA also functions as the template for replication, which occurs within nucleocapsids in the cytoplasm. Upon encapsidation with the viral polymerase, reverse transcription takes place. After plus-strand synthesis and rcDNA formation, capsids are either recycled to the nucleus, or enveloped with HBV surface proteins

and budded into multivesicular body (MVB) for virions secretion.

1.1.5 HBV reverse transcription

The reverse transcription of viral RNA to rcDNA is a key step for HBV life cycle and it is a complex multistep process. Duck hepatitis B virus (DHBV) is an invaluable model in elucidating the mechanism by which hepadnaviruses replicate. DHBV and HBV have similar genome organizations and are believed to use similar mechanisms for reverse transcription. Reverse transcription of hepadnaviruses takes place in the cytoplasmic nucleocapsids of infected cells (Figure 1.5). The first two steps are encapsidation of pgRNA and initiation of minus-strand DNA synthesis. Hepadnavirus polymerase protein binds with the encapsidation signal, epsilon (ε), which is an RNA stem-loop at the 5′ end of the pgRNA, to initiate encapsidation of pgRNA. Polymerase protein, acting as primer and reverse transcriptase, initiates minus-strand DNA synthesis using nucleotides within epsilon as a template (Figure 1.5A). After the synthesis of three or four nucleotides at epsilon, the nascent minus-strand DNA switches templates to a complementary sequence at direct repeat 1 (DR1), which is near the 3′ end of the pgRNA (Figure 1.5B), the minus-strand DNA synthesis resumes from this position. Following elongation, the RNase H activity of the polymerase degrades the pgRNA template that has been copied (Figure 1.5C). Minus-strand DNA synthesis proceeds to the 5′ end of pgRNA and results in a full-length minus-strand DNA with HBV polymerase (P protein) still covalently attached to its 5′ end (Figure 1.5D). The final RNase H activity of the polymerase generates a short RNA fragment of 17 or 18 nucleotides that is the primer for the initiation of the synthesis of plus-strand DNA (Figure 1.5D). The 3′ end of the primer contains the sequence of DR1. For the synthesis of the most abundant form of the mature genome, rcDNA, two template switches are required during plus-strand DNA synthesis. First, the plus-strand primer switches templates to anneal to DR2, which is near the 5′ end of the minus-strand DNA, and initiates plus-strand DNA synthesis from DR2. This template switch is called primer translocation (Figure 1.5E). Synthesis of plus-strand DNA proceeds to the 5′ end of the minus-strand DNA (Figure 1.5F). The nascent plus-strand DNA undergoes another template switch, called circularization, to permit elongation with the 3′ end of minus-strand DNA as a template. The minus-strand DNA is terminally redundant for 9

or 10 nucleotides (5′r and 3′r). The nascent plus-strand DNA, after copying the 5′r sequence, anneals to 3′r (Figure 1.5G). Elongation of the plus-strand DNA from 3′r ultimately generates the rcDNA form (Figure 1.5H). For a small fraction of the capsids, there is a second pathway for the synthesis of plus-strand DNA, which termed *in situ* priming. This pathway generates a duplex-linear (DL) DNA because the RNA primer initiates plus-strand DNA synthesis from DR1 on the minus strand. No template switch is involved during the synthesis of the plus strand of DL DNA (Figure 1.5I) [27].

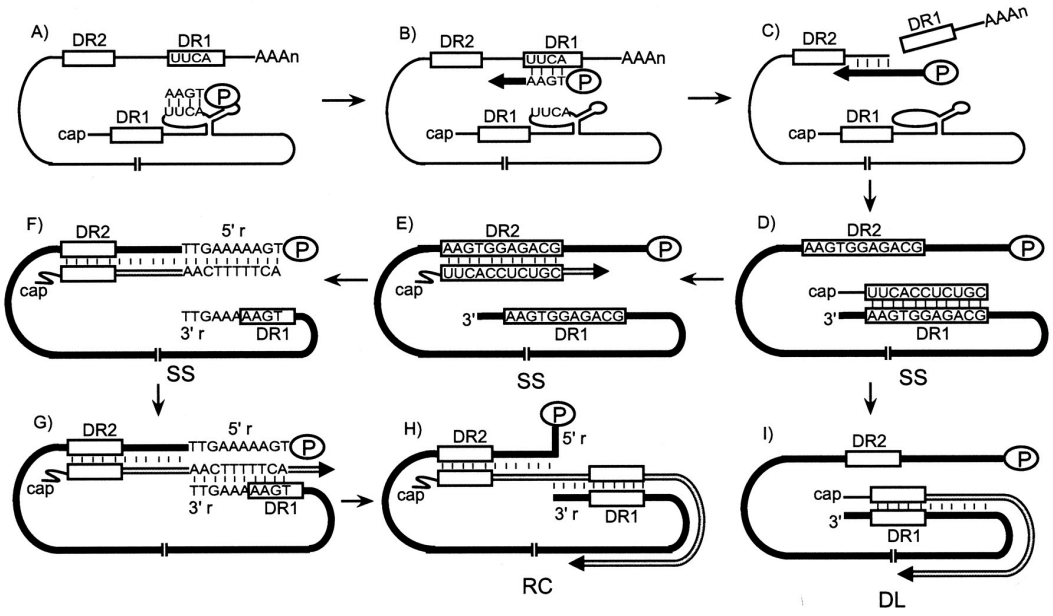

Figure 1.5 Model of HBV reverse transcription. P: HBV polymerase protein; DR1, DR2: direct repeat 1 and 2; SS: single strand; RC: relax cycle; DL: duplex-linear. (A) Initiation of minus-strand DNA synthesis. (B) Minus-strand template switch. Minus-strand DNA is indicated by a thick black line, and an arrow indicates the direction of elongation. (C) Elongation of minus-strand DNA. (D) Completion of minus-strand DNA synthesis and generation of the plus-strand primer. (E) Primer translocation. Plus-strand DNA is represented by a double line, with an arrow indicating the direction of its synthesis. (F) Elongation of plus-strand DNA from DR2. (G) Circularization. (H) Generation of rcDNA. (I) *In situ* priming. (From [27])

1.1.6 Experimental models for HBV research

As HBV exhibits a very narrow host range and shows a strong tropism for liver parenchymal cells, a major obstacle to the research of HBV has been the lack of an

efficient cell culture system or a readily available small-animal model, permissive for viral infection and replication. Although several *in vitro* cell culture systems and *in vivo* animal model has been established for HBV study, all these model systems suffer limitations in terms of functionality, reproducibility, and/or accessibility. A partial list of currently available *in vitro* cell culture models and *in vivo* animal models appears in Table 1.1 and Table 1.2.

Table 1.1 *In vitro* cell culture models for the study of HBV infection

***In vitro* cell culture models**	**Advantages**	**Disadvantages**	**References**
Human hepatoma cell lines (HepG2, Huh-7)	Mimic of acute HBV infection by transient transfection HBV genome;	No-infection.	[28]
HepG2.2.15 cell line	Integration with HBV genomes; Stable low HBV replication; Convenient to study of viral replication and screen anti-viral agents.	No-infection; HBV production is limited and difficult to control.	[29]
Primary human hepatocytes (PHH)	Susceptible to HBV infection.	Limited availability; Unpredictable variability of human liver.	[30]
Primary hepatocytes from Tupaia belangeri (PTH)	Susceptible to HBV infection; More readily available; Less variability between different preparations.	Cell culture system is less characterized.	[31]
HepaRG cell line	Susceptible to HBV infection.	Strictly dependent on the differentiation state induced by DMSO; Poor viral replication; Low viral yields; Absence of re-infection.	[32]
Human NTCP-hepatoma cell lines	Susceptible to HBV infection.	DMSO is essential for the robust infection.	[33]

Table 1.2 *In vivo* animal models for the study of HBV infection

***In vivo* animal models**	**Advantages**	**Disadvantages**	**References**
Chimpanzee	An immunocompetent host; Susceptible to HBV infection; Similar to human infection (including cccDNA).	Ethical constraints; Large size; High costs; Transient infection; Lack of chronic liver disease.	[35]

Tupaia belangeri	Susceptible to HBV infection; Similar to human infection (including cccDNA).	Relatively large size; Not easily available; Outbred animals; Transient infection.	[36]
Transgenic mouse	Convenient, inbred animals; High levels of HBV replication.	No-infection; Immune tolerance.	[37]
Transfected mouse by hydrodynamic injection	Analysis of mutant strains; Immunocompetent.	No-infection; Transient gene expression.	[38]
Transfected mouse by adeno-associated virus	High replication levels; Immunocompetent; Relatively long-time gene-expression.	No-infection; Transient gene expression; Vector-driven interferences.	[39]
Human liver-chimeric mouse	Susceptible to HBV infection (including cccDNA); Assessment of efficacy of anti-HBV agents.	High costs; Immunocompromised.	[40-42]

So far, a robust HBV *in vitro* infection has been difficult to achieve in the hepatocyte-derived cells, which is, presumably, due to the loss of HBV receptor(s) in the transformed or cancerous hepatocytes. Transient transfection with HBV genome to human hepatoma cell lines such as HepG2 and Huh-7 can mimic of acute HBV infection, but all of those cell lines are not susceptible to HBV infection [28]. Another human hepatoma cell line-HepG2.2.15 is derived from HepG2 cell by integration with HBV genome and stably produces HBV mRNAs, antigens and viral particles. Although HepG2.2.15 cells are convenient for studying of viral replication and screening of anti-viral agents, they are also not susceptible to HBV infection [29]. The primary human hepatocytes (PHH) and primary hepatocytes from Tupaia belangeri (PTH) are susceptible to HBV infection and can be used for studying HBV lifecycle and certain HBV infection experiments, but the PHH are costly with limited supply, and their genetic background and susceptibility to HBV infection vary from donor to donor. Different from PHH, PTH are more readily available and less variability between different preparations, but this cell culture system is less characterized [30,31]. The HepaRG is a hepatoma cell line that supports HBV infection, but the susceptibility of HepaRG cells to HBV is strictly dependent on the differentiation state induced by DMSO (dimethyl sulfoxide), causing variable toxic side effects. Moreover, the HepaRG

cells have a poor viral replication, low viral yields and absence of reinfection [32]. Recently, the NTCP has been identified as a functional HBV receptor [11], opening a new field to establish cell culture model for HBV research. Now, the reconstitution of NTCP expression in commonly used human hepatoma cells (e.g. HepG2 and Huh-7) was established, the human hepatoma cells stably expressing NTCP renders these cells able to support HBV infection and production, will allow a deeper understanding of the early steps of the HBV life cycle, including receptor-mediated HBV entry, uncoating, and first round cccDNA formation, etc. Although the reported HBV infectivity of NTCP-expressing cells is relatively high (about 70%) among different laboratories under different infection conditions, DMSO is required for efficient HBV infection, which may cause variable toxic side effects [33].

To understand the virus biology and pathogenesis in HBV-infected patients, several animal models have been developed to mimic hepatic HBV infection and the immune response against HBV [34], but the narrow host range of HBV infection and lack of a full immune response spectrum in animal models remain significant limitations. Although chimpanzees are susceptible to HBV infection and they are the immunocompetent host for HBV infection, their usage is limited for ethical and practical reasons such as large size, high costs and transient infection that lacks of chronic liver disease [35]. Another animal model susceptible to HBV infection is tupaias. We can observe viral DNA replication in the liver, HBsAg secretion into the serum, and the production of antibodies to HBsAg and HBeAg after infection, which is similar to human infection. But tupaias are outbred animals with a relatively large size, not easily available, and their immune systems have not been characterized [36]. Thus, due to the various restrictions for using the chimpanzees and tupaias for HBV infection, most recent developments have focused on mouse model, which is a well-defined, inbred, and small animal system.

HBV transgenic mice were developed by a 1.3 HBV-DNA insertion, the infectious virions produced at high levels in these mice are exactly alike from human-derived virions in morphology. This model, with its advantage of very-high-level HBV replication, provides the opportunity to assess the efficacy of anti-HBV agents. But as this animal model integratesthe HBV genome into the mouse chromosome, which inherently increases immune tolerance to transgenic products, and also this model does not lead to liver inflammation and forms cccDNA [37]. Because the HBV transgenic mice

are immunologically tolerant to the virus as constantly express HBV, it is difficult to study the host immune response and the resultant pathophysiology of HBV infection. To overcome this problem, several researchers applied hydrodynamic injection of a naked plasmid DNA encoding a supergenomic HBV 1.3-length transgene to transient expression of HBV protein in the liver of adult mice. The hydrodynamic injection could induce high levels of HBV replication in the liver, and the immune response to HBV and the concomitant hepatitis can be observed. However, the replication of HBV in the liver is rapidly terminated within 15 days after injection by specific antiviral antibodies and cytotoxic T lymphocytes (CTLs) if the mice are immunocompetent [38]. Thus, in this mouse model, only can cause acute hepatitis, but cannot establish HBV chronic infection. Another mouse model that infect mice with HBV by delivering the HBV genome to mice liver through the liver-targeted transduction of adeno-associated virus, which enabling the study of viral infection for up to one year, so this mouse model is useful for the development of new treatment and immune-based therapies or therapeutic vaccines for chronic HBV infections. But the adeno-associated virus based transduction system may interfere the host immune response [39].

Even the above mouse models have had important roles for clarifying the pathophysiology of the host immune response to HBV, but a common limitation of the above mouse models is that HBV particles produced by those mice do not enter into murine hepatocytes, which lack HBV-specific receptors, thus these mice do not recapitulate natural HBV infection, researchers thus cannot study the infection step of the HBV life cycle. To overcome this problem, researchers established human-liver chimeric mouse model by transplantation human hepatocytes into immunodeficient mice. The most widely chimeric mouse model used for HBV infection is transplantation human hepatocytes into urokinase-type plasminogen activator-transgenic SCID (severe combined immunodeficiency) mice ($uPA^{+/+}$/SCID mice), which are immunodeficient and undergo liver failure. The $uPA^{+/+}$/SCID mouse is generated from backcrossing the transgenic mouse carried the mouse urokinase-type plasminogen activator gene under the control of the mouse albumin enhancer/promotor (Alb-uPA mouse) onto a genetically severe combined immunodeficiency (SCID) mouse strain. In those chimeric mice, more than 90% mouse livers can be replaced by human hepatocytes [40,41]. Because the chimeric mice are immunocompromised, they are not suited for vaccine studies or evaluation of immune responses. However, because they are susceptible to HBV

infection and can formation of HBV cccDNA, they are a promising tool for evaluation of anti-HBV agents [41], and also are useful for assessment of susceptibility of mutant strains of HBV to various drugs [42].

1.2 Innate immune responses in viral infection

All living organisms have developed several kinds of mechanisms to protect themselves from different invading pathogenic microorganisms and eliminate infective pathogens, including the innate immune system and adaptive immune system [43]. In pathogens infections, the host innate immune system (also known as nonspecific immune system) is meant to act as a first line defense to prevent pathogens invasion or replication before more specific protection by the adaptive immune system is generated. The structural components (viral envelope proteins /bacterial lipopolysaccharide) and the genetic material (RNA/DNA) of pathogens (also known as PAMPs: pathogen-associated molecular patterns) activate innate immune responses via cell surface or intracellular pattern recognition receptors (PRRs), leading to the secretion of interferons (IFNs), cytokines, chemokines and many innate immune molecules [44]. Although multiple cytokines and chemokines are produced by several kinds of host cells in viral infection, IFNs are the principal cytokines involved in the antiviral response. There are three types of IFNs: type I, type II, and type III. In humans and mice, the type I IFN family is composed of 16 members, namely 12 IFN-α subtypes, IFN-β, IFN-ε, IFN-κ and IFN-ω. By contrast, the type II IFN family includes only one cytokine: IFN-γ, which also exhibits antiviral activities. The third type of IFNs is the IFN-λ family, which includes IFN-λ1 (also known as IL-29), IFN-λ2 (also known as IL-28A), IFN-λ3 (also known as IL-28B) and recently indentified IFN-λ4 [45,46]. In contrast to type II IFN that is only produced by activated T-cells and natural killer (NK) cells, type I IFNs can be produced by all nucleated cells in response to virus infection, and type III IFNs can be produced by a number of cell types, although the pattern of expression has not been elucidated [47]. These IFNs each have different receptors but share downstream signaling molecules and regulate the same genes. The produced IFNs after viral infection can active the Mx GTPase pathway, the 2', 5'-oligoadenylate-synthetase (2', 5'-OAS) directed ribonuclease L (RNase L) pathway, the protein kinase R (PKR) pathway and the IFN stimulated gene 15 (ISG15)

ubiquitin-like pathway through the Janus tyrosine kinase–signal transducers and activators of transcription (JAK-STAT) signaling. These pathways individually block viral transcription, degrade viral RNA, inhibit translation and modify protein function to control all steps of viral replication [48,49]. In addition, IFNs also activate DCs (dendritic cells) and NK cells and induce the activation of the adaptive immune system [50].

1.2.1 Pattern recognition receptors in innate immune responses

The innate immune system detects the presence of PAMPs from microbes through different classes of germline-encoded PRRs and initiates mechanisms to eliminate potentially infectious threats. Bacterial PAMPs are diverse and include various molecules ranging from lipoproteins, lipopolysaccharide (LPS), flagellin and peptidoglycan to unique bacterial nucleic acid structures, such as unmethylated CpG DNA, rRNA (ribosomal RNA) and CDNs (cyclic dinucleotides). By contrast, viruses are mainly recognized through viral fusion glycoproteins and through unique nucleic acids, such as double-stranded RNA (dsRNA), uncapped single-stranded RNA (ssRNA) and viral DNA [51].

Two main classes of PRRs have been described in mammalian cells: membrane-bound receptors (Figure 1.6), such as Toll-like receptors (TLRs) and C- type lectin receptors (CLRs), and cytoplasmic sensors (Figure 1.7), including NLRs (nucleotide-binding oligomerization domain (NOD)-like receptors), ALRs (absent in melanoma (AIM)-like receptors), RLRs (retinoic acid inducible gene 1 (RIG-I)-like receptors) and an increasing range of cytosolic nucleic acid sensors, including DAI (DNA-dependent activator of interferon regulatory factor), cGAS (Cyclic GMP-AMP synthase), DDX41 (DEAD (Asp-Glu-Ala-Asp) Box Polypeptide 41), etc. [51].

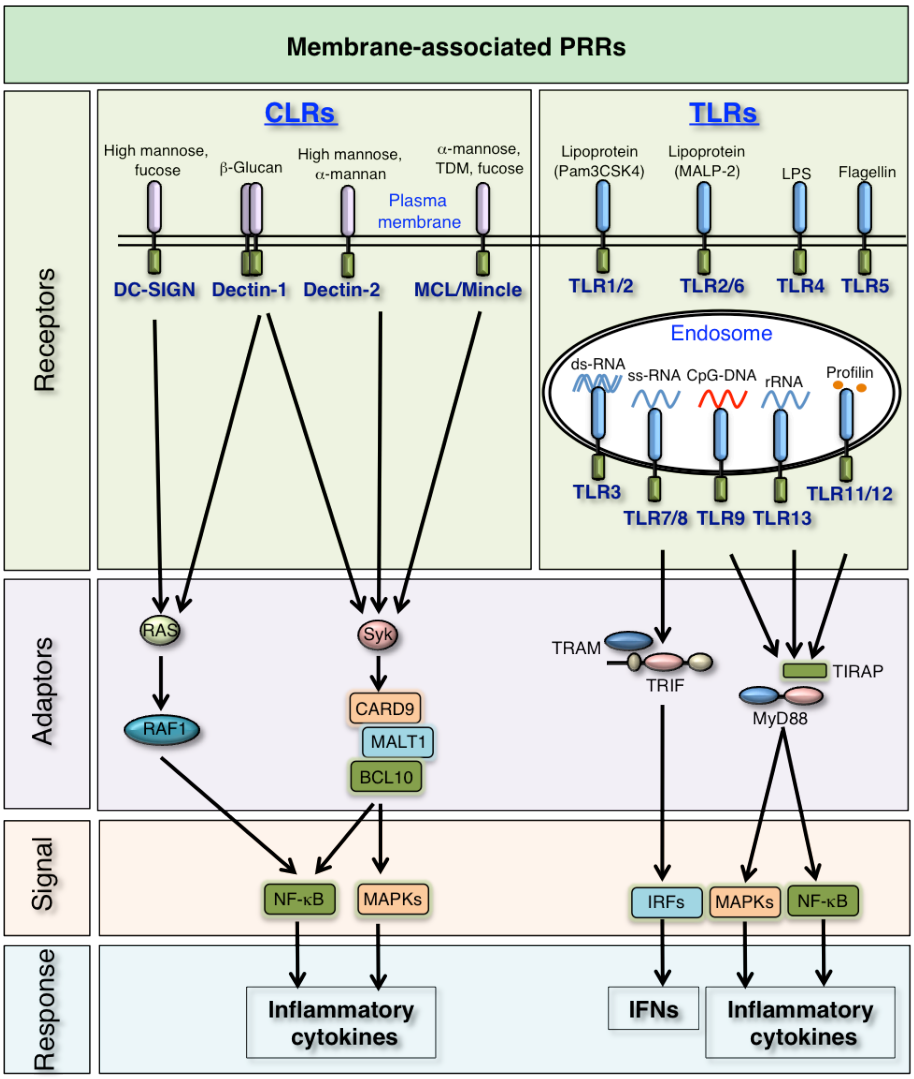

Figure 1.6 Sensing of PAMPs through membrane-associated PRRs: TLRs and CLRs. In macrophages and dendritic cells plasma membrane localized TLRs (TLR1, TLR2, TLR4, TLR5 and TLR6) and endosomal localized TLRs (TLR3, TLR7, TLR8, TLR9, TLR11, TLR12 and TLR13). TLR recruits MyD88, TRIFs, TIRAP, and TRAM adaptors for induction of inflammatory cytokines and type-I IFNs through activation of NF-κB, MAPKs and IRFs signaling. Dectin-1, Dectin-2, Mincle and MCL recruit Syk kinase to activate the CARD9–BCL10–MALT1 complex, inducing production of various inflammatory cytokines via NF-κB and MAPKs signaling. DC-SIGN and Dectin-1 can activate NF-κB pathway via the RAS-RAF1 signaling.

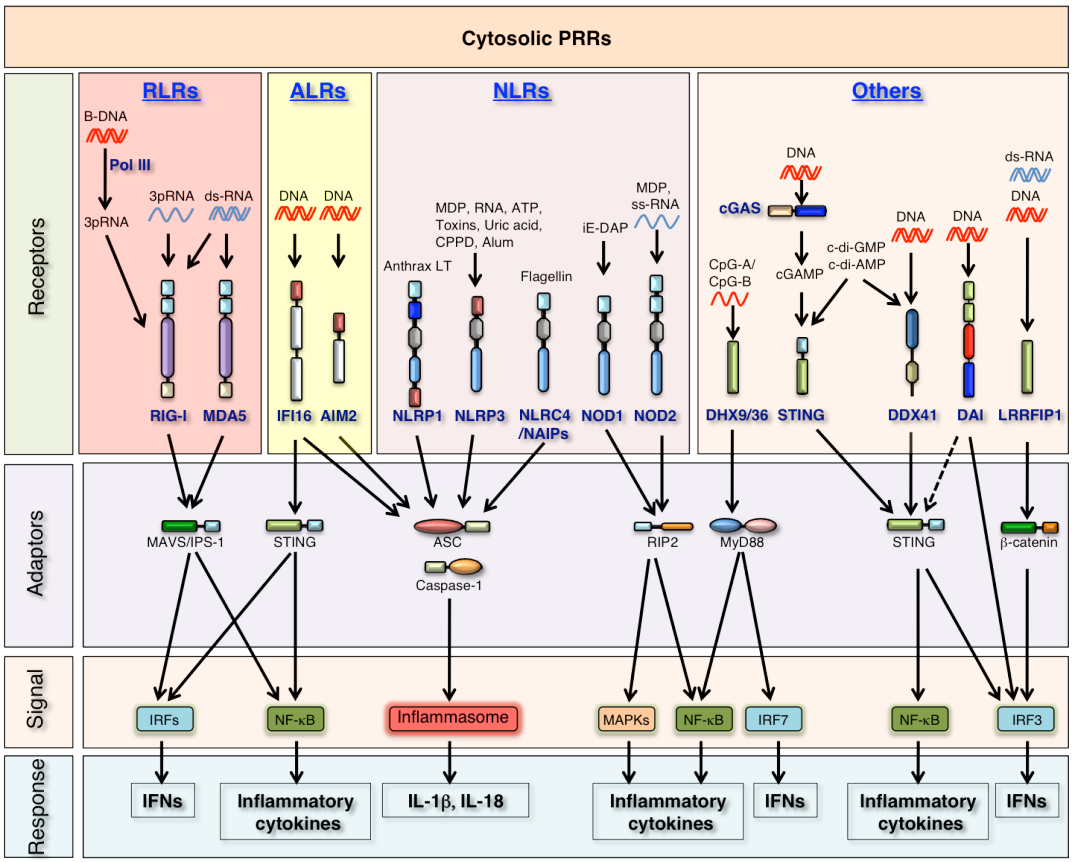

Figure 1.7 Sensing of different types of PAMPs through cytosolic PRRs: RLRs, ALRs, NLRs and other cytosolic nucleic acid sensors. RLRs family members RIG-I and MDA5 detect ssRNA and dsRNA and induce IFNs and cytokines through MAVS. ALRs IFI16 and AIM2 detect cytosolic DNA and initial inflammasome formation with ASC and IFI16 also activate IRF-3 and NF-κB pathway through STING. NLRs family members detect different types of PAMPs from bacteria or virus and initial inflammasome formation or induce inflammatory cytokines expression via NF-κB or MAPKs pathways. DAI is a DNA sensor that detects cytosolic DNA and interacts with TBK1 and IRF-3 to elicit type I IFN production. DAI also has been proposed to interact with STING (dashed arrow). LRRFIP1 detects both cytosolic dsDNA and dsRNA and enhances IFN-β production through β-catenin-IRF-3 pathway. DDX41 detects CDNs or B-form DNA and activates STING. Upon DNA binding, cGAS synthesizes cGAMP to activate STING. STING not only functions as a signaling adaptor for the cytosolic DNA responses but has also been shown to directly bind to CDNs and activate IFN signaling.

TLRs were the first group of PRRs to be characterized and they recognize PAMPs in the extracellular compartment or within endosomes of macrophages and DCs. So far,

10 members of the TLR family have been identified in humans (TLR1 to TLR10) and 12 in mice (TLR1 to TLR9, TLR11, TLR12 and TLR13). There are three general categories of TLR ligands: proteins, nucleic acids and lipid-based elements. The ligand specificities and expression in different cell types are as follows: TLR2 is expressed on monocytes, mature macrophages and DCs, and mast cells. It specifically recognizes components from gram-positive bacteria, including lipoteichoic acid (LTA) with the assistance of the scavenger receptor CD36. TLR2 can form a heterodimer with either TLR1 to recognize triacylated lipopeptides, such as the synthetic ligand Pam3CSK4, or TLR6 to recognize diacylated lipopeptides like MALP-2. TLR3 is an endosomal TLR expressed in dendritic cells and recognizes double stranded RNA, which is produced by replicating viruses and the synthetic ligand polyriboinosinic polyribocytidylic acid (poly I:C). TLR4 recognizes LPS from gram-negative bacteria and is expressed mainly on monocytes, mature macrophages and DCs, mast cells and the intestinal epithelium. TLR5 binds flagellin, a constituent of bacterial flagella and is expressed primarily on cell surface of the intestinal epithelium and in monocytes, macrophages and DCs. TLR7 and TLR8 are found in endosomes of monocytes and macrophages. Both these receptors recognize ssRNA from viruses. TLR9 is expressed in endosomes of monocytes, macrophages and plasmacytoid dendritic cells, and acts as a receptor for unmethylated CpG islands found in bacterial and viral DNA. Synthetic oligonucleotides that contain unmethylated CpG motifs are used to activate TLR9. TLR10 is expressed in endosomes of macrophages and DCs, it is the only one TLR in human that without a defined ligand. Both of mouse TLR11 and TLR12 are expressed in endosomes of DCs and macrophages, and recognize ignaling, which is a protein from the apicomplexan parasite *Toxoplasma gondii*. TLR12 can function either alone or as a heterodimer with TLR11. Although TLR11 and TLR12 expression overlaps in macrophages and DCs, TLR12 is predominantly expressed in myeloid cells, whereas TLR11 is mostly expressed in epithelial tissue. Recently found that mouse TLR13 recognizes large bacterial rRNAs, specifically the conserved CGGAAAGACC motif of 23S rRNA. TLR13 is also found expression in endosomes of macrophages and DCs. Following ligation with their ligands, TLRs interact with different combinations of the adaptor proteins TIRAP (Toll/interleukin-1 receptor domain containing adaptor protein, also known as MAL), MYD88 (Myeloid differentiation primary-response protein 88), TRIF (Toll/interleukin-1 receptor domain-containing adaptor inducing IFN-β, also known as

TICAM1) and TRAM (TRIF-related adaptor molecule, also known as TICAM2) to induce inflammatory cytokines and IFN-β. The MYD88-dependent pathway controls the activation of mitogen-activated protein kinases (MAPKs) and the transcription factor complex nuclear factor-kappa-B (NF-κB) to induce inflammatory cytokines expression, whereas the TRIF-dependent pathway mainly mediates type I IFN production through IRFs (interferon-regulatory factors) signaling [51-53].

In contrast to TLRs, CLRs and their signaling pathways are essential for antifungal immunity by recognition the major carbohydrate structures that are found in fungal cell walls, including β-glucan and mannan. The number of extracellular carbohydrate recognition domain (CRD) and their cellular localization classifies CLRs to type-I transmembrane, which contains multiple CRD, type-II transmembrane, which contains single CRD and soluble CLRs; Furthermore, based on domain organization and sequence homology, CLRs are grouped into 17 clusters. Among these clusters, DCs associate C-type lectin (Dectin)-1 and 2 clusters are the most widely explored. Dectin-1 senses fungal β-glucan and Dectin-2 senses α-mannans. Macrophage C-type lectin (MCL) and Macrophage inducible C-type lectin (Mincle) senses TDM (Trehalose dimycolate), which is the mycobacterial cord factor, α-mannose and fucose from pathogens. DC-SIGN (Dendritic cell-specific intercellular adhesion molecule-3 grabbing non-integrin, also known as CD209) a type-II CLR senses high mannose and fucose. Upon binding to fungal and bacterial PAMPs, Dectin-1, Dectin-2, MCL and Mincle use the signal transduction kinase Syk to activate MAPKs and NF-κB pathway through the CARD9 (caspase recruitment domain family, member 9)–BCL10 (B-cell CLL/lymphoma 10)–MALT1 (mucosa associated lymphoid tissue lymphoma translocation gene 1) complex. Dectin-1 and DC-SIGN can activate RAF1 (Raf-1 proto-oncogene, serine/threonine kinase) via small GTPase Ras proteins to control NF-κB activation, although the proximal mechanisms involved are unclear. Notably, these receptors also affect signaling by Toll-like receptors, and modulate the development of adaptive immunity, particularly responses of Th1 and Th17 subsets of helper T (Th) cells [51,54,55].

Mammalian RLRs are composed of three family members: RIG-I, which also known as DDX58 (DEAD box polypeptide 58), MDA5 (melanoma differentiation associated protein 5), which also named as IFIH1 (interferon induced with helicase C domain 1), and LGP2 (laboratory of genetics and physiology 2), which also kown as

DHX58 (DEXH (Asp-Glu-X-His) box polypeptide 58), and all are expressed in the cytoplasm of ubiquitous types of cells. These RLRs all share a DexD/H-box RNA helicase domain and a C-terminal domain (CTD), while RIG-I and MDA5, but not LGP2, have a N-terminal CARD domain, which is responsible for interacting with a downstream mitochondrial adaptor molecule, MAVS (mitochondrial antiviral signaling protein), which also named IPS-1 (interferon beta promoter stimulator protein 1) [56]. The helicase and CTD domains of RIG-I and MDA5 are implicated in the detection of viral RNA, and ATP-dependent conformational change allows CARDs to interact with MAVS and activate IFNs response through the IRFs and NF-κB pathway. RIG-I and MDA5 are major cytosolic receptors for detection of virus-derived RNAs. It has been shown that RIG-I binds preferentially to 5′-triphosphorylated RNA (5'-pppRNA or 3pRNA) and short dsRNA while MDA-5 recognizes preferentially long dsRNA [57]. Moreover, RNA polymerase III (Pol III) can also function as a sensor of B-form DNA (poly(dA:dT)) by converting it into dsRNA that is recognized by RIG-I [58]. In ligand-free resting state, RIG-I is auto-repressed, the second CARD domain (CARD2) interacts with helicase domain and prevents direct access of any RNA to the helicase domain, this also hinders the access of ubiquitination enzymes and polyubiquitin binding to the CARDs, thus inhibiting downstream signaling via MAVS. Upon virus infection, the viral RNA is recognized by CTD, ATP-dependent conformational change induces a packed complex formation of the helicase domain/CTD with dsRNA, the CARDs are released from auto-repression. The active RIG-I then interacts with MAVS, through RIG-I CARD and MAVS CARD interactions, and promotes MAVS filament formation on mitochondrial surface. Consequently, MAVS becomes active to stimulate downstream signaling effectors TBK1 (TANK-binding kinase 1) and IKK (inhibitor-κB kinase), which activates transcription factor IRFs (mainly IRF-1, IRF-3, and IRF-7) and NF-κB pathway, respectively. Activated IRFs and NF-κB are translocated into the nucleus, and interact with the promoter regions of target genes, including IFNs and inflammatory cytokines [59,60,61]. MDA5 is activated through a similar mechanism as RIG-I [62]. However, the LGP2 lacks CARDs and does not induce IFNs, it is though as a regulator in antiviral immune responses. LGP2 has been previously reported to inhibit RIG-I signaling and activity both *in vivo* and *in vitro*. In contrast, MDA5-induced signaling transduction is stimulated in the presence of LGP2 [63].

AIM2 (absent in melanoma 2) and IFI16 (interferon, gamma-inducible protein 16)

are ALRs with an N-terminal PYD domain (pyrin domain) and one or two C-terminal HIN domains (hemopoietic expression, interferon-inducibility, nuclear localization) for sensing cytosolic microbial dsDNA, and belong to the PYHIN (pyrin and HIN domain) protein family. The HIN domain contains partially conserved repeats, which assemble into an oligonucleotide/oligosaccharide-binding fold (OB-fold), which facilitates DNA binding. AIM2 preferentially binds dsDNA through the alone HIN-B domain, while IFI16 has two HIN domains, the HIN-A domain has a greater affinity for ssDNA than dsDNA, and the HIN-B domain alone can bind with dsDNA, which is enhanced when both HIN domains are present. However, only the dsDNA binding to IFI16 can induce IFNs signaling but not ssDNA [64]. Upon interaction with cytoplasmic dsDNA of sufficient length from invading pathogens through HIN domain, drives the IFI16 or AIM2 filament formation on dsDNA under the cooperation of PYD, the resulting IFI16 or AIM2 oligomers then robustly nucleate the assembly of the downstream adaptor protein ASC (apoptosis-associated speck-like protein containing a CARD) filaments via PYD-PYD interactions [65,66]. The formation of ASC filaments, in turn, acts as a platform for pro-caspase-1 CARD to form filaments. This brings the caspase domains of pro-caspase-1 into proximity for dimerization, cleavage and caspase-1 activation. Activated caspase-1 converts cytokines IL-1β (interleukin 1, beta) and IL-18 (interleukin 18) to their mature forms by proteolysis, and/or to induce caspase-1-dependent pyroptotic cell death [67]. Additionally, upon sensing DNA, IFI16 also activates the IRF-3 pathway through the adaptor molecule STING (stimulator of interferon genes protein), which is also known as TMEM173 (transmembrane protein 173), and finally induces the IFNs expression [68]. Moreover, IFI16 and AIM2 proteins can form heterodimers and regulate each other's signaling [69].

The NLR family includes 22 indentified protein members in humans and approximately 33 NLRs genes in mice. Most NLRs are involved in inflammasome complex formation and share common structural characteristics including a central NOD domain, which mediates the self-oligomerization occurring during activation, a variable N-terminal effector domain, and a C-terminal leucine-rich repeat (LRR) domain that detects PAMPs. The effector domains found in NLRs are CARD, PYD or BIR (baculoviral inhibitor of apoptosis repeat) domains. Based on the variation in their N-terminal effector domain, the NLRs family can be further subdivided into five families: NLRA subfamily consists of only one member, class II transactivators

(CIITA), which at least one splice variant expresses a CARD, and is involved in transcriptional activation of genes encoding major histocompatibility complex class II; NLRB subfamily expresses a BIR domain and consists of 7 members in mice (NAIP1-7, neuronal apoptosis inhibitor proteins 1 to 7) and only one member in humans (NAIP); NLRC subfamily includes the CARD-containing molecules (NOD1, NOD2, and NLRC3-5); The NLRP subfamily members (NLRP 1–14) express a PYD in the N-terminal; NLRX, an additional subfamily that has no homology to the N-terminal domain of any of the other four subsets and consists of one member, NLRX1, which is the only NLR protein that is localized in mitochondria [70,71]. NOD1 (which is categorized as NLRC1) and NOD2 (NLRC2) are well-characterized members of the NLR family, which recognize distinct structural motifs derived from PGN (peptidoglycan). NOD1 recognizes iE-DAP (g-D-glutamyl-meso-diaminopimelic acid), which is found in the PGN structures of all Gram-negative and certain Gram-positive bacteria, whereas NOD2 recognizes MDP (muramyl dipeptide), the largest component of the PGN motif that found in almost all bacteria. Upon binding of their ligands, NOD1 and NOD2 activate MAPKs and NF-κB signaling pathway throught the adaptor kinase RIP2 (receptor-interacting protein 2, also known as RIPK2, receptor-interacting serine-threonine kinase 2), and induce inflammatory cytokines expression. Additionally, NOD2 also can sense viral derived ssRNA and activate IRF-3 pathway through MAVS to induce IFNs expression [72,73]. Other three NLRs-NLRC4, NLRP1 and NLRP3-were definitely known to initiate inflammasome assembly after recognition with their ligands. NLRC4 is activated by bacterial flagellin, NLRP1 is activated by anthrax lethal toxin (LT), and NLRP3 is activated by a wide variety of signals including pore-forming cytotoxins, MDP, CPPD, ATP, uric acid, alum and also bacterial RNA. Similar as the formation of AIM2 and IFI16 inflammasome, the activated NLRs form an inflammasome complex with or without the adaptor, ASC, and recruit procaspase-1, which is subsequently cleaved into active caspase-1. Caspase-1 cleaves pro-forms of IL-1β and IL-18 into their active forms as well as induces cell death. In contrast to NLRP1 and NLRP3 inflammasome formation, which are dependent on ASC, NLRC4 possesses an N-terminal CARD that allows direct interaction with caspase-1 independently of ASC. And also NAIPs have been identified as critical components of the NLRC4 inflammasome, they are required for the recognition of bacterial components, as well as the scaffolding of the NAIP-NLRC4 inflammasome [51,64,73].

Other cytosolic PRRs such as DAI, LRRFIP1, DDX41, DHX9, DHX36 and cGAS are involved in cytosolic DNA sensing and induction of IFNs and other inflammatory cytokines. DAI (also known as ZBP1, Z-DNA binding protein 1) is the first indentified cytosolic DNA sensor, which was shown to bind DNA, and to be required for the response to transfected viral, bacterial and mammalian DNA in murine L929 cells. DAI has been reported to interact with TBK1 and IRF-3, and also with RIP1 and RIP3 to activate NF-κB, thus elicit type I IFN and inflammatory cytokine production [74-76]. DAI has been shown to play a role in DNA virus HSV-1 (herpes simplex virus 1) and HCMV (human cytomegalovirus) infection [77,78]. It is likely that the DAI pathway also involves STING, although this has not been formally demonstrated. LRRFIP1 is a cytosolic nucleic acid-binding protein that acts as a sensor for both dsDNA and dsRNA. Upon binding to ligands, LRRFIP1 promotes IRF-3 transcriptional activity at the IFNB1 promoter through β-catenin-dependent signaling [79]. In addition to DAI and LRRFIP1, DDX41, a DexD/H box helicase, was shown to induce IFN-β response upon stimulation with poly (dA:dT), cyclic dinucleotides from bacteria, HSV-1 and adenovirus via STING-TBK1-IRF-3 pathway [80,81]. Other two DexD/H box helicase members, DHX9 and DHX36 sense microbial DNA differently, DHX9 recognizes CpG-B using the DUF (the domain of unknown function) domain, and DHX36 senses CpG-A via DEAH (aspartate-glutamate-alanine-histidine box motif) domain. Upon DNA recognition, DHX9 induces TNF-α (tumor necrosis factor alpha) and IL-6 (interleukin 6) production via NF-κB pathway and DHX36 promotes IFNs production via IRF-7 pathway, and both processes are dependent on adaptor Myd88 [82]. Recently, 2′, 3’-cGAMP (cyclic [G(2’,5’)pA(3’,5’)p]) synthase (cGAS) has been identified as a sensor for cytosolic DNA. cGAS belongs to the nucleotidyltransferase (NTase) family and exhibits structural and sequence homology to the catalytic domain of OAS (oligoadenylate synthetase). When activated by DNA through direct binding, cGAS catalyzes the production of cGAMP from ATP and GTP. cGAMP in turn functions as an endogenous second messenger to activate STING and sequentially activate IRF-3 and NF-κB pathway signaling [83,84]. Even STING is thought to function as an adaptor protein, which links upstream PRRs to IRF-3 and NF-κB pathway activation, it also directly senses bacterial CDNs (cyclic dinucleotides), including c-di-GMP (cyclic 3′-5′diguanylate), c-di-AMP (cyclic 3′-5′ diadenylate) and 3′,3′-cGAMP (cyclic [G(3’,5’)pA(3’,5’)p]) [85,86], those CDNs are bacterial second messengers with a

regulatory role in several processes, such as biofilm formation, virulence, DNA integrity surveillance, chemotaxis and colonization [87-89]. Binding with bacterial CDNs or cGAS product-2′,3′-cGAMP can activate STING and recruit TBK1 to phosphorylate IRF-3 and promote IRF-3 nuclear translocalization and binding to IFNs promoter, and also STING can activate NF-κB pathway via TRAF6 (TNF receptor-associated factor 6, E3 ubiquitin protein ligase)-TBK1 pathway [90,91].

1.2.2 Mechanism for host to distinguish self and non-self PAMPs

Reorganization PAMPs by PRRs is a critical process for initiation innate immune responses after pathogens infection. As above description, different PRRs interact with different PAMPs, and show distinct expression patterns, activate specific signaling pathways and lead to distinct anti-pathogen responses. But basically, the immune system is able to distinguish self-components from non-self PAMPs and respond to non-self but not to self. The most common mechanism for host to distinguish self-components and non-self PAMPs is that many PAMPs recognized by PRRs are unique to the pathogen and not found in the host, for example, components of bacterial and fungal cell walls, flagellar proteins and viral surface proteins, and also c-di-GMP and c-di-AMP, which are bacteria- and archaea-specific secondary messengers that are not produced by host cells [87]. However, another major group of PAMPs specifically recognized by innate immune PRRs comprises microbial DNA and RNA. Even all microbes use DNA and/or RNA as genetic information carriers in their life cycle and could therefore potentially activate host nucleic acid sensors, nucleic acids are present not only in microbes but also in host, so this also introduces the risk of self nucleic acid recognition by innate immune sensors that may cause several autoimmune and autoinflammatory diseases. To avoid this self nucleic acid recognition, the host has evolved specific mechanisms to distinguish self from non-self nucleic acids based on modification or location of nucleic acid or PRRs to avoid inappropriate IFN production. For example, after infection by microbe, the pathogenic DNA is always presented in cytoplasm, which is different from the nuclear or mitochondrial localization of host DNA; thus, the host cytosolic DNA sensors can distinguish self and non-self DNA. However, the DNA sensor IFI16 is a special case. Different from other identified cytosolic DNA sensors, which only function in cytoplasm, IFI16 also operates in the nucleus, which is conventionally thought to be off limits to DNA sensors due to the

abundant self DNA. As the activation of IFI16 upon DNA recognition requires IFI16 filament formation on dsDNA, and the length of the exposed linker-dsDNA between nucleosomes (10-20 bp) or even that of the transcription bubble (~17 bases) in the host nucleus is too short to promote robust filament assembly of IFI16, thus, IFI16 can not sense self DNA even operates in the nucleus [65]. Another example is endosomal nucleic acid-sensing TLRs (TLR3, 7, 8, 9, 13), those TLRs are localized in intracellular compartments, such as endosomes, lysosomes, multivesicular bodies, and ER. However, they are only activated within acidic endosomal compartments, because TLRs-induced responses to foreign nucleic acids are suppressed by some endosomal acidification inhibitors, such as chloroquine, ammonium chloride or bafilomycin A1. Upon stimulation, nucleic acid-sensing TLRs are translocated directly from the ER to endosomes via the conventional secretory pathway through the Golgi. After pathogens are internalized, the TLRs enable them to recognize nucleic acids delivered to the endosomal compartments. By contrast, host nucleic acids presented outside endosomes are rapidly degraded by nucleases and are not detected by endosomal nucleic acid-sensing TLRs. Therefore, trafficking and localization of TLRs has emerged as a primary mechanism to facilitate self versus non-self discrimination [92,93].

In addition to the mechanism based on nucleic acids and PRRs location, nucleic acid modification is also involved in host to distinguish self from non-self nucleic acids. The classical ligand for TLR9 is CpG DNA, an immuno-stimulatory DNA composed of unmethylated CpG dinucleotides with particular flanking sequences. The CpG motif is abundant in bacterial genomes as well as in the DNA of viruses such as HSV-1, HSV-2 and MCMV (murine cytomegalovirus). In contrast, in mammalian genomes the CpG motif occurs much less frequently and is highly methylated, which is not recognized by TLR9 [94]. For the case of RNA sensing, one type of ligands for RIG-I recognition is RNAs containing a 5'triphosphate motif, which found in most RNA viruses but not in host as host mRNAs are capped at their 5' ends while mature tRNA and rRNA lack 5' triphosphate group and are covered as ribonucleoproteins respectively. This virus-specific RNA motif provides a way by which RIG-I can distinguish between host and viral RNAs [95]. However, RIG-I and MDA5 also can sense dsRNA, which also exist in host cells. Recent studies indicate that ADAR (adenosine deaminase acting on RNA) enzymes mediated adenosine-to-inosine (A-to-I) editing of host RNA can prevent the sensing of endogenous dsRNA as nonself by MDA5, and endogenous RNA

methyltransferases (N7 and N1/2-2′O-methyltransferases) mediated 2′O-methylation of the 5′-terminal nucleotide (N1) prevents the binding of self RNA to RIG-I and entirely abrogates the activation of RIG-I [96,97].

Although the host develops some mechanisms as described above to specifically recognize microbial nucleic acids, they can in some circumstances lead to the recognition of self DNA and RNA and the development of autoimmunity. For example, the mutations of the exonuclease TREX1 (three prime repair exonuclease 1) in humans leads to loss of function to degrade aberrant cellular self DNA and the undigested DNA induces excessive production of IFNs and inflammatory cytokines through the activation of host DNA-sensing pathway, so TREX1 mutation in humans links to autoimmune diseases including Aicardi-Goutieres Syndrome (AGS) and systemic lupus erythematosus (SLE) [98,99].

1.2.3 Viral strategies for evasion of host innate immune responses

When virus infects a host, the innate immune response functions as the first line of defence against infection to eliminate the invading pathogen. Viruses, in turn, have evolved an abundance of strategies to escape from the innate immune system, evasion of the host innate immune responses allow the virus to gain an early foothold during infection, replicating to a high titer before an effective adaptive immune response can be mounted. There are two main types of mechanism for viral evasion of host innate immune responses:

(1) Avoid detection by PRRs: Detection of the PAMPs form pathogens by host PRRs is the first step for innate immune responses. Some virus can shield themselves from immune system to avoid detection by PRRs, for example, the Dengue virus (DENV), which replicates in ER-derived membrane structures called vesicle packets and convoluted membranes. This has the advantage of keeping its proteins and RNA out of the cellular cytosol and, thus, limits triggering the innate response via PRRs [100]. Modifying or degrading viral PAMPs is another strategy. For example, some virus can hide or remove of 5'tri-phosphate to avoid recognition by RIG-I. Viral peptide linked to the genome (VPg) of poliovirus is covalently attached to the 5' end of viral RNA, thus lacking 5'-triphosphate [101]. Other virus such as Hantaan virus (HTNV) and Borna disease virus (BDV) do not trigger RIG-I-mediated IFN responses, because the 5'-triphosphate structure of these viral genomic RNA is removed by processing [102].

And Lassa virus encodes an exonuclease, nucleoprotein that hydrolyses RNA, thus Lassa virus is able to evade immune recognition by digesting its own PAMPs [103]. Human immunodeficiency virus type 1 (HIV-1) also can use host exonuclease TREX1 to degrade HIV DNA generated during HIV-1 infection and avoid detection by nucleic acid sensors [104].

(2) Disruption of PRRs or downstream signaling pathway: Viruses have evolved a variety of mechanisms to inhibit every step of the innate immune responses, including disruption of PRRs or downstream signaling pathway. The viral RNA receptor RIG-I is degraded during encephalomyocarditis virus (EMCV) infection through the viral-encoded 3C protease and caspase proteinase, thus, reduces the sensing of viral RNA by RIG-I [105]. The RLRs signaling pathway adaptor-MAVS is cleaved by Hepatitis C virus (HCV) non-structural (NS) proteins-NS3/4a, thus, inhibit further innate signaling [106]. The major IFNs regulator-IRF-3 is targeted by amount of viral proteins, including NS1 protein from Influenza A virus (IAV), VP35 (viral protein 35) of Ebola virus (EBOV), Npro (viral N-terminal protease) protein from pestiviruses, etc. Blocking IRF-3 prevents its phosphorylaton, dimerization and subsequent translocation to the nucleus to induce transcription of IFN-β [107].

Although viral evasion strategies may be the most elaborate and have been studied most extensively, other classes of pathogens have also developed several elegant evasion strategies, either by altering their PAMPs to be less immunogenic or through activation of anti-inflammatory responses induced by different virulence factors. For example, *Helicobacter pylori*, *Porphyromonas gingivalis*, and *Legionella pneumophila*, synthesize modified forms of LPS, which are not recognized by TLR4 [108], and similarly, *Campylobacter jejuni*, *Helicobacter pylori*, and *Bartonella bacilliformis* produce subclasses of flagellin that do not activate TLR5 [109].

1.2.4 HBV and innate immune responses

After HBV infection, the nucleocapsid is released and then the viral rcDNA is delivered to the nucleus, where the cccDNA is formed. The cccDNA serves as the template for the transcription of viral RNAs, which are then be capped and polyadenylated by host machinery. The transcripts are exported to the cytoplasm but the viral RNA-DNA chimeric replicative genome is sequestered within viral capsids. Thus, except for capped viral RNAs in cytoplasm, the naked viral DNA seems to be not

detectable by host cytosolic nucleic acid sensors. Thus, HBV was believed to be a stealth virus that did not trigger or only triggered a limited innate response in infected chimpanzees and patients during the acute phase of infection [110,111]. However, about 95% of adults infected with HBV recover completely and become immune to the virus, and not develop chronic HBV infection [112]. On the other hand, HBV replication is sensitive to the suppressive effects of IFNs in studies using the transgenic mouse model or hepatoma cell lines. HBV was shown to replicate in IFN-γ knockout (KO) and IFN-α/β receptor KO mice at levels higher than those observed in control mice, indicating that the low levels of these cytokines control HBV replication [113]. Both of those results suggest that the innate immune response to HBV may play an unexpected role in controlling HBV replication.

Previous study has shown that HBV was unable to interfere host cellular gene transcription significantly and to induce IFN stimulated genes (ISGs) expression in the liver of HBV infected chimpanzee model [110]. However, other study indicated that HBV infection was unable to elicit a strong production of IFNs and IL-15, but induced the production of anti-inflammatory cytokine IL-10 by quantification of cytokines from 21 HBV infected patients' serum samples [111]. In addition to this observation, another study suggested that many cytokines in serum samples from about half of HBV patients were weakly induced during acute HBV infection, including IFN-α, TNF-α, IL-15, IL-10, IL-6 and IL-1β [114]. When using cultured primary human hepatocytes and non-parenchymal liver cells, it was shown that HBV was recognized by kupffer cells and resulted in the activation of NF-κB pathway and production of IL-6, while no induction of type I IFNs [115]. In the chimeric uPA/SCID mice harboring human hepatocytes, a weak activation of ISGs was detected in HBV infected human hepatocytes, but not in mouse hepatocytes without HBV infection [116]. Moreover, some studies revealed that HBV exposure *in utero* promoted innate immune cell maturation and Th1 response development, which in turn enhanced the responses of cord blood immune cells to bacterial infection *in vitro* [117]. The circulating monocytes also were shown to respond to HBsAg *in vitro*, resulting in strong production of proinflammatory cytokines TNF-α and IL-6 [118].

Taken together, these data from recent studies suggested that liver cell populations, as well as circulating innate immune cells, could sense and respond to HBV infection, which enables the innate immune system to detect and restrict the invading virus, even

the response to HBV infection is relatively weak, as compared with other virus infection.

1.3 Therapeutic approaches for HBV

HBV infection is a major causative factor associated with not only inflammation but also cirrhosis and even cancer of the liver. Although about 95% of adults infected with HBV recover completely and become immune to the virus, and not develop chronic HBV infection. The development of chronic infection is very common (about 90%) in infants infected from their mothers or before the age of 5 years. Worldwide, an estimated 240 million people are chronically infected with HBV (defined as HBV surface antigen positive for at least 6 months), and more than 780 000 people die every year due to complications of HBV, including cirrhosis and liver cancer [112]. Even a vaccine against HBV has been available since 1982 and is 95% effective in preventing infection and the development of chronic disease and liver cancer due to HBV, HBV infection is still a major global health problem as lacking an effective therapeutic approach to cure the virus infection from chronic carriers. Currently, based on specifically targeting critical steps involved in HBV replication, various therapeutic approaches, alone or in combination, have been developed in clinical for HBV treatment or under development (Figure 1.8). Those approaches have been shown to have the potential to decrease the risk of liver disease progression by suppression of the virus replication [119,120].

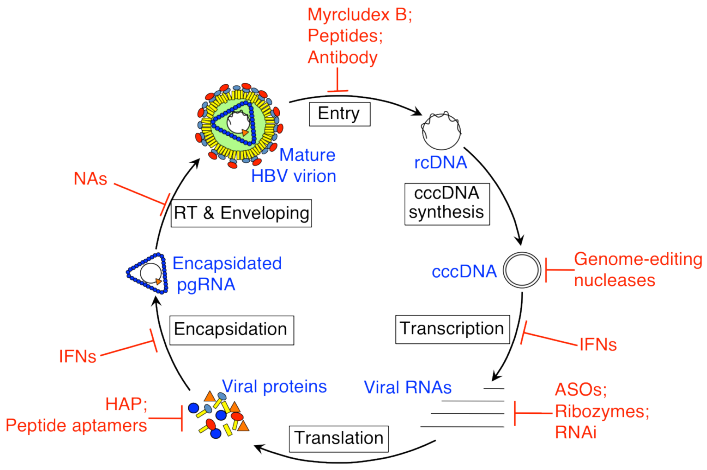

Figure 1.8 Diagram of HBV replication cycle and developed or under development therapeutic approaches for HBV infection. Based on specifically targeting critical steps

involved in HBV replication, various therapeutic approaches are approved or shown great potential for treatment of chronic HBV infection: Myrcludex B and other peptides or antibodies inhibit HBV enter into cell via binding to HBV receptor; genome-editing nucleases target to the cccDNA of HBV in the nucleus and disrupt the gene function; interferons (IFNs) not only inhibit transcription of viral RNAs from cccDNA but also inhibit the assembly of HBV capsid; viral RNAs could be specifically targeted and degraded by antisense oligonucleotides (ASOs), ribozymes and short small interfering RNAs (siRNAs); some HBV core protein inhibitors like heteroaryldihydropyrimidines (HAPs) and peptide aptamers directly bind HBV core protein and inhibit proper nucleocapsid assembly; nucleos(t)ide analogues (NAs) have strong ability to suppress HBV replication by inhibiting HBV polymerase/reverse transcriptase activity.

1.3.1 Interferon based antiviral therapy against HBV

IFNs have antiviral, antiproliferative, and immunomodulatory effects [121]. Though HBV does not trigger type I IFN production in hepatocytes and in the infected liver, IFN-α and IFN-β are shown to be able to suppress HBV replication *in vitro* and in HBV transgenic mouse models [122,123], and recombinant IFN-α has been approved and successfully used in clinical as a standard treatment for chronic HBV infection. IFN-α has multiple functions on inhibition of HBV replication via direct or indirect manners. IFN-α induces epigenetic modification of cccDNA minichromosomes or suppresses the activity of HBV enhancers, thus inhibits transcription of pgRNA and subgenomic RNA from cccDNA [124,125]. IFN-α also accelerates decay of nucelocapsids that contain pregenomic HBV RNA by the inhibition of HBV capsid assembly [126]. In addition, IFN-α can induce ISGs expression via JAK-STAT pathway and some ISGs are shown to have antiviral activity against HBV by degradation of viral mRNA, inhibition of viral protein synthesis, or prevention of infection of cells [127]. Recent study shows that high doses of IFN-α up-regulates the expression of the deaminase APOBEC3A (apolipoprotein B mRNA editing enzyme, catalytic polypeptide-like 3A), which results in cytidine deamination and degradation of HBV cccDNA in cell culture models [128]. Except for the antiviral effects of IFN-α on HBV infection, IFN-α also has relative low immunomodulatory effects including enhancement of antigen presentation to the immune system, activation of NK cells and other immune cells for lysis of infected hepatocytes, and increased production of cytokines for control of viral replication [129].

Additionally, type II and Type III IFNs are also shown to have anti-HBV activity. It was reported that IFN-γ was secreted by cytotoxic T-lymphocytes can inhibit both HBV gene expression and replication [130]. Type III IFNs also have ability to repress HBV replication use a common molecular mechanism as type I IFNs, and as type III IFNs receptors demonstrate a more restricted pattern of expression in epithelial cells, which may reduce any adverse event profiles on treatment, thus type III IFNs may play a local, rather than systemic, role in antiviral immunity [131,132]. However, Type I and Type III IFNs have predominantly antiviral effects, while Type II IFN has more marked immunoregulatory but less potent antiviral activity [133]. As the modification of IFNs through the attachment of a polyethylene glycol (PEG) molecule can improve pharmacokinetic and pharmacodynamic properties and result in relatively continuous drug exposure during the dosing interval, the PEG-IFN-α has largely replaced conventional IFN used in clinical to treat chronic HBV infection [134].

Though IFN-α was approved to treatment of CHB in most countries, only small percentage (about 30%) of patients with chronic HBV infection who respond to IFN-α-based therapy with HBeAg and HBsAg loss, seroconversion to anti-HBe and anti-HBs status, reduction of viral replication, and ALT (alanine aminotransferase) normalization [135]. Furthermore, there is a relative higher rate of adverse effects on the treatment of CHB by IFN-α, including fatigue, flu-like symptoms, neuropsychiatric symptoms and hematological abnormalities [136].

1.3.2 Nucleos(t)ide analogues based therapy

In contrast to IFN-α based therapy, which is given as subcutaneous injection, nucleos(t)ide analogues (NAs) are approved for the treatment of CHB by oral administration, including lamivudine (LAM), telbivudine (LdT), adefovir (ADV), entecavir (ETV) and tenofovir (TDF) [137]. Lamivudine and telbivudine are L-nucleoside analogues, adefovir and tenofovir are acyclic adenine nucleotide analogues, and entecavir is a cyclopentyl guanosine analogue. Tenofovir was shown to be superior to adefovir and is expected to replace adefovir. These agents are prodrugs and need intracellular activation before they can exert their potent action in inhibiting HBV polymerase/reverse transcriptase activity. Via this action, they are highly effective in the suppression of HBV replication, and in turn lead to rapid and profound decrease in HBV DNA synthesis and may thus block the amplification of cccDNA. However, in

contrast to IFN-α based HBV therapy, these agents have no direct effect on cccDNA; thus the translation of HBV proteins may lasts a long time after starting therapy, as a residual amount of the pre-existing cccDNA may be still in a very stable state. Therefore, NAs are highly effective in decreasing serum HBV DNA levels, but they are less likely to clear serum HBeAg and HBsAg. It is reported that the reduction in serum HBV DNA by these agents ranged from 3.6 to 6.9 $\log_{10}$, being highest with entecavir, followed by tenofovir, telbivudine, lamivudine and adefovir. However, the increased potency does not associate with increased HBeAg loss or seroconversion rate [138].

Though HBV DNA titers decline rapidly in blood and liver during treatment with NAs, the therapeutic efficacy is determined by two main factors: potency of inhibition and low risk of drug resistance in long-term therapy. Under a long-term therapy, selection pressure allows HBV mutants with reduced susceptibility to drugs by alter the interaction between the binding sites of HBV polymerase and antiviral drugs, thus frequency lead to treatment failure and progress to liver disease [139].

The limited efficacy of IFN-α or NAs monotherapy in achieving HBsAg seroconversion and/or sustained HBV control was the rationale for studies that combine the two classes of drugs. Because IFN-α targets HBV cccDNA and reduces viral RNAs and proteins synthesis, and NAs potently represses HBV replication by inhibiting the activity of viral polymerase, the combination of IFN-α and NAs may generate a better antiviral response and immune recovery in patients with chronic HBV infection. Unfortunately, the results from studies comparing the efficacy of various combinations of IFN-α and NAs versus IFN-α and NAs alone have been rather controversial. According to trials, there was no difference in HBsAg seroconversion and/or sustained HBV reduction between combination therapy of PEG-IFN-α and NAs and either PEG-IFN-α or NAs alone [140], despite some studies showed that combination PEG-IFN-α and NAs therapy have a higher sustained biochemical response rate or HBeAg loss than IFN-α or NAs monotherapy [141,142]. However, one major benefit of combination therapies is that they could significantly delay or decrease the emergency of drugs resistance.

1.3.3 Nucleic acid based therapy

Besides IFN-α and NAs based therapy for chronic HBV infection, nucleic acid based therapy is also potential therapeutic tool for HBV, and several genetic anti-HBV

strategies have been developed or under development. The most studied approaches include the use of antisense oligonucleotides (ASOs), ribonucleic acid enzymes (ribozymes), RNA interference (RNAi) effectors and gene editing tools [143]. In contrast to NAs based therapy, all of those approaches can reduce the escape mutants of HBV by targeting the conserved regions of HBV genes.

Antisense oligonucleotides (antisense DNA or antisense RNA) are short, synthetic, nucleic acid fragments that specifically bind to the target RNA sequences to form a DNA:RNA hybrid or RNA:RNA duplex. This binding may block targeted RNAs reverse transcription or translation by ribosomal blockage or induce RNase H-mediated RNA cleavage of RNA:DNA hybrids [144]. The first report of ASOs against HBV in 1990 indicated that ASOs can inhibit the HBV surface gene expression, later several studies have further demonstrated the potential of ASOs in gene therapy by targeting HBV pre-S1, pol, X, core genes, and also non-coding sequences, such as the packaging and polyadenylation signals, all of those ASOs are shown to effective against HBV replication. However, there are still some challenges for the clinical application of ASOs, such as instability, inefficient intracellular delivery, inadequate affinity to targets and toxicities [143]. Thus, most of recent studies focus on overcoming the deficiencies of ASOs, and several studies demonstrated that ASOs could easily be modified at the base, phosphodiester groups and the sugar to increase stability, solubility, specificity and affinity for targets [145], this may accelerate the clinical development of ASOs.

Ribozymes are naturally occurring catalytically active antisense RNA molecules. They are though as a more potential tool for HBV gene therapy as their RNA cleavage activities are independently of cellular pathways. In general, a potentially therapeutic ribozyme comprises an antisense sequence for specific RNA binding and a target cleaving enzymatic domain. Naturally occurring classes of ribozymes include Group I introns, Group II introns, Ribonuclease P (RNase P) and the hammerhead, hepatitis delta virus, hairpin and Neurospora Varkud satellite ribozymes. Group I introns, Group II introns and RNase P are larger and more structurally complex ribozymes. Among the larger ribozymes, RNase P is the most explored for use against viruses. RNase P ribozymes can be modified by linking the catalytic domain to an external guide sequence (EGS) that is complementaryto the target. A study which designed an RNase P-free EGS that targeted the pre-S1 and surface regions of the pgRNA is shown significant suppression of viral gene expression with reduced viral DNA levels in both

HBV replication cell culture model and mouse model [146]. In addition, hairpin and hammerhead ribozymes have also been engineered to confer sequence-specific cleavage of HBV mRNA. Hammerhead ribozymes are the best characterized and most commonly used small ribozyme against HBV. It is reported that targeting HBV packaging signal, polyadenylation signal, core, S, pol and X genes by hairpin ribozymes and hammerhead ribozymes resulted in efficient target RNA cleavage and suppression of HBV replication in cell culture and mouse model [143]. However, ribozymes generally have lower intracellular efficiency, which has delayed progress of anti-HBV ribozymes to clinical development.

RNAi is a post-transcriptional process triggered by the introduction of small dsRNA which leads to gene silencing in a sequence-specific manner. Two types of small dsRNAs are involved in RNAi, one is exogenous short small interfering RNAs (siRNAs), the other is endogenously expressed microRNAs (miRNAs). Both siRNAs and mature miRNAs can be incorporated into an RNA inducing silencing complex (RISC) containing Argonaute 2 (Ago2). One strand of the dsRNA is selected as a guide and the remaining strand is subsequently degraded or released from RISC by Ago2. The guide strand hybridizes to target mRNA to promote degradation by Ago2 or translation inhibition [147]. Different from vector-based small dsRNAs and endogenously expressed miRNAs, the *in vitro* synthesized siRNAs are easier to produce and control the dose, and also have a higher stability by chemical modification and lower immunostimulatory effects, thus widely used for RNAi. Due to the strong ability to degrade RNAs, RNAi-based technology has been suggested to be a potentially rational therapy for HBV infection, although significant challenges including the low delivery efficacy, poor RNA stability, and off-target effects need to be overcome before these can be successfully used in clinical treatment. Indeed, several siRNAs against HBV have entered clinical development. Recent pre-clinical studies with an RNAi based drug, ARC-520, showed promising results. ARC-520 comprises two cholesterol-conjugated siRNAs and a hepatocyte-targeted membrane-lytic-peptide (NAG-MLP) to improve the stability and liver-tropic of the siRNAs. Injection of ARC-520 in a chronically infected chimpanzee decreased HBV DNA levels 36-fold, HBeAg by 10-fold and HBsAg by 80% after two injections. It is also shown that ARC-520 was safe and well tolerated in the Phase 1 clinical trial, the Phase 2a clinical trial (gov ID: NCT02065336) in chronically infected patients showed significant HBsAg reduction and was well

tolerated [148].

Genome editing is a technique that utilizes engineered DNA-binding nucleases for targeted gene replacement, addition, or inactivation. Engineered nucleases with modular DNA-binding domains or RNA-guided DNA targets may be employed to bind and digest specific DNA sequences to enable permanent disruption of target genes through double-strand breaks (DSBs), homology-directed repair (HDR) or non-homologous end joining (NHEJ). There are three most commonly used designer nucleases, including zinc finger nucleases (ZFNs), transcription activator-like effector nucleases (TALENs), and the clustered regularly interspaced short palindromic repeats/Cas9 (CRISPR/Cas9) system, which are designed to target specific DNA sequences, represent highly promising potential therapeutic tools [143]. Several studies have shown that genome editing is a useful technique for achieving inhibition of HBV replication by targeting different regions of HBV cccDNA [149-151].

However, both RNAi- and genome editing-based HBV therapy may have potential off-target effects, which result in inaccurate cleavage of host RNA or DNA. Further more, as HBV genome may integrate into the host genome, genome-editing nucleases targeting on HBV genome may result in chromosomal translocation [143]. All of those undesired events might increase the risk of developing cancer.

Except for the above therapeutic approaches for HBV, which are all based on inhibition of HBV replication by targeting HBV DNA or RNAs, other alternative methods focus on HBV proteins. As the HBV functional receptor was indentified, some peptides or antibodies were developed for blocking HBV enter into cells. For example, myrcludex-B, which is an optimized synthetic lipopeptide corresponding to amino acids (aa) 2–48 of the pre-S1 domain of the HBV surface L protein, is able to strongly inhibit HBV infection in both cell culture and an *in vivo* mouse model via binding to HBV receptor-NTCP [152]. Moreover, some peptides or compounds bind to HBV core protein and inhibit the encapsidation, which is the critical step in the HBV life cycle involving assembly of the HBV polymerase, pre-genomic RNA, and HBV core protein into the nucleocapsid. One of the compounds heteroaryldihydropyrimidines (HAPs) was reported to bind to the HBV core protein and lead to dysfunctional polymer formation, degradation of core protein, and inhibition of proper nucleocapsid assembly [153]. In addition, some peptide aptamers have also been reported to have an inhibitory effect on nucleocapsid formation through binding to the core protein [154,155].

All together, although antiviral therapy of CHB infection has improved dramatically during the last decades, an effective treatment is still not available and CHB remains a serious clinical problem worldwide. Current available antiviral approaches based on IFN-α or NAs suppress viral replication and improve patient survival, but both of those treatments do not eradicate cccDNA of HBV in most cases, thus may result in viral reactivation after cessation of treatment and development of liver disease progression. Moreover, the response to IFN-α-based therapy is still not satisfactory, and long-term therapy by NAs increases the mutation of HBV with reduced susceptibility to drugs. As the high efficacy of reducing the replication of HBV and low possibility of generating escape mutants, the new therapeutic strategies which targeting viral RNAs or cccDNA by gene therapy approaches provide new promising expectations for more efficient therapies. However, new strategies should be clinically evaluated by large-scale trials or by the use of relevant experimental models.

1.4 Aims of the study: Elucidation of the innate immune activation by HBV and its mechanism of action

As described above, earlier studies have shown that the induction of type I IFNs in infection models was hardly detected, but several later studies indicated that HBV could induce a weak host innate immune response. However, the host innate immune response against HBV infection is largely unknown, and understanding of the nature of innate immunity induced by HBV will aid to characterize the immunopathogenesis of HBV infection and to further develop novel innate immune-based antiviral approaches for HBV infection or optimize the current therapy regimens of HBV.

Accordingly, in this study, I wanted to elucidate the innate immune activation upon HBV infection by analyzing the induction of IFNs and cytokines in several HBV infection models, and also clarify the mechanism of the innate immune activation by HBV through analyzing the role of several innate immune response associated molecules in HBV infection. Our study would accelerate the successful design of novel immune modulatory therapies based on the induction or reconstitution of efficient host antiviral innate immune responses in chronic HBV patients.

2. Materials and Methods

2.1 Biotic and abiotic materials

All solutions were prepared with deionised water from the Milli-Q Advantage A10 Water Purification System (Millipore, USA). At a resistance of 18.2 MΩ.cm at 25 °C and a TOC (Total organic carbon) value below 5 ppb obtained water is valid as desalted and is comparable to double-distilled water (ddH_2O).

2.1.1 Instruments

Table 2.1 Instruments used in this study

Device	Producer	Country
CO_2 incubator	Panasonic	Japan
CO_2 incubator (for virus infection)	WAKENBTECH	Japan
Fluorescence microscope IX81	Olympus	Japan
Culture Microscope CK40	Olympus	Japan
ABI StepOnePlusTM Real-Time PCR Systems	Applied Biosystems	USA
ABI Veriti 96 well Thermal Cycler	Applied Biosystems	USA
ABI 3100 Genetic Analyzer	Applied Biosystems	USA
Autoclave HG-50	HIRAYAMA	Japan
Digital electronic balance AT201	METTLER TOLEDO	Switzerland
High speed refrigerated micro centrifuge	KUBOTA	Japan
High speed refrigerated CR21E centrifuge	HITACHI	Japan
Centrifuge without cooling	KOKUSAN	Japan
Vortex mixer	Scientific industries	USA
Synergy 4 Hybrid Multi-Mode Microplate Reader	BioTek	USA
Centro LB 960 Microplate Luminometer	Berthold Technologies	USA
Sunrise Microplate reader	Tecan	Switzerland
Labo-shaker	Ever Seiko	Japan
Incubator shaker	TAITEC	Japan
Rotator	NIPPON THERMONICS	Japan
Double aluminum block bath	SCINICS	Japan
Agarose Gel chambers	ATTO	Japan
UV Transilluminators	TOYOBO	Japan
NanoVue Plus spectrophotometer	GE Healthcare	UK
Mini-PROTEAN Electrophoresis System	Bio-Rad	USA
Trans-Blot Semi-Dry Transfer Cell	NIHON EIDO	Japan
pH-Meter	Denver Instrument	USA
Freezer (4/-20/-80 ºC)	Panasonic	Japan
Clean bench	HITACHI	Japan
Water bath	TAITEC	Japan
LAS 4000 biomolecular imager	GE Healthcare	UK
Ovens (60/200 ºC)	EYELA	Japan

Pipettes (PIPETMAN P2, P20, P200, P1000)	Gilson	USA
Falcon Express Pipet-Aid	BD Biosciences	USA

2.1.2 Consumable items

Table 2.2 Consumable items used in this study

Consumable items	Producer	Country
1-200 µl, 100-1000 µl pipet tips	Corning	USA
Serological pipet (2 ml, 5 ml, 10 ml, 25 ml)	Corning	USA
Falcon tissue culture dishes (100 mm)	Corning	USA
Falcon tissue culture plates (6-, 12-, 24-, 96-well)	Corning	USA
Biocoat collagen I cellware 12-well plate	Corning	USA
1.5 ml and 2.0 ml microcentrifuge tubes	Corning	USA
15 ml and 50 ml centrifuge tubes	Corning	USA
0.2 mL 8 strip PCR tubes	NIPPON Genetics	Japan
96-well ultraAmp PCR plates	Sorenson BioScience	USA
qPCR adhesive seal	4titude	UK
96-well flat bottom white plates	Sterilin	UK
Nunc 96 well plates	Thermo Scientific	USA
0.1-10 µl pipet tips	Thermo Scientific	USA
0.2 µm Syringe Filter	Advantec	Japan
Hydrophobic immobilon-P polyvinylidene fluoride (PVDF) transfer membrane	Millipore	USA

2.1.3 Chemicals and reagents

Table 2.3 Chemicals and reagents used in this study

Chemicals and reagents	Producer	Country
Acrylamide	Wako	Japan
N,N'-Methylene-bis-acrylamide	Wako	Japan
Agarose	Wako	Japan
Ammonium persulfate (APS)	Wako	Japan
Bromophenol blue (BPB)	Wako	Japan
Sodium Fluoride (NaF)	Wako	Japan
Sodium orthovanadate (Na_3VO_4)	Wako	Japan
Magnesium acetate (MgOAc)	Wako	Japan
Ethylenediaminetetraacetic acid (EDTA)	Wako	Japan
Sodium dodecyl sulfate (SDS)	Wako	Japan
Sodium acetate (NaOAc)	Wako	Japan
Polyoxyethylene(10) octylphenyl ether (Triton X-100)	Wako	Japan
10w/v% Polyoxyethylene(20) (Tween-20)	Wako	Japan
0.25w/v% Trypsin	Wako	Japan
Dithiothreitol (DTT)	Wako	Japan
Phenylmethanesulfonyl fluoride (PMSF)	Wako	Japan
Leupeptin	Wako	Japan
Tetramethylethylenediamine (TEMED)	Wako	Japan

4% Paraformaldehyde (PFA)	Wako	Japan
Tris (hydroxymethyl) aminomethane (Tris)	Nacalai	Japan
Sodium chloride (NaCl)	Nacalai	Japan
Isopropanol	Nacalai	Japan
Ethanol (99.5%)	Nacalai	Japan
Methanol	Nacalai	Japan
Nonidet P-40 (NP-40)	Nacalai	Japan
Geneticin (G418)	Nacalai	Japan
Phenol:chloroform:isoamyl alcohol (25:24:1)	Sigma	USA
Ethidium bromide (EtBr)	Sigma	USA
Polyethyleneglycol 8000 (PEG 8000)	Sigma	USA
Bovine serum albumin (BSA)	Sigma	USA
Coomassie brilliant blue (CBB)	Sigma	USA
Chloroform	KANTO CHEMICAL	Japan
$NaHCO_3$	KANTO CHEMICAL	Japan
Bacto Agar	BD Biosciences	USA
Bacto Yeast Extract	BD Biosciences	USA
Bacto Tryptone	BD Biosciences	USA
L-Glutamine	Gibco	USA
Dulbecco's Modified Eagle's Medium (DMEM)	Nissui Pharmaceutical	Japan
DMEM/F-12+GlutaMax	Life Technologies	USA
4-(2-hydroxyethyl)-1-piperazineethanesulfonic acid (HEPES)	Life Technologies	USA
Fetal bovine serum (FBS)	Life Technologies	USA
Sf-900 II SFM	Life Technologies	USA
Opti-MEM I reduced-serum medium	Life Technologies	USA
Ribo m7G cap analog	Promega	USA
FuGENE HD transfection reagent	Promega	USA
FuGENE 6 transfection reagent	Promega	USA
Lipofectamine RNAiMAX Reagent	invitrogen	USA
Lipofectamine 2000 Reagent	Invitrogen	USA
RNaseOUT	Invitrogen	USA
Dynabeads M-280 Streptavidin	Invitrogen	USA
Protein G Sepharose 4 Fast Flow	GE Healthcare	UK
Glutathione Sepharose 4B	GE Healthcare	UK
Immunoreaction Enhancer Solution 1/2	TOYOBO	Japan
Tissue-Tek O.C.T compound	SAKURA	Japan
ISOGEN	NIPPON GENE	Japan
Bambanker Cell Freezing Media	LYMPHOTEC	Japan

2.1.4 Kits

Table 2.4 Kits used in this study

Kits	Producer	Country
GenElute HP Plasmid Miniprep Kit	Sigma	USA
PureLink HiPure Plasmid Maxiprep Kit	Invitrogen	USA

QIAamp DNA Blood Mini Kit	QIAGEN	Germany
Wizard SV Gel and PCR Clean-Up System	Promega	USA
ReverTra Ace qPCR RT kit	TOYOBO	Japan
DNase I (Amplification Grade)	Invitrogen	USA
SyBr premix Ex Taq (Tli RNaseH Plus)	TaKaRa	Japan
MEGAscript Kit T7	Ambion	USA
Label IT CX-Rhodamin/Biotin Labeling Kit	Mirus Bio	USA
SYBR Gold Nucleic Acid Gel Stain Kit	Invitrogen	USA
Bac-to-Bac baculovirus expression system	Invitrogen	USA
BCA Protein Assay Kit	Pierce	USA
Pierce Western Blotting Substrate Plus	Thermo Scientific	USA
BigDye Terminator v3.1 Cycle Sequencing Kit	Applied Biosystems	USA
BigDye Xterminator Purification Kit	Applied Biosystems	USA
Cell Counting Kit-8	Dojin	Japan
Human IL-29 Platinum ELISA Kit	eBiosciences	USA
Dual-Luciferase ReporterAssay system	Promega	USA

2.1.5 Enzymes and antibodies

Table 2.5 Enzymes and antibodies used in this study

Enzymes and antibodies	Producer	Country
Proteases K	Life Technologies	USA
Deoxyribonuclease I (DNase I)	Promega	USA
Ribonuclease A (RNase A)	Life Technologies	USA
Precision protease	GE Healthcare	UK
Restriction enzymes	TaKaRa	Japan
Anti-cGAS (HPA031700) antibody (rabbit polyclonal)	Sigma	USA
Anti-Flag (M2) antibody (mouse monoclonal)	Sigma	USA
Anti-beta-actin (AC-15) antibody (mouse monoclonal)	Sigma	USA
Anti-HA (Y-11) antibody (rabbit polyclonal)	Santa Cruz	USA
Anti-IFI16 (1G7) antibody (mouse monoclonal)	Santa Cruz	USA
Anti-IRF-3 (FL-425) antibody (rabbit polyclonal)	Santa Cruz	USA
Anti-RIG-I (1C3) antibody (mouse monoclonal)	KeraFAST	UK
Anti-RIG-I (D14G6) antibody (rabbit monoclonal)	Cell Signaling	USA
Anti-MDA5 (D74E4) antibody (rabbit monoclonal)	Cell Signaling	USA
Anti-phospho-Ser396 IRF-3 (4D4G) antibody (rabbit monoclonal)	Cell Signaling	USA
Anti-IL-29/IFN-lambda1 (AF1598) antibody (goat polyclonal)	R&D Systems	USA
Anti-m3G/m7G-cap (H-20) antibody (mouse monoclonal)	Millipore	USA
Anti-HA (3F10) antibody (rat monoclonal)	Roche	Switzerland
Anti-HBc antibody (rabbit polyclonal)	Dako	Danmark
Anti-human albumin (labeled with FITC) antibody (goat polyclonal)	Bethyl Laboratories	USA
Rabbit/Mouse/Goat control IgG antibody	Santa Cruz	USA
Anti-goat IgG HRP-conjugated secondary antibody	Santa Cruz	USA
Anti-rat/mouse/rabbit IgG HRP-conjugated secondary antibodies	GE Healthcare	UK
Alexa Fluor 488/594-conjugated secondary antibodies	Molecular Probes	USA

2.1.6 Solutions

Table 2.6 Solutions used in this study

Soultion	Component
Running buffer	25 mM Tris, 192 mM Glycine, 0.1% SDS.
Transfer buffer	25 mM Tris, 192 mM Glicine, 0.037% SDS, 20% methnol.
TBST buffer	20 mM Tris, 150 mM NaCl, 0.1% Tween-20, pH 7.4.
4x SDS sample buffer	40% Glycerol, 200 mM Tris pH 6.8, 8% SDS, 4% beta-mercaptoethanol, 0.08% bromophenol blue, 60 mM EDTA.
4x native PAGE sample buffer	25 mM Tris pH 6.8, 0.02% bromophenol blue, 60% glycerol.
1x Phosphate-buffered saline (PBS)	137 mM NaCl, 2.7 mM KCl, 10 mM Na_2HPO_4, 2 mM KH_2PO_4.
DMEM medium	DMEM with 10% FBS, 3.4 mM L-glutamine, 10% $NaHCO_3$.
PHH culture medium	DMEM with 10% FBS, 100 U/ml penicillin, 100 µg/ml streptomycin, 20 mM HEPES, 44 mM $NaHCO_3$, 15 µg/ml L-proline, 0.25 µg/ml insulin, 50 nM dexamethazone, 5 ng/ml epidermal growth factor (EGF), 0.1 mM Asc-2P, 2% dimethyl sulfoxide (DMSO).
HepG2-hNTCP-C4 culture medium	DMEM/F-12+GlutaMax with 10 mM HEPES, 200 U/ml penicillin, 200 µg/ml streptomycin, 10% FBS, 50 µM hydrocortisone , 5 µg/ml insulin, 400 µg/ml G418.
Sf9 culture medium	Sf-900 II SFM with 5% FBS, 25 µg/ml gentamycin.
Lysogeny broth (LB) medium	1.0% Tryptone, 0.5% Yeast Extract, 1.0% NaCl, pH 7.0.

2.1.7 Oligonucleotides

Table 2.7 Sequences of primers for qPCR in this study

Gene	Forward (5'→3')	Reverse (5'→3')
IFNL1	CGCCTTGGAAGAGTCACTCA	GAAGCCTCAGGTCCCAATTC
IFNA1	GCCTCGCCCTTTGCTTTACT	CTGTGGGTCTCAGGGAGATCA
IFNA4	ACCTGGTTCAACATGGAAATG	ACCAAGCTTCTTCACACTGCT
IFNB	ATGACCAACAAGTGTCTCCTCC	GCTCATGGAAAGAGCTGTAGTG
IFNG	ACTGACTTGAATGTCCAACGCA	ATCTGACTCCTTTTTCGCTTCC
IFNL2/3	AGTTCCGGGCCTGTATCCAG	GAGCCGGTACAGCCAATGGT
CXCL10	GTGGCATTCAAGGAGTACCTC	GCCTTCGATTCTGGATTCAGACA
OAS2	AACTGCTTCCGACAATCAAC	CCTCCTTCTCCCTCCAAAA
RSAD2	TTCACTCGCCAGTGCAACTAC	CGGTCTTGAAGAAATGGTCT
RIG-I	GATGCCCTAGACCATGCAGG	GCCATCATCCCCTTAGTAGAGC
IFI16	CCGTTCATGACCAGCATAGG	TCAGTCTTGGTTTCAACGTGGT
cGAS	GGGAGCCCTGCTGTAACACTTCTTAT	CCTTTGCATGCATGCTTGGGTACAAGGT
HBV-RNAs	GCACTTCGCTTCACCTCTGC	CTCAAGGTCGGTCGTTGACA
HBV pgRNA	TGTTCAAGCCTCCAAGCT	GGAAAGAAGTCAGAAGGCAA
HBV copy number *	CTTCATCCTGCTGCTATGCCT	AAAGCCCAGGATGATGGGAT
pcDNA3.1 transcripts	AGAGAACCCACTGCTTACT	TACCAAGCTTAAGTTTAAA
GAPDH	CATGAGAAGTATGACAACAGCCT	AGTCCTTCCACGATACCAAAGT

* This primer is used for detection of HBV encapsidated DNA.

Table 2.8 Sequences of primers for plasmids construction

Name	Forward (5'→3')	Reverse (5'→3')
HBV 3.5K	AAAGGTACCAACTTTTTCACCTCTGCCTA	GGGCTCGAGTTTATAAGGGTCAATGTCCAT
HBV 2.4K	AAAGGTACCATCATTTTGCGGGTCACCATA	GGGCTCGAGTTTATAAGGGTCAATGTCCAT
HBV 2.1K	AAAGGTACCGACAGTCATCCTCAGGCCATG	GGGCTCGAGTTTATAAGGGTCAATGTCCAT
HBV 0.7K	AAAGGTACCCCTTTGTGGCTCCTCTGCCG	GGGCTCGAGTTTATAAGGGTCAATGTCCAT
HBV△5	AAAGGTACCTTGACCCTTATAAAGAATTTG	GGGCTCGAGTTTATAAGGGTCAATGTCCAT
HBV△3	AAAGGTACCAACTTTTTCACCTCTGCCTA	GGGCTCGAGTTTATAAGAGATGATTAGGCAG AGGT
HBV-P	GGGCTCGAGATGCCCCTATCTTATCAACAC	AAAGCGGCCGCTCACGGTGGTCTCCATGCA
GFP	AAAGGTACCATGGTGAGCAAGGGCGAG	TTCTCGAGCTTGTACAGCTCGTCCAT
STM	CATGTCCCACTGTTCAAGCCTCCAAG	GTACAGGGTGACAAGTTCGGAGGTTC
pLKO.1	CCCACTAGTTTTCCCATGATTCCTTCATATTT	CCCAGATCTAAAATTGTGGATGAATACTGCC

Table 2.9 DNA oligonucleotides for εRNA and 3pRNA

Name	Sequence (5'→3')	Description
p-εRNA	**Sense:** CCGGTGTACATGTCCCACTGTTCAAGCCTCCAAGCTGTGCCTTGG GTGGCTTTGGGGCATGGACATTTTTG **Antisense:** AATTCAAAAATGTCCATGCCCCAAAGCCACCCAAGGCACAGCTTG GAGGCTTGAACAGTGGGACATGTACA	For vector construction
3pRNA	**Sense:** TAATACGACTCACTATAGGGAAACTAAAAGGGAGAAGTGAAAGTG **Antisense:** CACTTTCACTTCTCCCTTTTAGTTTCCCTATAGTGAGTCGTATTA	For *in vitro* transcription
εRNA	**Sense:** TAATACGACTCACTATAGTGTACATGTCCCACTGTTCAAGCCTCCA **Antisense:** XXTGTCCATGCCCCAAAGCCACCCAAGGCACAGCTTGGAGGCTTG	For *in vitro* transcription
Control RNA	**Sense:** TAATACGACTCACTATAGTTCGCAGTCCCCAACCTCCAATCACTCA **Antisense:** YXAACCAGGACAAATTGGAGGACAGGAGGTTGGTGAGTGATTGGA	For *in vitro* transcription

"X" denotes the 2'-O-methyl-modified UTP (2-O-Me U), "Y" denotes 2'-O-methyl-modified ATP (2-O-Me A).

Table 2.10 siRNA sequence of target genes in this study

Target gene	Target sequence (5'→3')
DDX58 (RIG-I)	GUUGGAGGAGUAUAGAUUA
IFI16	UGCUGAACGCAACAGAAUCAU
MB21D1 (cGAS)	GCUGUAACACUUCUUAUUA
TRIM25	CCAUAGACCUCAAAAACGA
MAVS	CCACCUUGAUGCCUGUGAA
TBK1	GCGGCAGAGUUAGGUGAAA
IRF-3	CCUUCAUUGUAGAUCUGAU

TICAM1 (TRIF)	GCCAUAGACCACUCAGCUU
MYD88	CUGGAACAGACAAACUAUC
HBV-RNAs	GCACUUCGCUUCACCUCUGCA
HBV-pgRNA	GAUCAGGCAACUAUUGUGG

2.1.8 Plasmids

(1) pUC19-HBV plasmids (genotype Ae, Bj, and C) contain 1.24-fold HBV genome are provided by Dr. Y. Tanaka (Department of Virology and Liver Unit, Nagoya City University Graduate School of Medical Sciences, Nagoya, Japan), as described previously [156,157].

(2) pIRM-3HA-RIG-I, pCXN2-Flag-RIG-I and pCAGGS-YFP-RIG-I wild type (WT) plasmids were constructed by inserting the full length of human RIG-I open reading frame (ORF) into the *Xho*I and *Not*I sites of pIRM-3HA, pCXN2-Flag and pCAGGS-YFP vectors (kindly provided by Dr. A. Miyawaki, Laboratory for Cell Function Dynamics, Brain Science Institute, RIKEN, Saitama, Japan), and deletion mutants of RIG-I (N-, C-, Helicase-, RD-domain) were generated by inserting the truncated RIG-I ORFs into pIRM-3HA and pCXN2-Flag vectors, as previously reported [158]. PCR-based site-directed mutagenesis was carried out to produce several RIG-I mutants, including T55I, K270A and K888E.

(3) pIRM-3HA-HBV-Polymerase (HA-P) and pCAGGS-YFP-HBV-Polymerase (YFP-P) expression vector was generated by cloning full length of HBV-polymerase ORF into the *Xho*I and *Not*I sites of pIRM-3HA and pCAGGS-YFP vectors using the primers as shown in Table 2.8.

(4) pcDNA3.1(+)-HBV-RNAs, including 3.5-, 2.4-, 2.1-, 0.7-kb, Δ5, Δ3 and stem-loop mutaion (STM), and pcDNA3.1(+)-GFP were constructed by inserting the respective cDNAs, which amplified with the primers given in Table 2.8, into pcDNA3.1(+) vector. The sequence of ε structure from nt 1851 to 1876 of HBV pgRNA was complementarily changed to disrupt the ε structure by PCR-based site-directed mutagenesis using pcDNA3.1(+)-HBV-3.5kb as template and the primer described in Table 2.8, thus generate 5'STM, 3'STM and 5'&3'STM plasmids.

(5) IFN-λ1-luciferase reporter (IFN-λ1-Luc) was generated by inserting the promoter region of human IFNL1 gene (-1106 to +10) into pGL4.18 vector (Promega).

P-55C1B-Luc plasmid, which is a luciferase activity of an IRF-driven reporter plasmid, was provided by Dr. T. Fujita (Laboratory of Molecular Genetics, Institute for Virus Research, Kyoto University, Kyoto, Japan). The pRL-TK renilla luciferase reporter plasmid which provided as an internal control was purchased from Toyo INK company.

(6) pCpGfree-U6-HBV-εRNA (p-εRNA) plasmid was used to express HBV εRNA under the U6 promoter, to construct p-εRNA, the oligo nucleotides shown in Table 2.9 are annealed and inserted into an *Age*I-*Eco*RI doubly digested pLKO.1-puro (Sigma) vector. The U6 promoter and εRNA-coding fragment is amplified through PCR with the pLKO.1-εRNA expression vector by a pair of pLKO.1 primers as shown in Table 2.8, the PCR product is digested with *Spe*I and *Bgl*II and inserted into pCpGfree-mcs vector (Invivogen).

(7) pFAST-Bac-GST-RIG-I WT and mutants (RD-WT, RD-K888E) plasmids were generated by cloning the cDNA of RIG-I WT and mutants into pFAST-Bac-GST vector, which was derived from inserting a Glutathione S-transferase (GST) tag into pFAST-Bac vector (Invitrogen). The generated plasmids were used for expression of GST-tagged RIG-I WT and its mutant proteins.

2.1.9 Mice

Human hepatocyte-chimeric mice (purchasable from PhoenixBio Co., Ltd., Hiroshima, Japan) were generated by transplantation commercially available cryopreserved human hepatocytes (a 2-year-old Hispanic female; BD Bioscience) into uPA$^{+/+}$/SCID mice as described previously [159].

2.1.10 Cells

HepG2, HEK293T and Vero cells were purchased from ATCC. Immortalized human hepatocytes, HuS-E/2 cells were kindly provided by Dr. M. Hijikata and Dr. K. Shimotohno (Laboratory of Human Tumor Viruses, Institute for Virus Research, Kyoto University, Kyoto, Japan). Huh-7.5.1/Rep-Feo-1b HCV replicon cells were kindly provided by Dr. N. Sakamoto (Department of Gastroenterology and Hepatology, Hokkaido University Graduate School of Medicine, Sapporo, Japan). PHH prepared from human hepatocyte-chimeric mice were purchased from Phoenix Bio Co., Ltd. (Japan) and cultured as described previously [159]. HepG2-hNTCP-C4 cells were kindly provived by Dr. K. Watashi and Dr. T.Wakita (Department of Virology II, National

Institute of Infectious Diseases, Tokyo, Japan), Huh-7.5 and Huh-7 cells were kindly provided by Dr. C. M. Rice (Laboratory of Virology and Infectious Disease, The Rockefeller University, New York, USA). All cells were cultured at 37 °C in a 5% CO_2-incubator. HepG2, HEK293T, Vero, Huh-7, Huh-7.5, and Huh-7.5.1/Rep-Feo-1b HCV replicon cells were cultured in DMEM medium, HepG2-hNTCP-C4 cells ware cultures in HepG2-hNTCP-C4 culture medium, PHH were cultured in PHH culture medium as shown in Table 2.6.

Sf9 for recombinant protein expression was purchased from Invitrogen (USA) and cultured at 28 ºC in Sf9 culture medium shown in Table 2.6. *E.coli* DH5α and GT115 competent cells were purchased from TaKaRa (Japan) and Invivogen (USA), respectively, and growth in LB medium as shown in table Table 2.6.

2.1.11 Virus

HBV for infection were generated as described previously [156], Briefly, $1x10^6$ cells/10-cm dish of Huh-7 cells were transfected 10 μg HBV plasmid (pUC19-HBV-C) by FuGENE 6 transfection reagent following the manufacturer's protocol, after 24 hours transfection, medium was changed. At 3 days after transfection, medium was harvested and cleared by centrifugation for 5 min (minutes) at 5,000 rpm at 4 °C. The supernatant contain HBV was stocked at -80 °C. 100 μl supernatant, which was taken for detection the HBV DNA copies, was mixed with 1 μl MgOAc (600 mM), 0.5 μl RNase A (20 mg/ml), 1 μl DNase I (1 unit/μl) and incubated for 3 hous at 37 °C to remove the HBV plasmid. The reaction was terminated by adding 2 μl EDTA (0.5 M, pH 8.0) and incubation for 10 min at 65 °C. Then the HBV DNA was extracted using QIAamp DNA Blood Mini Kit following the manufacturer's protocol, and HBV DNA copies were determined by qPCR using the primers as shown in Table 2.7. In order to rule out contaminations of the inocula during virus production, 50 μM Lamivudine (LAM, Sigma) was added in Huh-7 culture media during HBV production.

Vesicular stomatitis virus (VSV, Indiana strain) and Newcastle disease virus (NDV, LaSota) were kindly provided by Dr. A. Takada (Division of Global Epidemiology, Research Center for Zoonosis Control, Hokkaido University, Sapporo, Japan) and Dr. H. Kida (Laboratory of Microbiology, Department of Disease Control, Graduate School of Veterinary Medicine, Hokkaido University Sapporo, Japan), respectively.

All virus were stocked at -80 °C until use for infection.

2.2 Methods

2.2.1 Preparation of nucleic acids

(1) *In vitro* transcribed RNAs: Control RNA, εRNA and 3pRNA (5'-triphosphorylated RNA) oligo nucleotides shown in Table 2.9 which containing T7 promoter sequence were annealed and used as templates (300 ng template in 20 μl reaction mixture) for *in vitro* transcription under the control of the T7 promoter with MEGAscript kit following the manufacturer's protocol, the transcribed RNAs were purified by Isogen reagent. To generate capped-εRNA and control RNA, 7.5 mM of Ribo m7G cap analog instead of the GTP was added in the reaction mixture. In order to avoid the non-templated nucleotide addition to the 3'-terminus of transcribed RNAs, the oligonucleotide was modified with 2-O-Me (2'-O-methyl) at the first two nucleotides of the 5'-terminus of antisense strand [160]. All of the *in vitro* transcribed RNAs were separated by urea denaturing gel electrophoresis to check the integrity, and gel shift analysis with anti-m7G cap antibody to confirm the 5'-capping efficiency of RNAs. 3pRNA was used for stimulation at a concentration of 1.0 μg/ml, while εRNA and control RNA were used for stimulation at a concentration of 1.6 μg/ml.

(2) Nucleic acid purification from HBV transfected cells: After 48 hours transfection of pUC19 control empty plasmid or HBV genome-containing plasmid (pUC19-HBV-Ae) into Huh-7 cells, the cellular nucleic acids were extracted by phenol:chloroform:isoamyl alcohol (25:24:1) extraction and ethanol precipitation, and then subjected to treatment with RNase A (333 μg/ml) or DNase I (100 U/ml) for 37 °C for 1 hour. Enzyme-treated DNAs or RNAs were precipitated with isopropanol before transfection and 2 μg/mL of nucleic acid wad used for stimulation.

(3) Plasmid extraction: All of the plasmids used in this study were firstly purified by GenElute HP Plasmid Miniprep Kit for small-scale extraction following the manufacturer's protocol, and after the sequences were confirmed by sequencing using the BigDye Terminator v3.1 sequencing kit, large-scale extraction were performed by using PureLink HiPure Plasmid Maxiprep Kit according the manufacturer's protocol. All of plasmids were dissolved in TE (tris-EDTA) buffer and stored at -20 °C until use.

(4) Encapsidated HBV DNA extraction: Encapsidated HBV DNA was purified from intracellular core particles as described previously [161,162]. Briefly, cells were transfected with HBV plasmid or infected with HBV, after 72 hours, cells were

suspended in lysis buffer containing 50 mM Tris-HCl (pH 7.4), 1 mM EDTA and 1% NP-40. Pellet nuclei and insoluble fractions were removed by centrifugation at 4 ˚C and 15,000 rpm for 5 min. The supernatant was adjusted to 6 mM MgOAc and treated with DNase I (200 μg/ml) and of RNase A (100 μg/ml) for 6 hours at 37 ˚C. The reaction was stopped by addition of 10 mM EDTA and the mixture was incubated for 15 min at 65 ˚C. After treatment with proteinase K (200 μg/ml), 1% SDS and 100 mM NaCl for 2 hour at 55 ˚C, viral nucleic acids were isolated by phenol:chloroform:isoamyl alcohol (25:24:1) extraction and precipitated with 1 volume isopropanol, 1/10 volume of NaOAc (3 M, pH 5.2) and 20 μg glycogen as carrier. The viral nucleic acids were final dissolved in 200 μl ddH_2O and analyzed by qPCR.

(5) RNA extraction from cells, liver tissues or RNA immunoprecipitated samples: Isogen reagent was used for RNA isolation and then subjected to RT-qPCR analysis. Briefly, 0.5 ml of ISOGEN reagent was added to cells, homogenized liver tissues or RNA immunoprecipitated samples and mixed, and 0.1 ml of chloroform was added to the mixture, which was then vortexed and centrifuged at 15,000 rpm for 15 min at 4 °C. RNA was precipitated from the aqueous phase by addition of 0.25 ml of isopropanol, and the RNA was collected by centrifugation at 15,000 rpm for 10 min at 4°C. The RNA pellet was washed with 70% ethanol and dissolved in ddH_2O. The RNA concentration was detected by NanoVue Plus spectrophotometer.

2.2.2 RT-qPCR/qPCR

1 μg of RNA was treated with 1 μl DNase I (1 U/μl, Amplification Grade) at 25 °C for 15 min in a 10 μl reaction volume, and the reaction was stopped by addition of 1 μl EDTA (25 mM) and the mixture was incubated for 10 min at 65 ˚C. DNase treated RNA sample was used for reverse transcription (RT) by ReverTra Ace qPCR RT kit, 7 μl of RNA was mixed with 2 μl RT Buffer, 0.5 μl Enzyme mix and 0.5 μl primer mix (random primer plus oligo(dT) primer), and the traction was incubated for 15 min at 37 ˚C, and then 98 ˚C for 5 min to stop reaction. The reverse transcribed cDNA sample was added 40 μl ddH_2O and stocked at -20 ˚C or performed real-time qPCR analysis immediately. The cDNA samples from reverse transcription or HBV DNA samples extracted from encapsidated HBV virons were quantified by using SyBr Premix Ex Taq reagent and StepOnePlus real-time PCR system. For cDNA sample analysis, a 20 μl mixture including 6.8 μl ddH_2O, 10 μl SyBr Premix Ex Taq reagent, 0.4 μl ROX

reference dye (50×), 0.4 μl forward primer (10 μM), 0.4 μl reverse primer (10 μM) and 2 μl cDNA sample was placed in the StepOnePlus real-time PCR system and started the reaction as the following program: 95 °C, 10 sec; 50 cycles of (95 °C, 5 sec; 60 °C, 30 sec), and collected data at 60 °C step. Melting (dissociation) curve was included at the terminal of reaction to monitor whether there were single and specific products during the reaction. Data analysis was performed by the instrument's software and data were normalized to the expression of GAPDH or HBV RNAs for each sample. For HBV DNA quantification, 5 μl DNA sample was used to instead of 2 μl cDNA sample, and a 10-fold serial diluted HBV DNA sample, which ranged from 0.2 x 10^3 to 10^9 copies/μl (1 μg pUC19-HBV plasmid contains 1.46 × 10^{11} DNA copies) was used as standard sample for absolute quantification.

2.2.3 Preparation of protein

(1) Protein extraction from cells: Whole cell lysate used for SDS-PAGE (polyacrylamide gel electrophoresis) analysis was prepared by lysising cell in lysis buffer (0.5%SDS/1×PBS), for detection of phosphorylation state of target protein, 10 mM NaF and 1 mM Na_3VO_4 were added in the lysis buffer. The cell lysate was further disrupted by sonic disintegration and then heat at 100 °C for 10 min. The protein concentration was measured by using BCA Protein Assay Kit.

(2) Recombinant protein extraction and purification from Sf9 cells: GST-tagged RIG-I WT and its mutant proteins were expressed in Sf9 cells according to the manufacturer's instructions for Bac-to-Bac baculovirus expression system. Briefly, pFAST-Bac-GST-RIG-I WT or its mutants vectors were transformed into DH10Bac *E.coli* cells, and the recombinant bacmid DNA was isolated and transfected into Sf9 cells, after 3 days transfection, the produced recombinant baculovirus particles were collected for second time infection of Sf9 cells. After 3 days infection, the Sf9 cells were harvested by centrifugation (3,000 rpm for 10 min at 4°C), resuspended in lysis buffer (1% Triton X-100, 50 mM Tris, 150 mM NaCl, 1 mM EDTA, and 1 mM PMSF [pH 8.0]), and lysed by sonication. The lysate was incubated on ice for 30 min and then centrifuged at 12,000 rpm for 10 min at 4 °C, the supernatant was incubated with Glutathione Sepharose 4B beads for 2 hours at 4 °C, then the beads were washed 3 times with wash buffer (0.1% Triton X-100, 50 mM Tris, 300 mM NaCl, 1 mM EDTA [pH 8.0]) and wash one time with cleavege buffer (50 mM Tris, 150 mM NaCl, 1 mM

EDTA, 1 mM DTT [pH 7.5]), the GST tags were cleaved from recombinant GST protein by using Precision protease in cleavege buffer overnight at 4 °C. The concentration of cleaved recombinant RIG-I WT and mutants proteins were measured by using BCA Protein Assay Kit, and the purity of recombinant proteins were higer than 95% as judged by CBB staining.

2.2.4 SDS-PAGE and Western-blotting

Protein samples were mixed with 4x SDS sample buffer (As shown in Table 2.6) and boiled for 10 min at 100°C. The indicated amount of protein was applied to a SDS-PAGE gel. As a standard for protein size, a pre-stained protein marker was added. After proteins were separated by electrophoresis, then transferred with transfer buffer (As shown in Table 2.6) from the SDS-PAGE gel onto a methanol-activated PVDF membrane using a semi-dry transfer cell. The amperage was calculated with the following formula: 2.4 mA/cm^2 of the gel for 70 min transfer. After protein transfer the membrane was blocked in blocking solution (5% w/v skim milk in TBST buffer. As for the detection of phosphorylation state of target protein, 2% BSA in TBST buffer with 1 mM Na_3VO_4 was used for blocking) for 1 hour at RT (room temperature) and probed over night at 4°C with the indicated antibody (As shown in Table 2.5) in Immunoreaction Enhancer Solution 1. After 3 times wash with TBST 10 min each, the respective secondary HRP-conjugated antibody (1:5000) was added in Immunoreaction Enhancer Solution 2 and incubated for 1 hour at RT. Membranes were again washed 3 times, 15 min each with TBST buffer. The detection was performed with the Pierce Western Blotting Substrate Plus detection kit by using LAS 4000 biomolecular imager system.

2.2.5 siRNA mediated gene knock down

To knock down the indicated target genes, HBV-derived RNAs or pgRNA, chemically synthesized 21-nucleotide siRNAs as well as control siRNA (siPerfect Negative Control) were obtained from Sigma (sequence information are shown in Table 2.10). Cells were transfected with 10 nM siRNA by using Lipofectamine RNAiMAX transfection reagent following the manufacturer's protocol and then used for the subsequent analyses.

2.2.6 Plasmid and RNA transfection *in vitro*

Lipofectamine 2000, FuGENE 6 and FuGENE HD transfection reagents were used

for plasmid and RNA transfection according to their manufacturer's protocol. Plasmids transfer into HepG2, Huh-7, Huh-7.5 and HuS-E/2 cells was mediated by FuGENE HD, while Lipofectamine 2000 reagent was used for plasmid transfer into HEK293T cells or RNA transfection for cell stimulation.

2.2.7 ELISA (enzyme-linked immunosorbent assay)

The levels of IFN-λ1 protein in culture supernatants were measured by using the Human IL-29 Platinum ELISA kit following the manufacturer's protocol. This ELISA is for the detection of human IFN-λ1 with a minimum detection limit of 31.2 pg/ml. There is no cross reactivity or interference detected according to the product specification of the vendor.

2.2.8 Luciferase assay

Huh-7 or HepG2 cells were transiently co-transfected with 100 ng of IFN-λ1-Luc or p-55C1B-Luc (C1B-Luc) and 10 ng of pRL-TK renilla luciferase reporter plasmid as an internal control, and then stimulated with nucleic acids prepared as above (Methods 2.2.1). At 24 hours after stimulation, luciferase activities were measured with the Dual-Luciferase Reporter Assay system according to the manufacturer's instructions by using Centro LB 960 Microplate Luminometer.

For detection of HCV replication, Huh-7.5.1/Rep-Feo-1b cells were transfected with Control or εRNA expression vector. At 48 hours after transfection, cell numbers were measured by using Cell Counting Kit-8, and subsequently lysed with 100 μl of Passive lysis buffer. Firefly luciferase activities were measured using the Dual-Luciferase Reporter Assay system and normalized to cell numbers.

2.2.9 RNA immunoprecipitation assay

HEK293T or HepG2 cells were lysed with buffer A (20 mM HEPES, 150 mM NaCl, 1 mM EDTA, 1% NP-40, 1 mM PMSF, 1 mM DTT, 1 μg/ml leupeptin, 100 U/ml RNaseOUT [pH 7.3]) and 20 μl of the supernatant was saved as input for qRT-PCRanalysis. Primary antibody including anti-Flag, anti-HA, anti-RIG-I (1C3), anti-IFI16, anti-MDA5 antibody or control IgG was added to cell lysates. After 2 hours incubation with the antibody as indicated for immunoprecipitation at 4 °C with gentle rotation, protein G sepharose beads were added and further incubated for 1 hour with gentle rotation. Beads were washed 3 times with wash buffer (20 mM HEPES, 150 mM NaCl, 1 mM EDTA, 0.5% NP-40 [pH 7.3]). The precipitated RNAs were eluted with

Isogen and analyzed by qRT-PCR with appropriate primers to detect the target RNA. The amount of immunoprecipitated RNAs is represented as the percentile of the amount of input RNA (%input). The result for the quantification of the co-immunoprecipitated pgRNA was normalized to the band intensities of the immunoprecipitated proteins.

2.2.10 HBV infection

PHH were seeded on biocoat collagen I cellware 12-well plate with PHH culture medium as 1×10^5 cells/well. HepG2-hNTCP-C4 cells were seeded on 12-well tissue culture plate as 1×10^5 cells/well.

After 24 hours, PHH or HepG2-hNTCP-C4 cells were incubated for 24 hours at 37 °C with HBV stock aliquots containing the appropriate number of genome equivalents (Geq) (PHH or HepG2-hNTCP-C4 cells was performed at 10 or 100 Geq per cell, respectively.), which are diluted with 1 ml of culture medium supplemented with 4% PEG 8000. At the end of the incubation, cells are washed three times with culture medium, and harvested for analysis.

Chimeric mice were intravenously infected with HBV-C (10^6 copies per mouse). Three weeks after HBV infection, the infection efficiency was confirmed by measuring the number of viral genome copies in the sera of HBV-infected chimeric mice by qPCR analysis.

2.2.11 εRNA treatment *in vivo*

p-εRNA plasmid or empty pCpGfree plasmid was loaded in a liposome carrier which based on the procedure that was previously described [163]: p-εRNA or empty pCpGfree-mcs vector is formulated into lipid nanoparticles (MEND). 80 μg of p-εRNA or empty vector (in H_2O) was dissolved with 120 μl of citrate buffer (12.5 mM citrate, 500 mM NaCl). Addition of this solution to 480 μl of the tertiary butanol containing YSK lipid (2,100 nmol), cholesterol (900 nmol), and 1, 2-dimyristoyl-sn-glycerol, methoxypolyethyleneglycol (150 nmol) leaded to spontaneous formulation of liposomal particles (εRNA-MEND or control-MEND). The prepared εRNA-MEND and control-MEND were stocked at 4 °C until use. At 4-week postinfection of HBV, chimeric mice were treated with εRNA-MEND or control-MEND by intravenously injection at a dose of 0.5 mg/kg of body weight (n=3 per group) every two days for 14 days. Serum and liver samples were subjected to qPCR for the quantification of HBV DNA copy numbers or other analyses.

2.2.12 Gel shift assay

For the detection of εRNA–RIG-I complex formation, the indicated amounts of purified RIG-I RD or RD K888E protein were incubated at 37 ˚C for 15 min with 10 pmol of the capped εRNA (see Preparation of nucleic acids) in the reaction buffer (20 mM Tris-HCl, 1.5 mM $MgCl_2$, 1.5 mM DTT [pH 8.0]). After incubation, 4x native PAGE sample buffer (25 mM Tris-HCl, 0.02% bromophenol blue, 60% glycerol [pH 6.8]) was added. The mixture was then subjected to electrophoresis on a 1.2% agarose gel. The gel was stained with SYBR Gold Nucleic Acid Gel Stain Kit and visualized using a UV illuminator.

For confirmation of the 5'-capping efficiency of RNAs from *in vitro* transcription, gel electrophoresis of εRNA or control RNA following incubation with anti-m7G cap antibody or control IgG was performed, 0.3 pmol of ppp- or capped-eRNA and control RNA were incubated with 4 μg of anti-m7G antibody or IgG control at 4 ˚C overnight, the complexes were separated by 5% native polyacrylamide gel and stained with SYBR Gold, the bands were visualized using a UV illuminator.

2.2.13 FRET (fluorescence resonance energy transfer) analysis

Rhodamine (ROX)-labeled εRNA or control RNA was prepared using Label IT CX-Rhodamine Labeling Kit according to the manufacturer's instructions. Huh-7.5 cells transfected with the YFP-tagged RIG-I or HBV polymerase protein expression vector were stimulated with ROX-labeled εRNA or control RNA (0.5 μg/ml) for 4 hours and then FRET analysis was performed with IX81 fluorescence microscope as described previously [74]. Following filters in this study were used: BP490-500HQ (Olympus) and FF01-542/27-25 (Semrock) excitation and emission filters for the YFP images; BP535-555HQ and BA570-625HQ (Olympus) for ROX; and BP490-500HQ and BA590 for FRET. As a dichroic mirror, a DM505HQ glass reflector (Olympus) was used. Corrected FRET ($FRET^C$) was calculated with the following equation: $FRET^C = FRET - 0.1076 \times YFP - 0.0082 \times ROX$, where FRET, YFP and ROX indicate fluorescence intensity acquired for the FRET, YFP and ROX channels, respectively, with background fluorescence intensity subtracted. FRET efficiency was calculated as a quotient of background-subtracted FRET and YFP images and was presented in an intensity-modified display mode with MetaMorph software. In the intensity-modified display mode shown here, eight colors from red to blue are used to represent the

emission ratio, with the intensity of each color.

2.2.14 RNA pull down

In vitro transcribed RNAs described above were labeled with biotin using Label IT Biotin Labeling Kit. HEK293T or HepG2 cells were lysed with lysis buffer (20 mM HEPES, 150 mM NaCl, 1 mM EDTA, 1% NP-40, 1 mM PMSF, 1 mM DTT, 1 μg/ml leupeptin [pH 7.3]). Biotin-labeled RNA (1 μg) was incubated with lysates (2 mg) for 1 hour with gentle shaking. Subsequently, Dynabeads M-280 Streptavidin were added and incubated for 1 hour with gentle shaking. Beads were washed three times with wash buffer (20 mM HEPES, 150 mM NaCl, 1 mM EDTA, 0.5% NP-40 [pH 7.3]). The pull-down complexes were eluted with sample buffer and analyzed by immunoblotting with the indicated antibodies.

2.2.15 Immunofluorescence study

Freshly prepared liver tissues in OCT compound were cut at 5-6 μm by cryostat, mounted on glass slides air-dried, and fixed in acetone-methanol (1:1) at -20 ˚C for 10 min. Sections were blocked with Antibody Diluent (Dako), incubated with rabbit anti-HBc at 37 ˚C for 1 hour, washed in PBS, and then incubated with goat anti-rabbit IgG conjugated with Alexa Fluor 594 and goat anti-human albumin labeled with FITC. Sections were washed with PBS and observed in a fluorescence microscope.

2.2.16 Plaque reduction assay

Conditioned media were prepared from HepG2 cells transfected with Control or HBV-C plasmid vector for 72 hours. And then, Vero cells pretreated with the conditioned media for 24 hours were infected with VSV (Indiana serotype) at 100 pfu per well for 1 hour in serum-free DMEM. Cells were subsequently overlaid with DMEM containing 2.4% methyl cellulose and incubated for 48 hours. The number of plaques was then counted. The inhibition of VSV replication was calculated as followed; %inhibition = [(plaque number of uninfected HepG2 culture media – plaque number of infected HepG2 culture media) / plaque number of uninfected HepG2 culture media] x100. For neutralization of IFN-λ1, anti-Human IL-29/IFN-lambda 1 antibody was used at the concentration of 1.0 μg/ml.

3. Results

3.1 IFNs induction in human hepatocytes during HBV infection

The induction of IFNs was known to be the hallmark of innate responses for virus infection, to investigate the innate immune activation during HBV infection, I first examined type I and type III IFN responses in human hepatocytes and human hepatocytes-chimeric mice upon HBV plasmid transfection and HBV infection.

3.1.1 Induction of IFNs by HBV plasmid transfection in human hepatocytes

Two human hepatoma cell lines, HepG2 and Huh-7, and also immortalized human primary hepatocytes-HuS-E/2 cell were used for detection IFNs induction upon HBV plasmid transfection. As shown in Figure 3.1, after transfection with plasmids carrying 1.24-fold the HBV genome of three major different genotypes (genotype Ae, Bj or C) into cells, the expression levels of HBV RNAs were detectable by using a pair of primers which was able to amplify all 4 different length HBV mRNAs, and the peak of HBV RNAs expression levels was 48 hours after HBV plasmid transfection. However, the induction of type I IFNs, IFN-α4 (*IFNA4*) and IFN-β (*IFNB1*) in response to HBV plasmid transfection at least during seven days after transfection in HepG2 cells and three days in Huh-7 and HuS-E/2 cells was hardly observed, despite the IFN-α4 (*IFNA4*) was slightly elevated (about 4 times compared with the mock group) at 48 hours after HBV genotype Bj and C transfection in HuS-E/2 cells. This result was consistent with the previous report [110], which also shown that there were no type I IFNs induction after HBV infection. On the other hand, type III IFN, IFN-λ1 (*IFNL1*), was induced in all of the three types of human hepatocyte cell lines with a peak at 48 hours after transfection, indicating that type III IFN is predominantly induced in hepatocytes after HBV plasmid transfection.

In addition, the IFN-λ1 protein levels in HepG2 cells after HBV plasmid transfetion 48 and 72 hours were also measured by enzyme-linked immunosorbent assay (ELISA) (Figure 3.2A), HBV-C transfection was shown the highest protein induction, which was consistent with the mRNA induction. Although the IFN-λ1 protein levels were weak, the HBV replication was increased after blocking the IFN-λ1 activity by using neutralizing antibody (NAb) (Figure 3.2B), and the increased viral replication was strongly abolished by treatment with nucleoside analogue-lamivudine

(LAM), an HBV inhibitor. Moreover, Vero cells exposed to HBV-tranfected HepG2 culture supernatant could inhibit Vesicular stomatitis virus (VSV) replication in plaque reduction assay (Figure 3.2C), and this inhibiting activity was also dependent on the IFN-λ1 protein in the culture supernatant because blocking the IFN-λ1 activity by using anti-IFN-λ1 NAb reduced this inhibiting activity. These results indicate that the induced IFN-λ1 after HBV plasmid transfection exhibits potent physiological antiviral activities.

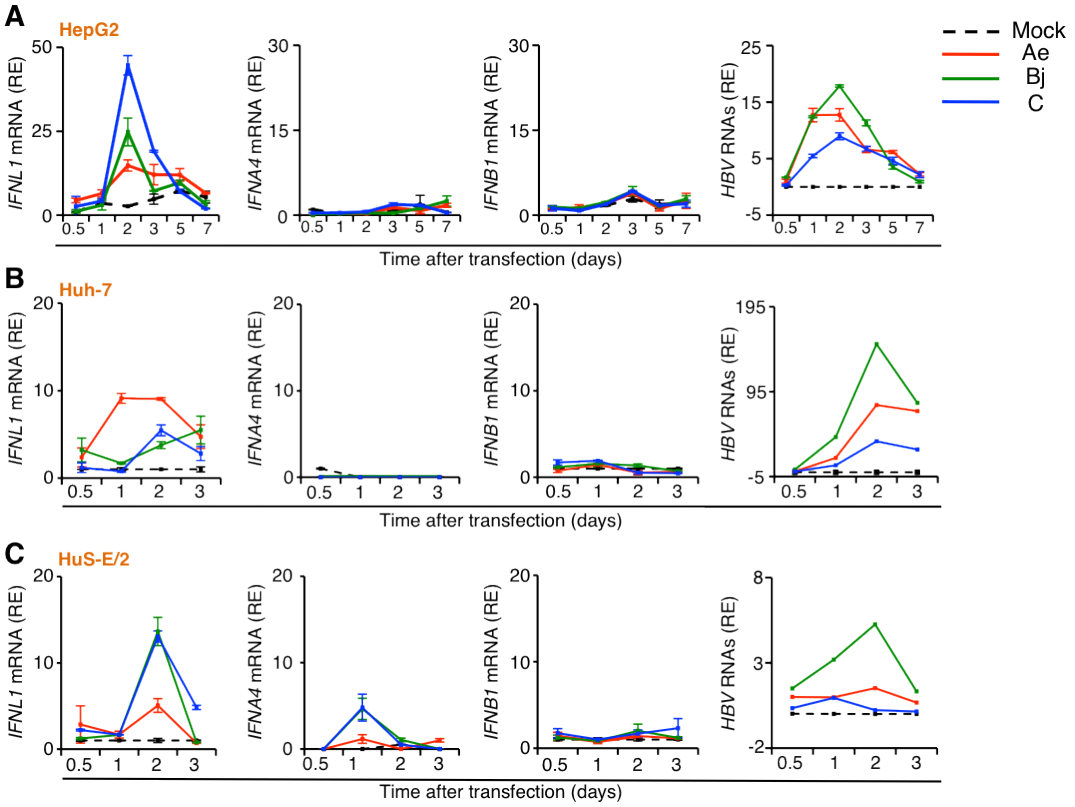

Figure 3.1 Expression of IFNs and HBV-RNAs upon HBV plasmid transfection. qRT-PCR analysis of *IFNL1*, *IFNA4, IFNB1* and *HBV*-RNAs RNA expression levels at the indicated times after transfection with 1.24-fold the HBV genome (genotype Ae, Bj or C) or empty vector (Mock) in HepG2 (A), Huh-7 (B) and HuS-E/2 (C) cells. RE, relative expression. Except for the data of *HBV*-RNAs expression in Huh-7 and HuS-E/2 cells, all data are presented as mean and SD (*n* = 3) and are representative of three independent experiments.

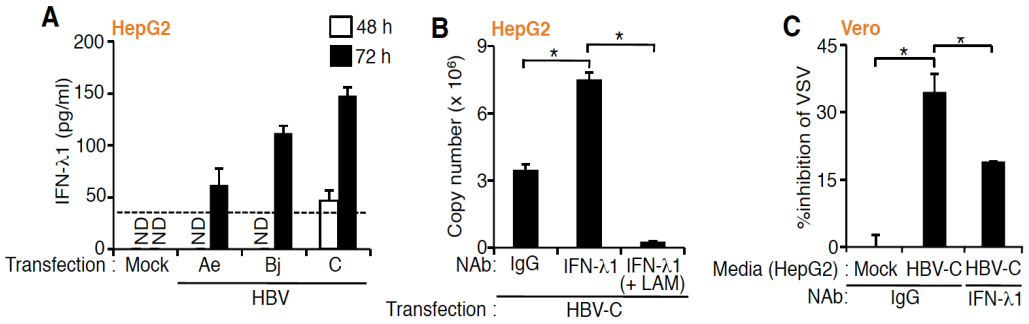

Figure 3.2 Antiviral activity of HBV-induced IFN-λ1. (A) ELISA of IFN-λ1 at 48 or 72 hours after transfection with the HBV genome in HepG2 cells. The dot line indicates the minimum detectable amount (31.2 pg/ml) of IFN-λ1 by the ELISA kit. ND, not detected, indicates below the minimum detectable amount. (B) qPCR analysis of copy numbers of encapsidated HBV DNA in control IgG or anti-IFN-λ1 neutralizing antibody (NAb) or anti-IFN-λ1 NAb plus Lamivudine (LAM)-treated HepG2 after 4 days of transfection with HBV-C genome. (C) Plaque reduction assay analysis of the inhibition of VSV replication by pretreatment Vero cells 24 hours with conditioned medium from HepG2 cells which transfected with HBV-C or empty vector (Mock) 3 days with or without anti-IFN-λ1 NAb. The inhibition of VSV replication was calculated as %inhibition. *$P < 0.05$, Student's *t*-test. Data are presented as mean and SD ($n = 3$) and are representative of three independent experiments.

3.1.2 Induction of IFNs by HBV infection in human hepatocytes

Although HBV plasmid transfection into above human hepatocytes could mimic the viral gene expression and DNA replication, those cell lines were not susceptible to HBV infection. Thus, primary human hepatocytes (PHH) and HepG2-hNTCP-C4 cell lines that were susceptible to HBV infection were used in the next study. Consistent with the HBV plasmid transfection results, the significant induction of not only IFN-λ1 (*IFNL1*) but also IFN-λ2/3 (IFNL2/3) in PHH at 24 hours after infection with HBV-C was observed, genotype Ae and Bj infection also induced a weak type III IFNs expression. However, neither of type I IFN (IFN-α1 and IFN-β) mRNAs (*IFNA1* and *IFNB1*) nor type II IFN (IFN-γ) mRNA (*IFNG*) tested was induced, even the successful establishment of HBV infection was assayed by determining HBV pgRNA (Figure 3.3A). Although it is difficult to simply compare the amount of IFN induced by different types of virus, the induction of IFN-λ1, λ2/3 mRNAs (*IFNL1*, *IFNL2/3*) in

response to HBV infection was much weaker than that of Newcastle disease virus (NDV) infection (Figure 3.3A). In this regard, in order to rule out the possibility that the IFN-λ response is due to contaminants in the inocula, one of HBV inhibitor-LAM was added during virus preparation. Treatment with LAM inhibited IFN-λ mRNA (*IFNL1*, *IFNL2/3*) induction in response to HBV infection in PHH, suggesting that the IFN response is actually induced by HBV infection (Figure 3.3A). Furthermore, in HepG2-hNTCP-C4 cell line, which stably expressing a functional receptor-human NTCP for HBV, also confirmed that IFN-λ1 (*IFNL1*) but not IFN-β (*IFNB1*) were induced in these cells after infection with HBV-C (Figure 3.3B). These results indicate that HBV infection predominantly induces type III IFNs expression.

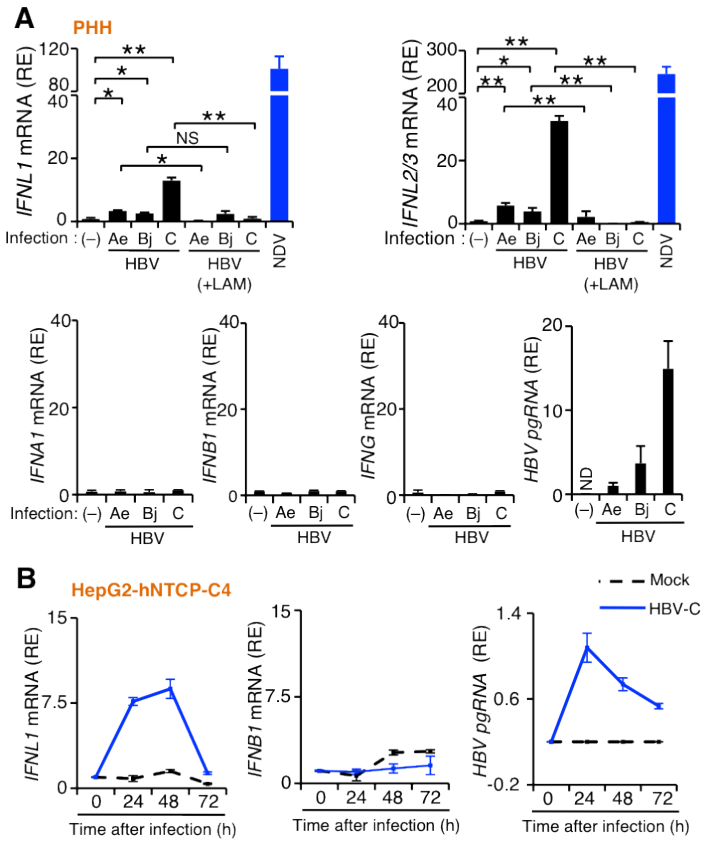

Figure 3.3 Expression of IFNs and HBV pgRNA upon HBV infection in PHH and HepG2-hNTCP-C4 cells. (A) qRT-PCR analysis of *IFNL1*, *IFNL2/3*, *IFNA1, IFNB1, IFNG mRNA* and HBV *pgRNA* at 24 hours after infection with HBV, NDV (multiplicity of infection=10, blue bar) or mock (–), or media-treated Lamivudine (LAM) as control in primary human hepatocytes (PHH). (B) Time course analyses by qRT-PCR of *IFNL1, IFNB1* mRNA and HBV *pgRNA* at the indicated times after HBV infection in HepG2-hNTCP-C4 cells. **P* < 0.05, ***P* < 0.01, Student's *t*-test. NS,

not significant. ND, not detected. RE, relative expression. Data are presented as mean and SD (n = 3) and are representative of three independent experiments.

3.1.3 Induction of IFNs by HBV infection in human hepatocytes-chimeric mice

To next assess the innate immune responses *in vivo* during HBV infection, I exploited human-hepatocytes chimeric mice, which generated by transplantation human hepatocytes into severe combined immunodeficiency mice that carry the urokinase-type plasminogen activator transgene controlled by an albumin promoter (uPA$^{+/+}$/SCID mice). After the chimeric mice were intravenously infected with HBV-C, which was derived from patient with chronic hepatitis, the expression of type III IFNs mRNAs increased in the liver tissue, whereas type I IFNs (IFN-α4 and IFN-β) mRNAs (*IFNA4* and *IFNB1*) were compared with uninfected mice, even a successful infection was assessed by measuring the HBV pgRNA (Figure 3.4). In parallel with this type III IFNs (*IFNL1*, *IFNL2/3*) response, the significant induction of IFN-stimulated genes (ISGs), such as *CXCL10*, *OAS2,* and *RSAD2*, in the human liver of these infected mice was also observed (Figure 3.4).

Taken together, all of these findings indicate that a moderate type III but not type I or type II IFNs is predominantly induced in human hepatocytes in response to HBV infection, and this induced type III IFNs are shown to have potent physiological antiviral activities.

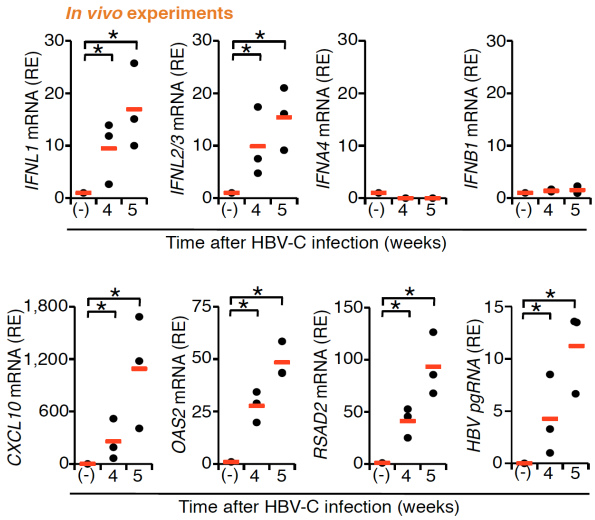

Figure 3.4 Expression of IFNs, ISGs and HBV pgRNA after HBV infection in human

hepatocytes-chimeric mice. qRT-PCR analysis of *IFNL1*, *IFNL2/3*, *IFNA4, IFNB1, CXCL10, OAS2, RSAD2* mRNA and HBV *pgRNA* of liver tissues at 4 or 5 weeks after infection with HBV-C in human hepatocytes-chimeric mice. (–), uninfected mice. Red lines represent the mean of each dataset. *$P < 0.05$, Student's *t*-test. RE, relative expression.

3.2 Innate immune sensor(s) for the induction of IFN-λ1 during HBV infection

It is well known that the pattern recognition receptors (PRRs) play a crucial role in innate immune responses and recognize invading viruses mainly by sensing viral nucleic acid and trigger key immune responses for viral elimination. Thus, I next determined which nucleic acid sensor-mediated signaling pathway is responsible for the HBV-induced type III IFN response.

3.2.1 Role of RIG-I in IFN-λ1 induction

As HBV is a DNA virus, I assessed the contribution of previously reported cytosolic DNA sensors including RIG-I, IFI16 and cGAS in human hepatocytes. Knockdown analyses revealed that IFN-λ1 (*IFNL1*) induction in HepG2 or Huh-7 cells by plasmid transfection for HBV-C or HBV-Ae, respectively, was suppressed by the knockdown of RIG-I but not that of the other sensors (Figures 3.5A and 3.5B), and a sufficient knockdown was confirmed by immunoblotting (HepG2 cells) or qRT-PCR (Huh-7 cells). To further confirm the involvement of RIG-I in HBV-triggered type III IFN response, Huh-7.5 cells that derived from Huh-7 hepatoma cells but carry a dominant-negative mutant RIG-I allele that prevents RIG-I signaling were used [164]. Compared with Huh-7 cells that have an intact RIG-I pathway, Huh-7.5 cells failed to induce IFN-λ1 mRNA (*IFNL1*) expression in response to HBV-Ae genome plasmid transfection, as in the case of stimulation with 5'-triphosphate RNA (3pRNA), a defined RIG-I ligand (Figure 3.5C). In addition, I confirmed that the knockdown of RIG-I but not IFI16 and cGAS abolished IFN-λ1 (*IFNL1*) induction in PHH infected with HBV-C (Figure 3.5D). Furthermore, by knockdown assay, I also observed that the induction of IFN-λ1 and OAS2 mRNA (*IFNL1* and *OAS2*) in HepG2-hNTCP-C4 cells in response to HBV-C infection was dependent on RIG-I (Figure 3.5E). These data indicate that IFN-λ1 gene induction during HBV infection depends on RIG-I.

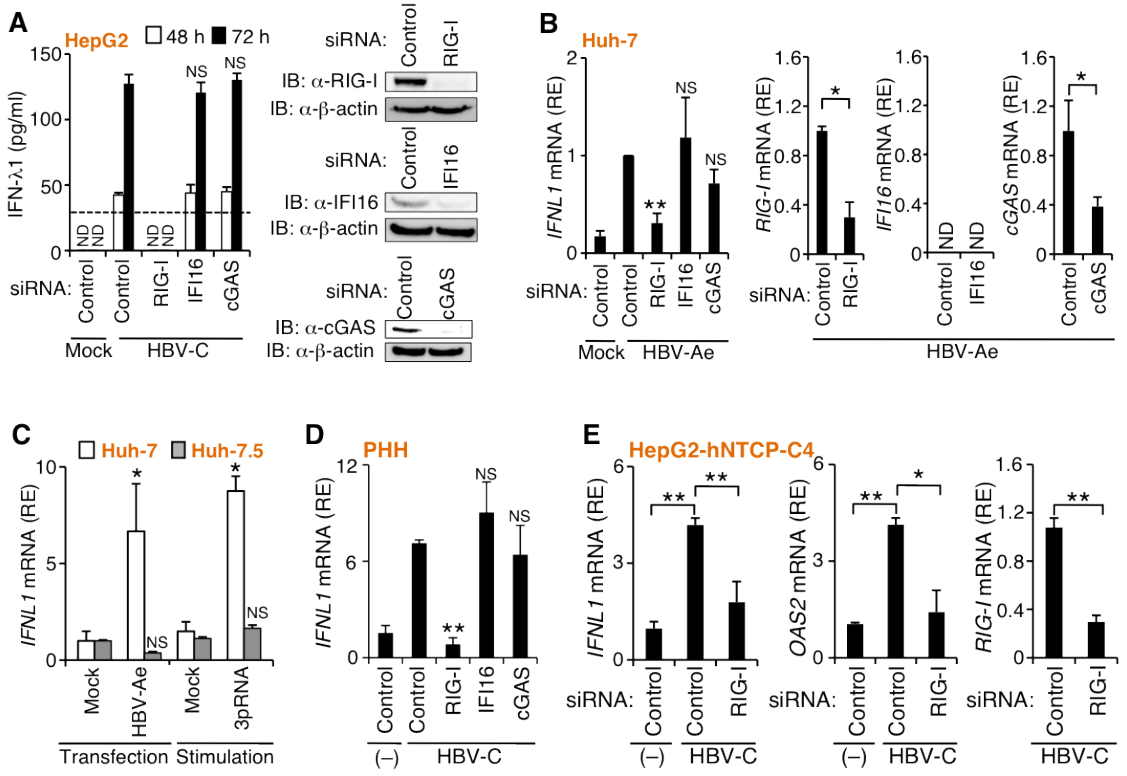

Figure 3.5 RIG-I-dependent IFN-λ induction in response to HBV infection. HepG2 cells (A) and Huh-7 cells (B) treated with control siRNA (Control) or siRNA targeting RIG-I, IFI16 or cGAS were transfected with the HBV-C (HepG2 cells) and HBV-Ae (Huh-7 cells) genome for 24 hours (Huh-7 cells) or 48 and 72 hours (HepG2 cells). The induction of IFN-λ1 was measured by ELISA (A) or qRT-PCR (B). The dot line indicates the minimum cytokine expression detected (31.2 pg/ml) of IFN-λ1 by the ELISA kit. ND, not detected, indicates below detectable concentrations. Knockdown efficiency was analyzed by immunoblotting (A) or qRT-PCR (B). (C) qRT-PCR analysis of *IFNL1* mRNA in Huh-7 or Huh-7.5 cells transfected with the HBV-Ae genome (at 24 hours after transfection) or stimulated with 3pRNA (1 μg/ml) for 6 hours. PHH **(D)** or HepG2-hNTCP-C4 cells (E) treated with control siRNA or the indicated siRNAs were infected with the HBV-C for 24 hours. Total RNAs were subjected to qRT-PCR analysis for *IFNL1*, *OAS2* and *RIG-I* mRNA. Data are presented as mean and SD (n = 3) and are representative of three independent experiments. *P < 0.05 and **P < 0.01, Student's t-test. RE, relative expression. ND, not detected. NS, not significant.

3.2.2 Role of RIG-I signaling molecules in IFN-λ1 induction

It is known that upon PRRs recognition, the CARD domains of RIG-I

subsequently undergo K63-linked polyubiquitylation by the E3 ubiquitin ligase TRIM25 (tripartite motif containing 25), which facilitates the interaction of RIG-I with the mitochondrial adaptor MAVS. The interaction of RIG-I and MAVS promotes activation of MAVS and triggers IFNs expression by TBK1-IRF-3 signaling pathway (see Introduction 1.2.1). Thus, I assessed the contribution of RIG-I signaling molecules on IFN-λ1 induction upon HBV infection.

Knockdown of RIG-I signaling molecules including TRIM25, MAVS, TBK1 and IRF-3, resulted in the suppression of IFN-λ1 mRNA (*IFNL1*) induction in HepG2 cells after transfection with the HBV-C genome. On the other hand, knockdown of TRIF or MYD88, which are not involved in RIG-I signaling pathway, did not observe the suppression of IFN-λ1 mRNA (*IFNL1*) induction (Figure 3.6A). In addition, I also confirmed that the knockdown of MAVS abolished IFN-λ1 (*IFNL1*) induction in PHH infected with different HBV genotypes (Figure 3.6B).

These data indicate that IFN-λ1 gene induction during HBV infection depends largely on RIG-I signaling pathway.

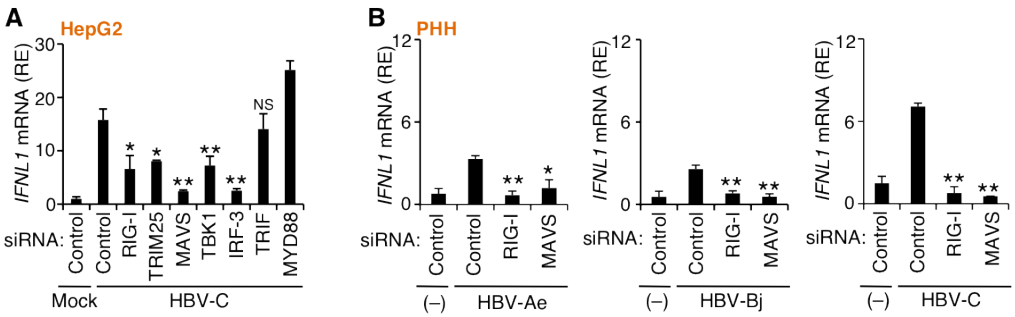

Figure 3.6 RIG-I signaling pathway in HBV induced IFN-λ1 expression. HepG2 cells (A) or PHH (B) treated with control siRNA or the indicated siRNAs were transfected with empty vector (Mock) or HBV-C genome for 48 hours (HepG2 cells) or infection with different HBV genotypes or uninfection (–) for 24 hours (PHH). Total RNAs were subjected to qRT-PCR analysis for *IFNL1*. Data are presented as mean and SD (n = 3) and are representative of three independent experiments. *P < 0.05 and **P < 0.01, Student's t-test. RE, relative expression. NS, not significant.

3.3 Ligand(s) for the induction of IFN-λ1 during HBV infection

After virus infection, the viral PAMPs are detected by host PRRs and trigger the

induction of IFNs. As the above results indicate that HBV-induced type III IFNs expression depends on RIG-I signaling pathway, and also it is known that RIG-I recognizes not only virus-derived RNA but also DNA in the cytoplasm [56,58]. To further clarify how RIG-I recognizes HBV, I next determined the ligand(s) of HBV that are responsible for the induction of type III IFNs.

3.3.1 HBV-derived RNAs and IFN-λ1 induction

To examine either or both of which nucleic acid (DNA and RNA) derived from HBV-infected cells can activate IFN-λ1 gene expression, nucleic acid from Huh-7 cells that transfected with empty vector or HBV-Ae for 48 hours were extracted, same amount of nucleic acid was treated with RNase A or DNase I, or no any treatment as control, and purified them before transfection into Huh-7 cells. Luciferase reporter assay demonstrated that pretreatment with RNase A but not DNase I reduced the *IFNL1* promoter activation, suggesting that virus-devired RNAs may be ligands for RIG-I activation and induce the IFN-λ1 expression (Figure 3.7A). In addition, knockdown of HBV RNAs by an siRNA that target all four types of HBV RNA transcripts (3.5-, 2.4-, 2.1- and 0.7-kb transcripts) sufficiently reduced the expression of HBV RNAs, and also suppressed IFN-λ1 (*IFNL1*) induction in Huh-7 cells transfected with HBV-Ae (Figure 3.7B). These results indicate that HBV-devired RNAs may be candidates of the RIG-I ligands and trigger IFN-λ1 induction during HBV infection.

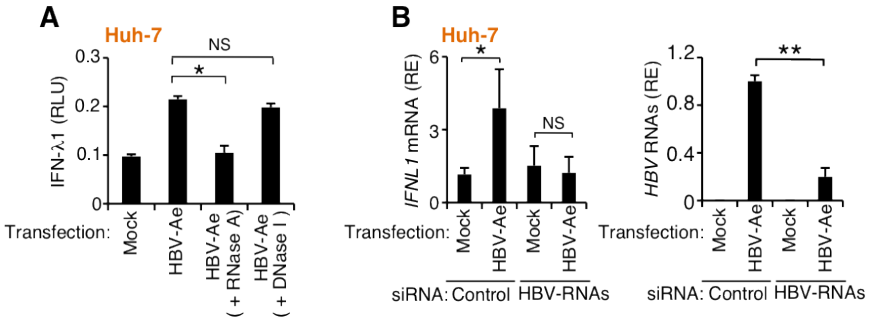

Figure 3.7 HBV-derived RNAs are ligand for RIG-I activation and trigger IFN-λ1 induction. (A) Luciferase activity of an IFN-λ1 reporter plasmid after 24 hours of stimulation with nucleic acids (2 μg/ml) extracted from Huh-7 cells transfected with control plasmid (Mock) or the HBV-Ae genome with or without RNase A or DNase I treatment. RLU, relative luciferase units. (B) Huh-7 cells treated with control or HBV RNA-targeted siRNA were transfected with the HBV-Ae

genome or mock. After 24 hours of transfection, total RNAs were subjected to qRT-PCR for *IFNL1*. Data are presented as mean and SD (n = 3) and are representative of three independent experiments. *P < 0.05 and **P < 0.01, Student's t-test. RE, relative expression. NS, not significant.

As four different lengths of HBV transcripts are generated during the life cycle of HBV in hepatocytes. Next, to determine which of these HBV RNA transcripts is/are involved in the RIG-I-mediated IFN-λ1 induction, several expression vectors (pcDNA-HBV-3.5K, 2.4K, 2.1K, and 0.7K) to express each of these four viral transcripts were transfected in HEK293T cells that are often used to analyze RIG-I signaling pathway in human cells. As shown in Figure 3.8A, the longest 3.5-kb transcript, that is, pgRNA, but not the three shorter HBV RNA transcripts has the potential to elicit a significant induction of IFN-λ1 mRNA (*IFNL1*). As a control, GFP construct (pcDNA-GFP) that express a GFP transcript did not induce any IFN-λ1 (*IFNL1*) response, even a much higher GFP RNA expression than HBV pgRNA (Figure 3.8B). These results suggest that HBV-derived pgRNA are required for activation of RIG-I pathway to induce IFN-λ1 expression. Furthermore, the knockdown assay by using a pgRNA-targeted siRNA also indicated that suppression of HBV pgRNA expression reduced the IFN-λ1 (*IFNL1*) induction in HepG2 cells transfected with HBV-Ae (Figure 3.8C).

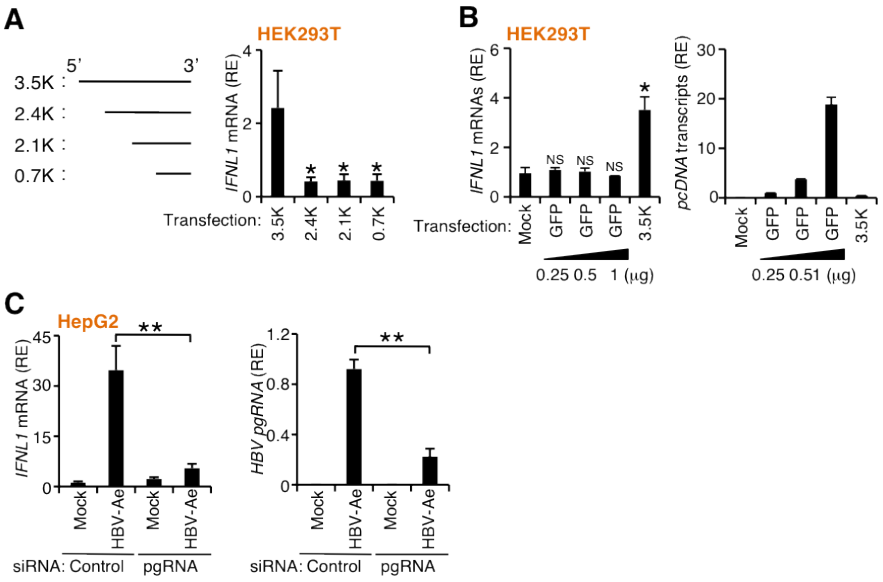

Figure 3.8 pgRNA of HBV is ligand for RIG-I activation and IFN-λ1 induction. (A) A

schematic representation of four types of HBV RNAs: pgRNA (3.5-kb), 2.4-kb, 2.1-kb and 0.7-kb RNAs. qRT-PCR analysis of *IFNL1* mRNA of HEK293T cells after 24 hours of transfection with the indicated HBV expression vectors. Data were normalized to the amount of each HBV RNA expression. (B) qRT-PCR analysis of the expression level of IFN-λ1 mRNA and vector derived RNAs in HEK293T cells at 24 hours after transfection with the indicated expression vectors. (C) HepG2 cells treated with control or pgRNA-targeted siRNA were transfected with the HBV-Ae genome or mock. After 48 hours of transfection, total RNAs were subjected to qRT-PCR for *IFNL1* and HBV *pgRNA*. Data are presented as mean and SD (*n* = 3) and are representative of three independent experiments. *P < 0.05 and **P < 0.01, Student's t-test. RE, relative expression. NS, not significant.

3.3.2 The 5'-ε region of HBV pgRNA and IFN-λ1 induction

All of four types of HBV RNAs are transcribed at different start site but share a common single polyadenylation signal, thus the longest 3.5-kb pgRNA have a special 5'-1.1-kb region compare with other three shorter HBV transcripts. The above results indicated that this 5'-1.1-kb region of HBV pgRNA is critical for the activation of RIG-I pathway to induce IFN-λ1 expression. In addition, as the pgRNA is longer than full-length HBV genomic DNA and contains terminally redundant sequences, thus the 5'-1.1-kb region of HBV pgRNA contains a overlapping sequence (90 nt, Figure 3.9A, blue line) that is same as the 3'-end of all HBV transcripts. Artificially deletion of this 90 nt overlapping sequence at the 5'-region (Δ5) or 3'-region (Δ3) of HBV pgRNA showed that Δ3 mutant pgRNA and wild type full-length pgRNA induced a comparable mRNA expression of IFN-λ1 (*IFNL1*), whereas such response was not observed for Δ5 mutant pgRNA (Figure 3.9A). These data suggest that the 5'-overlapping sequence of HBV pgRNA is important for RIG-I-mediated IFN-λ1 induction.

As the 5'-end of HBV pgRNA is known to contain the encapsidation sequence, called "epsilon (ε)", which takes a stem-loop secondary structure [165], and also the short double-stranded RNA is one type of ligand for RIG-I [57]. Therefore, this 5'-ε structure may confer a possible pathogen-associated molecular pattern (PAMP) motif for RIG-I recognition. To test this hypothesis, several stem-loop mutant (STM) forms of HBV pgRNA by disrupting the stem-loop structure were generated. Due to the overlapping sequence of 5'- and 3'-ends of HBV pgRNA as mentioned above, this ε element is

found at both ends of pgRNA. Thus, I generated the vector expressing pgRNA that disrupting the stem-loop structure of 5'- or 3'-ε region or both (5STM, 3STM or 5&3STM, respectively). In concordance with the results shown in Figures 3.9A, IFN-λ1 mRNA (*IFNL1*) induction was detected upon expression of the 3STM transcript that has an intact 5'-ε region, as similar to that of intact 3.5-kb pgRNA. In contrast, either 5STM or 5&3STM did not show significant response (Figure 3.9B). To further confirm the contribution of this stem-loop structure in IFN-λ1 induction, the capped ε region-derived RNA (hereafter called εRNA) by *in vitro* transcription was generated, and used for stimulation in HEK293T and HepG2 cells. Consequently, IFN-λ1 mRNA (*IFNL1*) was significantly induced by this εRNA stimulation in a RIG-I dependent manner, while such response was not detected upon stimulation with the equivalent length of RNA that is derived from HBV pgRNA but does not contain any ε element (Control RNA) (Figures 3.9C and 3.9D). I also confirmed RIG-I-dependent IRF activation by detecting the phosphorylation status of IRF-3 (Figure 3.9E) and IRF-driven luciferase activity (Figure 3.9F) in response to stimulation with this εRNA. These findings indicate that the 5'-ε region of HBV pgRNA is critical for IFN-λ1 induction through the recognition by RIG-I.

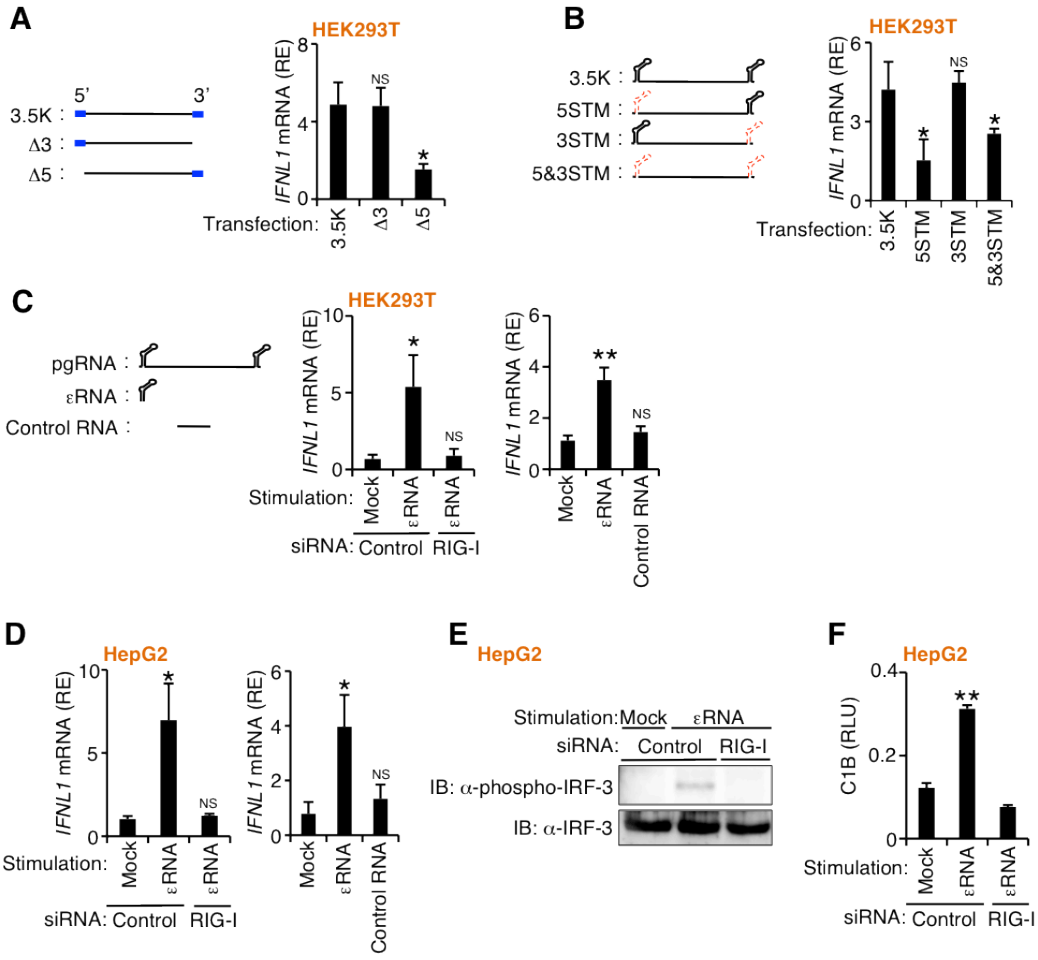

Figure 3.9 The 5'-ε region of HBV pgRNA is ligand for RIG-I activation and IFN-λ1 induction. (A, B) A schematic representation of HBV pgRNA (3.5-kb) and two deleted forms of pgRNA, Δ3 and Δ5 (A left), and three stem-loop mutated forms of pgRNA, 5STM, 3STM and 5&3STM (B left). The overlapping region is shown in blue, and red dotted line represents the mutated stem-loop. qRT-PCR analysis of *IFNL1* mRNA of HEK293T cells at 24 hours after transfection with the indicated expression vectors. Data were normalized to the amount of each HBV RNA expression. (C-E) A schematic representation of pgRNA, εRNA and Control RNA (C left). HEK293T cells (C) or HepG2 cells (D and E) untreated (C right and D right) or treated with control or RIG-I siRNA (C middle, D left and E) were unstimulated (Mock) or stimulated with εRNA or Control RNA for 12 hours. Total RNAs were subjected to qRT-PCR for *IFNL1* (C and D), while total proteins were subjected to immunoblotting with anti-phospho-IRF-3 antibody and anti-IRF-3 antibody (E). (F) Luciferase activity of an IRF-reporter plasmid (p-55C1B-Luc) after 24 hours of stimulation with εRNA in HepG2 cells treated with control or RIG-I siRNA. Data are presented as mean and SD (*n* = 3) and are representative of three independent experiments. *P

< 0.05 and **P < 0.01, Student's t-test. RE, relative expression. NS, not significant.

3.4 Role of RIG-I in antiviral response to HBV infection

As the 5'-ε region of HBV pgRNA is critical for initiation of encapsidation and HBV polymerase binding for reverse transcription [165], the 5'-ε region is an important element for HBV replication in HBV life cycle. And the above results indicate that the 5'-ε region of HBV pgRNA is also critical for IFN-λ1 induction possibly through the recognition by RIG-I. Therefore, the RIG-I may affect the HBV replication via an IFN-independent manner that directly counteract the interaction of HBV polymerase with the 5'-ε region of HBV pgRNA.

3.4.1 Interaction of RIG-I and 5'-ε region of HBV pgRNA

I first assessed the interaction of RIG-I and HBV pgRNA by using RNA-binding protein immunoprecipitation (RIP) assay. As shown in Figure 3.10A, endogenous RIG-I but not other nucleic acid sensors, such as IFI16 and MDA5 was shown to interact with HBV pgRNA in HepG2 cells. In order to further determine which region of RIG-I mediates its interaction with HBV pgRNA, several Flag-tagged wild type (WT) and deletion mutants of RIG-I were transfected into HEK293T cells together with HBV pgRNA expression vector, and RIP assay showed that the C-terminal portion of RIG-I (C-RIG) including its helicase domain (Helicase) and repressor domain (RD) except for N-terminal two CARDs domain (N-RIG) can bind to HBV pgRNA (Figure 3.10B). Moreover, a point mutation (K888E) of C-RIG that abolishes its RNA-binding activity [166] was used for further analysis of the interaction of RIG-I and HBV pgRNA. Result showed that HBV pgRNA was co-immunoprecipitated with the wild type C-RIG but not the K888E mutant, like HCV RNA that was previously reported to interact with RIG-I [167] (Figure 3.10C). To further determine which region of HBV pgRNA interacts with RIG-I, full-length of HBV pgRNA and two deletion mutants of pgRNA-Δ5 and Δ3 pgRNA expression vectors were transfected into HEK293T cells together with HA-tagged RIG-I vector. RIP assay results showed that not only full-length of HBV pgRNA but also Δ5 pgRNA as well as Δ3 pgRNA were detected in the RIG-I-immunoprecipitated complex (Figure 3.10D), which is seemingly inconsistent with the results by the functional assay (Figures 3.8A, 3.9A and 3.9B) that only 5'-ε region is critical for RIG-I-mediated IFN-λ1 induction, one explanation is that the ε

region is required for its interaction with RIG-I, but only the 5'-ε region is necessary to activate RIG-I pathway.

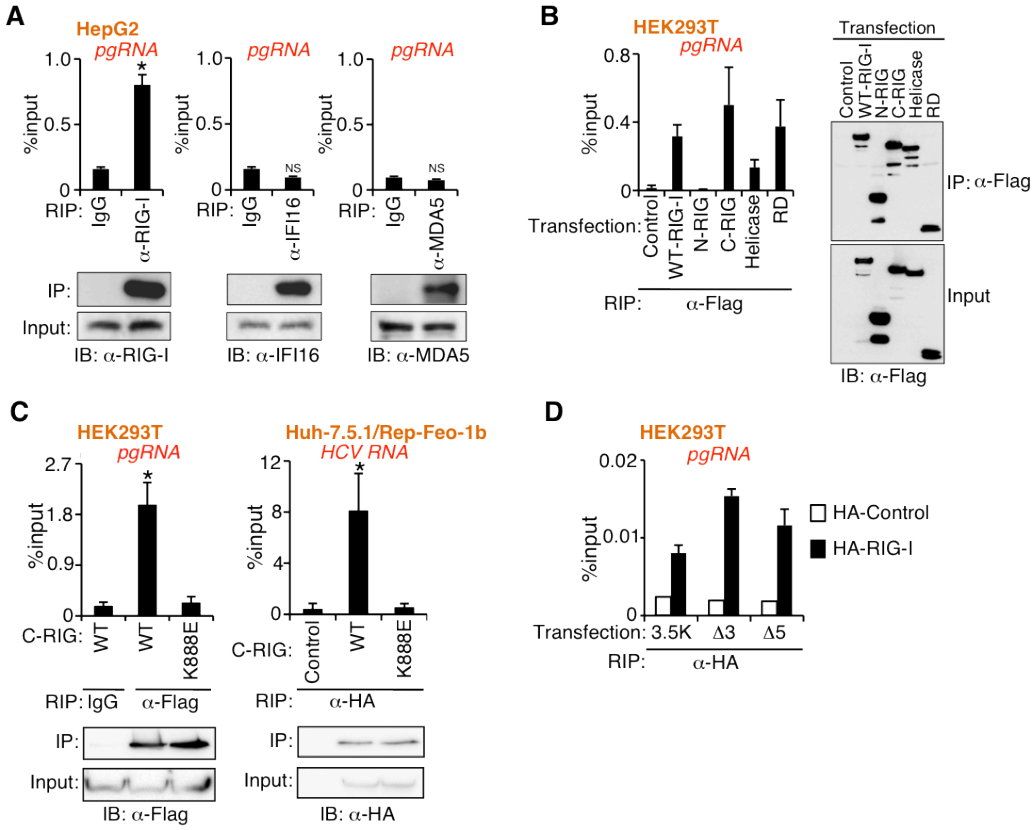

Figure 3.10 Interaction of pgRNA and RIG-I. RIP assay analysis of the interaction of endogenous nucleic acid sensors-RIG-I, IFI16 and MDA5 (A) or tagged wild type (WT) and mutants of RIG-I (B, C and D) with HBV pgRNA (A, B, C left and D) or HCV RNA (C right). The immunoprecipitated pgRNA or HCV RNA by using indicated antibodies was measured by qRT-PCR and is represented as fraction of input RNA prior to immunoprecipitation (%input). Whole cell expression and immunoprecipitated amounts of proteins are detected by immunoblotting with indicated antibodies. Data are presented as mean and SD (n = 3) and are representative of three independent experiments. *P < 0.05, Student's t-test.

Next, to further determine the interaction of RIG-I with the ε region of HBV pgRNA, biotin-labeled εRNA or Control RNA prepared by *in vitro* transcripton was incubated with the HEK293T cell lysate that transfected Flag-tagged RIG-I, and RNA pull-down assay showed that RIG-I was co-precipitated with εRNA but not with Control RNA (Figure 3.11A, top). Similarly, endogenous RIG-I in HepG2 cells also

interacted with εRNA albeit weakly comparing with the defined RIG-I ligand-3pRNA (Figure 3.11A, bottom). I also demonstrated the intracellular co-localization of RIG-I with εRNA in Huh-7.5 cells by FRET (Fluorescence resonance energy transfer) analysis (Figure 3.11B). RNA pull-down assay with several deletion mutants of RIG-I also showed that the C-RIG including its helicase and RD domain but not N-RIG bound to εRNA (Figure 3.11C), which is consistent with RIP assay results (Figure 3.10B). In addition, to confirm the directly interaction of RIG-I and ε region of HBV pgRNA, HBV εRNA was incubated with WT or K888E mutant of RIG-I RD recombinant protein (rRIG-I RD), gel shift assay results demonstrated that the HBV εRNA interacted with WT rRIG-I RD but not the K888E mutant (Figure 3.11D). These data indicate that the 5'-ε region of viral pgRNA directly interacts with RIG-I.

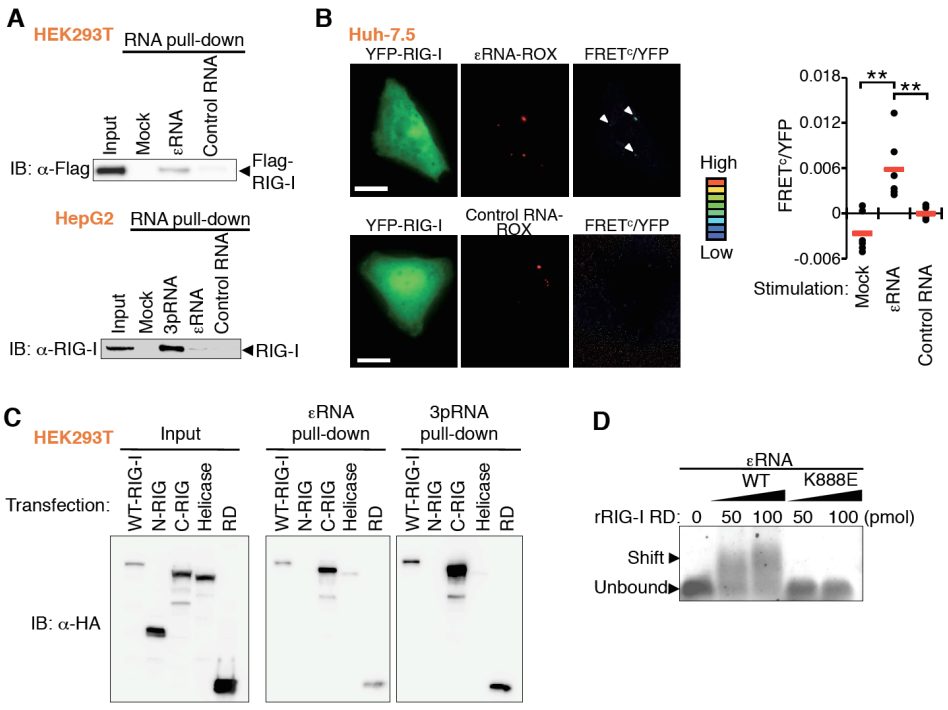

Figure 3.11 Interaction of εRNA and RIG-I. (A, C) RNA pull-down assay showing the binding activity of the indicated RNAs to Flag-tagged WT RIG-I (A, top) or its mutants in HEK293T cells (A, top and C) or endogenous RIG-I in HepG2 cells (A, bottom). (B) FRET analysis for the interaction of YFP-tagged RIG-I (YFP-RIG-I) with rhodamine (ROX)-conjugated εRNA (εRNA-ROX) or Control RNA (Control RNA-ROX). Representative fluorescence images of YFP, ROX and $FRET^C$/YFP (the ratio of corrected FRET ($FRET^C$) to YFP). Arrowheads indicate area showing high FRET efficiency. Bar: 20 μm. Right, Dot plot of $FRET^C$/YFP ratio (small horizontal

bars, mean). (D) Gel-shift analysis of complex formation between εRNA and recombinant RIG-I RD (WT) or RD (K888E). Arrowheads denote position of unbound RNA and RNA–RIG-I complexes. $^{**}P < 0.01$, Student's t-test.

3.4.2 Antiviral activity of RIG-I

As mentioned above, the 5'-ε region of HBV pgRNA that specifically recognized by RIG-I is also the binding site for HBV polymerase. Therefore, I hypothesized that the RIG-I may affect the HBV replication via an IFN pathway-independent manner that directly block the access of viral polymerase protein toward the 5'-ε region of HBV pgRNA.

Firstly, I tested the contribution of RIG-I pathway in antiviral defense against HBV infection, siRNA-mediated RIG-I knockdown in HuS-E/2 or PHH resulted in a higher HBV genome copy number after transfection or infection with HBV, as compared with control siRNA treated group (Figures 3.12A and 3.12B, left). These results indicate an implicated role of RIG-I as an innate sensor to activate antiviral response against HBV infection. However, the increased HBV genome copy number in RIG-I knockdown cells might result from the impaired IFN-λ1 (*IFNL1*) induction (Figure 3.12B, right). To further test the IFN-independent antiviral activity of RIG-I, I first tested whether RIG-I could block the interaction of HBV polymerase (P) protein toward the ε region. HEK293T cell lysates expressing pgRNA and HA-tagged P protein (HA-P) were incubated with the indicated amount of recombinant RIG-I (rRIG-I) protein, and RIP assay showed that rRIG-I protein suppressed the interaction of P protein with pgRNA in a dose-dependent manner (Figure 3.12C). Such an inhibitory effect was also observed in Huh-7.5 cells by overexpression of wild type RIG-I as well as its T55I[164,168] or K270A[169] mutant (Figure 3.12D), both of which are not able to induce ligand-dependent activation of the downstream signaling but retain their RNA-binding activities. On the other hand, the K888E mutant that lost its RNA-binding activity could not inhibit the binding of P protein with pgRNA (Figure 3.12D). In addition, treatment with recombinant IFN-λ1 (rIFN-λ1) in Huh-7.5 cells upregulated the amount of the mutant RIG-I protein (T55I) (Figure 3.12E, bottom), resulting in a partial inhibition of the P protein interaction with pgRNA, and this inhibitory effect was abrogated by RIG-I knockdown (Figure 3.12E, top). These results indicate that RIG-I protein can counteract

the interaction of HBV polymerase with pgRNA, which is a critical step for initiation of RNA reverse transcription and encapsidation during HBV life cycle. This finding suggests that RIG-I may be able to affect the HBV replication via an IFN pathway-independent manner.

To assess the IFN-independent antiviral activity of RIG-I, I used Huh-7.5 cells carrying a dominant-negative mutant RIG-I allele that failure to induce IFN response upon HBV transfection (Figure 3.5C) and RIG-I RD vector only expresses the repressor domain of RIG-I that can not active IFN response, thus, in this transfected Huh-7.5 cells, no any IFN induction is observed. In this condition, Huh-7.5 cells were transfected with WT or K888E mutant of RIG RD expression vector together with HBV-Ae plasmid. The results showed that WT RIG-I RD suppressed the HBV replication, while the mutant RD (K888E) did not affect viral replication (Figure 3.12F). These findings revealed another aspect of RIG-I as a direct antiviral factor through its interference with the binding of HBV P protein to pgRNA in an IFN pathway-independent manner.

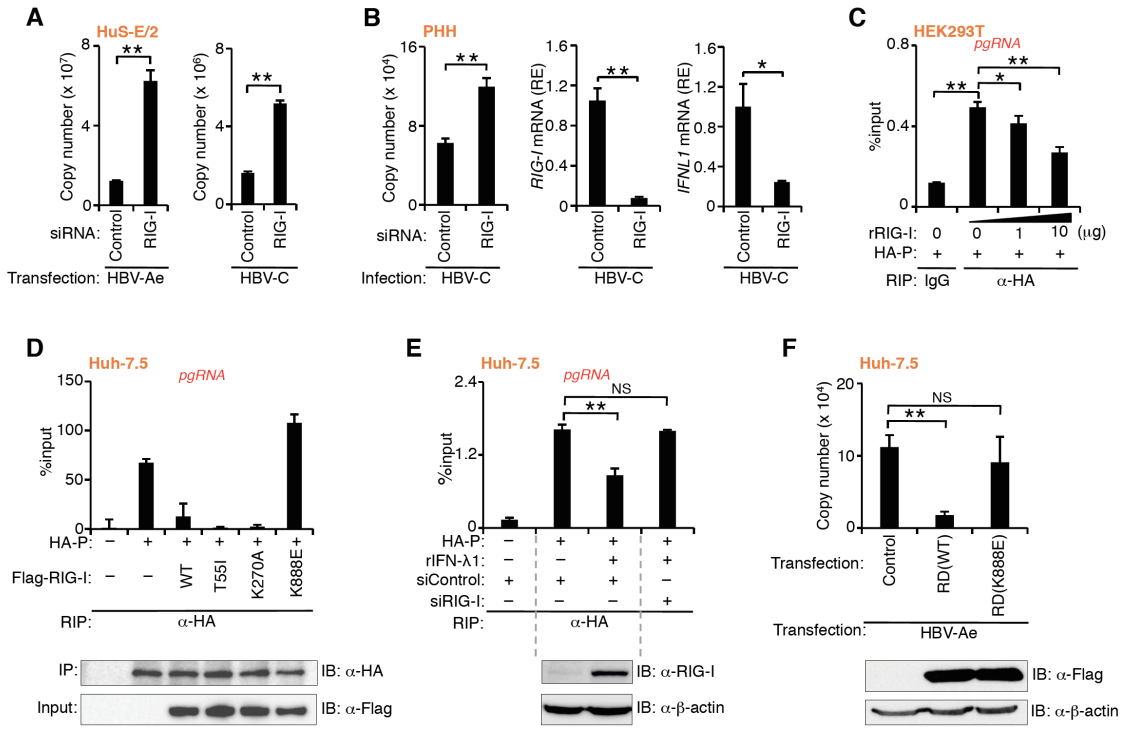

Figure 3.12 Antiviral effect of RIG-I by counteracting the interaction of HBV polymerase with pgRNA. (A, B) qPCR analysis of copy numbers of encapsidated HBV DNA in control or RIG-I siRNA-treated HuS-E/2 cells at 48 hours after transfection with the genome of HBV-Ae (A,

left) and HBV-C (A, right) or PHH at 10 days after infection with HBV-C (B, left). *RIG-I* (B, middle) and *IFNL1* mRNA (B, right) in control or RIG-I siRNA-treated PHH are analyzed by qRT-PCR. (C, D) HEK293T cell lysates expressing pgRNA and HA-tagged P protein (HA-P) were incubated with the indicated amount of recombinant RIG-I (rRIG-I) (C) or Huh-7.5 cell lysates expressing pgRNA, HA-tagged P and Flag-RIG-I or its mutants (D) were subjected to RIP assay and qRT-PCR analysis of the interaction of pgRNA with HA-P. Expression of Flag-RIG-I and its mutants, and immunoprecipitated amounts of HA-P is analyzed by immunoblotting (D, bottom). (E) Huh-7.5 cells expressing both pgRNA and HA-P were treated with rIFN-λ1 (100 ng/ml) for 24 hours with or without RIG-I siRNA, and subjected to RIP assay. rIFN-λ1 induced RIG-I expression was analyzed by immunoblotting with anti-RIG-I or anti-β-actin antibody (E, bottom). (F) Huh-7.5 cells were transfected with an expression vector for WT or K888E RIG-I RD, together with the HBV-Ae genome. After 72 hours of transfection, copy numbers of encapsidated HBV DNA were measured by qPCR (left), and expression of Flag-RIG-I RD (WT) and RD (K888E) was analyzed by immunoblotting. Data are presented as mean and SD (n = 3) and are representative of three independent experiments. *P < 0.05 and **P < 0.01, Student's t-test. NS, not significant.

3.5 εRNA and HBV replication

The above results indicate that the RIG-I binding to 5'-ε region of HBV pgRNA not only triggers IFN-λ expression, but also counteracts the interaction of HBV polymerase and pgRNA, both of them are shown to repress HBV replication. Therefore, treatment with εRNA may trigger IFN expression via RIG-I pathway, and also the εRNA may function as antagonist to prevent HBV polymerase binding to 5'-ε region of HBV pgRNA, both of those functions may repress HBV replication. Thus, in the last of this study, I tried to harness the therapeutic potential of the εRNA for the control of HBV infection.

3.5.1 Antiviral effect of εRNA treatment *in vitro*

To test the antiviral effect of the εRNA, I first confirmed the interaction of HBV polymerase (P) protein and εRNA in Huh-7.5 and HEK293T cells by FRET analysis (Figure 3.13A) and RNA pull-down assay (Figure 3.13B), respectively. In addition, a vector was designed to include a 63-bp DNA oligo, which is transcribed into εRNA under a U6 promoter. *In vitro* experiments showed that vector-driven expression of

εRNA in Huh-7.5 cells block the interaction of HBV P protein with HBV pgRNA (Figure 3.13C). Consistent with this, vector-driven expression of εRNA in Huh-7.5 cells showed repression of HBV replication (Figure 3.13D, left), but did not show any difference in HCV replication as compared with control (Figure 3.13D, right). This result suggest that εRNA induced by this vector-driven expression is capable to function as a decoy RNA to interfere with the binding of HBV P protein to pgRNA and to inhibit viral replication in an IFN-independent manner.

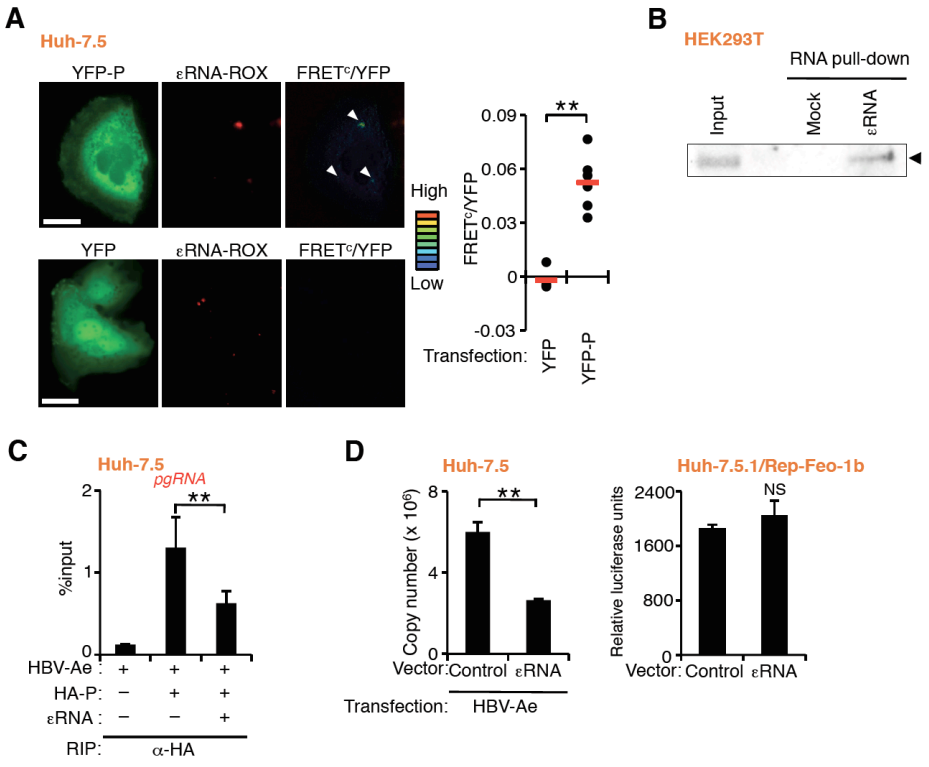

Figure 3.13 Antiviral effect of εRNA treatment *in vitro*. (A) FRET analysis for the interaction between YFP-tagged P protein (YFP-P) or YFP and εRNA-ROX as described in Figure 3.11B. (B) Biotin-labeled εRNA was incubated with lysates from HEK293T cells expressing Flag-tagged P protein (Flag-P). Flag-P pulled down by εRNA was detected by immunoblotting with anti-Flag antibody. (C) Huh-7.5 cells were transfected with expression vectors for HA-P and εRNA, together with the HBV-Ae genome. RIP assay was performed to evaluate the effect of εRNA on the interaction between HA-P and pgRNA. (D) qPCR analysis of copy numbers of encapsidated HBV DNA in Huh-7.5 cells expressing the HBV-Ae genome and εRNA (left). Luciferase assay analysis of HCV replication in Huh-7.5.1/Rep-Feo-1b cells expressing εRNA (right). Data are

presented as mean and SD (*n* = 3) and are representative of three independent experiments. ***P* < 0.01, Student's t-test. NS, not significant.

3.5.2 Antiviral effect of εRNA treatment *in vivo*

In order to evaluate the therapeutic efficacy of εRNA *in vivo*, HBV infection model of human hepatocyte-chimeric mice were intravenously infected with HBV-C. Three weeks after HBV infection, the infection efficiency was confirmed by measuring the number of viral genome copies in the sera of HBV-infected chimeric mice by qPCR analysis and the mice were randomly divided into two groups. Four weeks postinfection of HBV, infected chimeric mice underwent intravenous administration with the εRNA expression vector or empty vector loaded in a liposomal carrier, a multifunctional envelope-type nanodevice (MEND) for efficient delivery to liver tissue, every two days for 14 days. As shown in Figure 3.14A, treatment with εRNA-MEND significantly suppressed the elevation of the number of viral genome copies in the sera by less than one tenth of those for control mice. Consistently, immunofluorescence analyses showed that the expression of HBV core antigen (HBcAg) in the liver tissues of εRNA-MEND-treated chimeric mice was remarkably reduced as compared with those of control mice (Figure 3.14B). These results indicate that εRNA has therapeutic potential for the control of HBV infection.

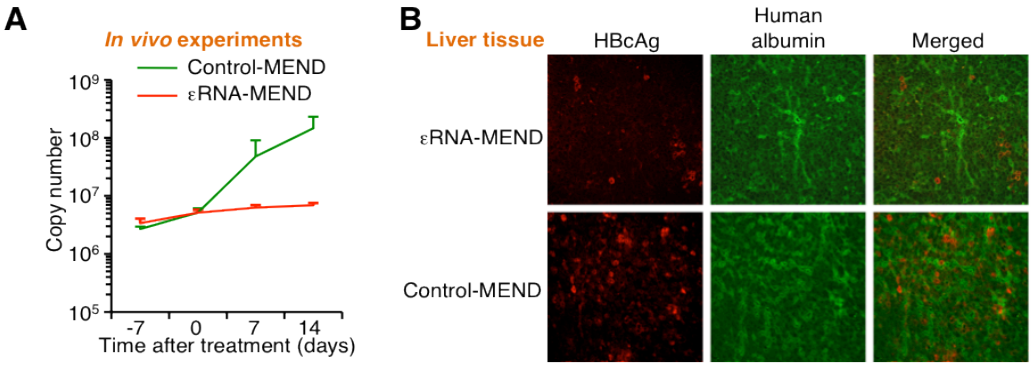

Figure 3.14 Antiviral effect of εRNA treatment *in vivo*. HBV-infected mice were intravenously administrated with the εRNA expression vector (εRNA-MEND) or empty vector (Control-MEND) loaded in liposomal carrier at a dose of 0.5 mg/kg of body weight every two days for 14 days. Serum HBV DNA in HBV-infected chimeric mice was determined by qPCR (A) (*n* = 3 per group),

HBcAg (red) and human albumin (green) in the liver sections were detected by Immunofluorescence stain (B). Day 0 indicates the first time to delivery εRNA-MEND or Control-MEND.

4. Discussion

The innate immune system acts as a front line of host defense against viral infection. In this step, PRRs (pattern recognition receptors) play a crucial role in the recognition of invading viruses. In particular, nucleic acid sensing of viruses is central to the initiation of antiviral immune responses. However, the nucleic acid sensor(s) for HBV and the host innate immune response against HBV infection has not been identified. On the other hand, the currently approved clinical therapies of chronic hepatitis B include administration of antiviral active IFN-α, as well as nucleos(t)ide analogues can control replication of HBV, but the long-term response rates are still not satisfactory. Thus, elucidation of host immune response against HBV infection is crucial for better understanding of the pathological processes and viral elimination to control HBV infection. In this study, I tried to identify a nucleic acid sensor(s) for HBV and to characterize the IFN response during HBV infection.

As a result, this study demonstrated: (1) Type III but not type I IFNs are predominantly induced in human hepatocytes during HBV infection; (2) RIG-I senses the HBV genotype Ae, Bj, and C for the induction of type III IFNs; (3) The 5'-ε region of HBV pgRNA is a key element for the RIG-I-mediated recognition and type III IFNs induction; (4) RIG-I directly counteracts the interaction of HBV polymerase with pgRNA to suppress viral replication in an IFN-independent manner; (5) εRNA can funcation as a decoy RNA to interfere with the binding of HBV polymerase protein to pgRNA and to inhibit viral replication.

The observations of this study reveal an innate recognition mechanism by which RIG-I dually functions as an HBV sensor activating innate signaling and to counteract viral polymerase in human hepatocytes. Moreover, this study also evaluate the therapeutic potential of the εRNA for the control of HBV infection, which may provide a better approach to the strategies for development of nucleic acid medicine, and offer an attractive clinical option for the therapy against not only HBV but also possibly other virus infections.

4.1 Inhibiton of innate immune responses by HBV proteins

This study identified RIG-I as an important innate sensor of HBV to predominantly

induce type III IFNs in hepatocytes through its recognition of the 5'-ε stem-loop of HBV pgRNA (Figures 3.1-3.11). While results showed that the induced-IFN-λ by HBV infection has antiviral activity (Figure 3.2), the type III IFN response upon HBV infection does not seem to be efficient as compared with the case with NDV infection (Figure 3.3). In this respect, there have been also several reports showing that HBV proteins such as HBV X and polymerase inhibit the activation of RIG-I pathway (Table 4.1). It was shown that HBV X protein interacts with MAVS and promotes the degradation of MAVS through Lys136 ubiquitin in MAVS protein [170,171], and HBV polymerase protein competes for DDX3 binding with TBK1 [172,173], both of them inhibit RIG-I-mediated IFNs expression, which possibly enables HBV to evade from antiviral innate immune response. Except for RIG-I signaling pathway, HBV proteins also repress other PRRs-mediated innate immune responses (Table 4.1). In the late 80's of the 20th century, Dr. Schloemer group firstly reported that HBV core protein was able to inhibit the transcription of the IFN-β gene in hepatoma cells [174,175]. Later, other groups also highlighted the involvement of HBV core protein in the inhibition of the IFN pathway. It was shown that the MxA protein, an effector of the IFN response, is totally inhibited in the HBV-replicating HepG2.2.15 cell line or HepG2 cells transfected with a re-circularized HBV DNA or HBV preC/C expression plasmids [176], as well as in PBMCs from HBV chronically infected patients [177]. They also demonstrated that the inhibition was due to a direct binding of the core protein with the ISRE (interferon-sensitive response element) sequence of the human MxA promoter [176]. Beside core, other HBV proteins were also involved in the inhibition of IFN pathway. HBsAg and HBeAg, two kinds of secretory proteins produced during the HBV replication cycle, are the markers of HBV infection and present in circulation at high levels. A possible explanation for the production of these proteins by the virus could be that they may have some immunomodulatory effects, which may help the virus to evade the immune system [178]. Indeed, it was reported that the TLR2 expression on Kupffer cells, peripheral monocytes and hepatocytes was significantly reduced in samples from HBeAg-positive CHB patients compared with HBeAg-negative CHB patients [179]. Furthermore, it was clarified that the unique 10-mer amino acid sequence located at the HBeAg N terminus (SKLCLGWLWG), which is highly conserved in all orthohepdnaviruses, shares sequence similarity with sequences of TIR (Toll/IL-1 receptor) domains that are encoded by TLRs and numerous adaptors. Thus, HBeAg can

directly interacts with key adaptors in the TLR2 pathway, particularly the TIRAP adaptor, and suppresses the activation of TLR2 signaling [180,181]. HBeAg was also shown to suppress IL-1β-mediated NF-κB activation in hepatocytes [182]. Another secretory protein HBsAg has been shown to abrogate TLR9-mediated IFN-α production in pDCs (plasmacytoid DCs) [183,184] and interfere with TLR-induced ERK (extracellular regulated protein kinases), JNK (c-Jun N-terminal kinase) pathways in monocytes/macrophages [185,186]. Recombinant HBsAg are also shown to inhibit LPS-induced IL-12/IL-18 production in THP-1 cells via interfering with the NF-κB pathway [187].

Table 4.1 Summary of innate immune responses directly manipulated by HBV proteins

HBV proteins	Cellular targets	References
HBxAg	RIG-I/MDA5–MAVS	[170,171]
Polymerase	RIG-I/TLR3–TBK1/IKKε–DDX3–IRF-3–IFN-β	[172,173]
HBcAg	IFN-β–MxA	[174,175,176,177]
HBeAg	TLR2–TIRAP	[179,180,181]
	IL-1β–NF-κB	[182]
HBsAg	TLR9–IFN-α	[183,184]
	TLRs–ERK/JNK	[185,186]
	NF-κB–IL-12/IL-18	[187]

The data from this study also indicated that HBV polymerase protein interacts with the 5'-ε stem-loop of HBV pgRNA, which is also a critical region for RIG-I-mediated recognition of viral pgRNA and the subsequent downstream signaling events. Therefore, the interaction of HBV polymerase and the 5'-ε stem-loop of HBV pgRNA may likely suppress the induction of IFN-λs, which may provide a novel aspect of HBV polymerase protein in terms of viral evasion from RIG-I activation. The inhibition of RIG-I pathway by HBV proteins also mirrored the important role of RIG-I-mediated signaling for antiviral defense against HBV infection, although further investigation will be required to determine whether other sensing molecules except for RIG-I are engaged in the activation of innate responses in other cell types including dendritic cell subsets and Kupffer cells.

4.2 HBV infection and IFN-λ induction

The other interesting issue for RIG-I-mediated IFNs induction during HBV infection in human hepatocyte is the mechanism of predominant induction of type III but not type I IFNs (Figures 3.1, 3.3 and 3.4), since it was believed that viral infections induce type I and type III IFNs expression through a common mechanism activating transcription factors such as NF-κB and IRF-3 [188]. However, it was reported that inhibition of the NF-κB pathway supresses IFN-λ expression but only has a minor effect on type I IFN expression in DCs and in whole animals strongly [189]. A recently study also indicated that type I and III IFNs are differentially regulated at the transcriptional level: IRF-3/7 and NF-κB were activated by both mitochondrial and peroxisomal MAVS to mediate the expression of both IFN classes in response to viruses that trigger activation of RIG-I signaling pathway. However, MAVS on peroxisomes activated IRF-1 to only regulate type III IFNs while MAVS on mitochondria could activate MAP kinases to induce type I IFNs via AP-1, which is not required for type III IFN production [190]. These findings suggested that some transcription factors predominantly induce type I or type III IFNs expression, despite they share a common signaling pathway.

For this study, results showed that RIG-I–MAVS–TBK1–IRF-3 signaling pathway is involved in the induction of type III but not type I IFNs during HBV infection (Figure 3.6), and also showed that εRNA recognized by RIG-I activates downstream target IRF-3 (Figures 3.9E and 3.9F), suggesting that the predominant production of type III IFNs is not simply explained by the type III IFNs special regulator-IRF-1, other factor(s) may exist to regulate this predominant expression of type III IFNs. Indeed, there have been several reports showing that type III IFNs were predominantly produced by hepatocytes during infection of HCV, which is also known to induce IFNs expression via RIG-I signaling pathway [167,191,192]. Except for the hepatocytes, other reports also indicated that IFN-λ is the dominant IFN produced by respiratory epithelial cells after infection with influenza virus or other respiratory viruses that trigger activation of RIG-I signaling pathway [193-196]. These findings may imply a key role for IFN-λ in mediating antiviral immunity in the liver and respiratory tract, and a specific factor(s) which is selectively involved in type III IFNs induction may exist in liver and respiratory tract, although this issue merits further investigation including epigenetic

evaluation.

4.3 The 5'-ε region of pgRNA-induced IFN-λ expression

This study found that either of the 5'- or 3'-ε region of pgRNA could interact with RIG-I (Figure 3.10D) but it was only the 5'-ε region that contributed to the induction of IFN-λ1 (Figures 3.8A, 3.8B, 3.9A and 3.9B), which is similar as the case of encapsidation of the HBV pgRNA during HBV replication. Despite the fact that both 5'- and 3'-ε elements have an identical sequence, only the 5'-ε, but not the 3'-ε, is functional for encapsidation, which is preceded by recognition and binding of HBV polymerase to the 5'-ε element of pgRNA. It was indicated that the 5' cap structure is required for encapsidation of the pgRNA, and 5'-ε element also needs to be positioned within 65 nt from the 5' cap to be encapsidated efficiently [197], suggesting that HBV polymerase somehow recognize the cap structure and/or its associated factors, as well as the 5'-ε, for encapsidation to occur.

In this study, the RIG-I protein was found to interact with either of the 5'- or 3'-ε region of pgRNA, however, the RNA binding is just the first prerequisite for RIG-I activation, the final RIG-I-mediated IFNs induction requires following complex multistep process that include ATP binding and hydrolysis, oligomerization, phosphorylation, ubiquitination, and several host proteins are involved in this process [56,59,61]. Therefore, only RNA binding to RIG-I is not sufficient for IFNs induction. Huh-7.5 cells used in this study contains a RIG-I T55I mutation that has no effect on the ability of RIG-I to bind dsRNA, but abolishes its TRIM25 binding ability, leading to the loss of TRIM25-induced RIG-I ubiquitination and IFNs induction. Thus, it could be speculated that some 5' end of pgRNA-associated factor(s) may additionally promote the activation of RIG-I after binding to the 5'-ε region of HBV pgRNA and/or some 3' end of pgRNA-associated factor(s) specially inhibit the activation of RIG-I.

4.4 Dual roles of RIG-I

In addition, this study demonstrated a hitherto-unidentified function of RIG-I as a direct antiviral factor against HBV infection (Figure 3.11). Mechanismly, RIG-I was found to counteract the accessibility of HBV polymerase to the 5'-ε region of pgRNA, which is an important process for the initiation of viral replication [165]. As is the case

with this, several viral PAMPs known to be recognized by RIG-I, for example, the poly-U/UC tract in the 3' non-translated region of HCV genome [167] and 5' terminal region of influenza virus (IAV) genome [298] were previously reported to be directly or indirectly critical for viral replication [199-201]. In this respect, one could envisage that such an exquisite targeting by RIG-I would confer a unique machinery to ensure efficient antiviral activities of RIG-I. Therefore, RIG-I is likely to play dual roles as an innate sensor and as a direct antiviral effector for host defense during viral infection. Indeed, recent study already reported that binding of RIG-I to 5′-triphosphorylated panhandle-RNA structure of IAV RNPs (ribonucleoproteins, contain viral RNA, multiple nucleoproteins, and the viral polymerase complex that composed of PA, PB1, and PB2) could directly restrict IAV infection in an IFN-independent manner [202].

Therefore, this study and recent study [202] revealed that RIG-I not only acts as a sensor, but can also exert direct effector function to restrict viral replication. For HBV, RIG-I does so by binding the 5′-ε region of pgRNA to block binding of the P protein. For IAV, the mechanistic details of how viral RNA binding by RIG-I restricts virus replication are still unknown. However, it could be speculated that RIG-I disrupts binding of components of the IAV polymerase complex to the viral RNA.

4.5 Type III IFNs and chronic HBV infection

Type I IFNs (IFN-β and the multiple IFN-α subspecies) bind to a common type I IFN receptor (IFNAR) that associated with the JAK1 (Janus activated kinase 1) and TYK2 (tyrosine kinase 2). Activation of the JAK1 in response to type I IFNs binding to IFNAR results in tyrosine phosphorylation of STAT2 (signal transducer and activator of transcription 2) and STAT1; this leads to the formation of STAT1–STAT2–IRF-9 (IFN-regulatory factor 9) complexes, which are known as ISGF3 (IFN-stimulated gene factor 3) complexes. These complexes translocate to the nucleus and bind ISREs (IFN-stimulated response elements) in the promoter region of ISGs, some of ISGs code for antiviral proteins. PEG-IFN-α (pegylated IFN-α) has long been used to treat chronic viral infections such as Hepatitis B/C, which infects hepatocytes. However, this treatment is associated with increasing viral resistance and undesirable systemic side effects due to the fact that virtually all cell types express type I IFN receptor-IFNAR [203]. Different from the type I IFNs that utilize IFNAR complex to trigger their biological

activities, the IL-10R2 (Interleukin 10 receptor 2) chain and IFNLR1 (Interferon, lambda receptor 1) chain are involved in type III IFNs mediated activation of intracellular signaling [204,205], and it is reported that IFNLR1 is only preferentially expressed in few cell types, notably epithelial cells, including hepatocytes [206]. Therefore, cellular response to type III IFN is restricted to a narrow range of cell types/tissues [132]. Despite the lack of similarities between the receptor systems used by type I and type III IFNs, the intracellular signaling pathway activated by these two types of IFNs is very similar, which is supported by the comparable cellular gene expression profiles induced after stimulation with type I IFNs (IFN-α and IFN-β) or type III IFNs (IFN-λ1, -λ2 and -λ3) in human hepatoma Huh-7 cells or primary human hepatocytes [207]. Because of the similar intracellular signal transduction, it is not surprising that type III IFNs have a potential antiviral activity similar as type I IFNs. It was reported that type III IFNs can not only against HBV but also other virus replication in cell culture systems or *in vivo* animal models [208,209]. Due to the similar antiviral ability and restricted expression of receptor, IFN-λ clinical trials for Hepatitis B/C have been very promising in both effectiveness and limitation of side effects [210].

This study also revealed that a moderate type III IFNs are induced by HBV infection rather than type I IFNs via RIG-I signaling pathway, and indicated that the induced IFN-λ has antiviral activity to against HBV and VSV replication (Figure 3.2). In consideration of about 95% of adults infected with HBV can eliminate the virus and recover completely [112], the induced type III IFNs during the early stage of HBV infection may play an important role on elimination of virus. Therefore, treatment with type III IFNs may provide a better approach for chronic HBV infection. Although the antiviral activity of type III IFNs was proved *in vitro* and *in vivo* animal models, using IFN-λ to treat chronic HBV infection in humans needs further investigation. However, recent report showed promising results that in Phase 2b clinical studies, PEG-IFN-λ1 administered in combination with ribavirin (RBV) was efficacious in patients with HCV infection representing genotypes 1 through 4, and was associated with more rapid declines in HCV RNA compared to PEG-IFN-α plus RBV [211].

4.6 εRNA-mediated anti-HBV replication

As HBV-encoded proteins have various functions to counteract the innate immune

responses, which may result in the establishment and maintenance of viral infection [212], restoration of impaired innate immune responses to produce sufficient cytokines by using viral protein inhibitors or PRRs agonist during the treatment of chronic HBV infection may also contribute to the elimination of virus. This study indicated that the εRNA can induce IFN-λ expression via activation of RIG-I signaling pathway (Figures 3.9D, 3.9E, 3.9F), which may repress HBV replication. This result is consistent with previous study that has demonstrated activation of RIG-I by 5'-triphosphorylated siRNA (small interfering RNA) induced a vigorous IFN response against HBV in hepatocytes [213]. Besides activation of RIG-I pathway, numerous studies have clarified that HBV replication and gene expression can be inhibited by other PRRs agonist stimulation *in vitro* and *in vivo* [214]. For example, intravenous injection of TLR3, TLR4, TLR5, TLR7 or TLR9 ligands inhibited HBV replication by type I IFN induction in HBV transgenic mice model [215]. Additionally, in hepatoma cell lines, it had been shown that TLR2 or TLR4 ligands were able to inhibit HBV via IFN-independent pathways, which directly activate MAPK-ERK and PI3K (phosphatidylinositol 3-kinase)-Akt (serine/threonine-protein kinases, also known as protein kinase B) pathways [216]. STING agonists also can induce an innate antiviral immune response dominated by type I IFNs and reduce HBV replication in HBV hydrodynamic mouse model [217]. These studies mentioned above indicated that the inhibition of HBV replication by activated PRRs was dependent on the secreted cytokines or the intracellular signaling pathways of immune cells or hepatocytes. Moreover, recent studies revealed that oral administration of a TLR7 agonist GS9620, which was capable of stimulating robust IFNα responses in plasmacytoid DCs and triggering ISGs expression in PBMCs (peripheral blood mononuclear cells) and liver, resulted in HBV suppression in chronically infected chimpanzees model. And this antiviral activity is also associated with activation of intrahepatic T, NK, and NKT cell responses that produce IFN-γ. Therefore, the suppression of HBV replication by activation of TLR7 involves both innate and adaptive immune systems [218,219].

Overall, activation of the innate immunity using agonists of PRRs has been proposed as therapeutic strategies for HBV infection. However, activation of PRRs may also lead to acute and chronic inflammation. Therefore, it is necessary to further clarify the intracellular signaling and antiviral proteins responsible for control of the viral infection in order to selectively augment the antiviral responses and to reduce the

harmful inflammatory side effects [178].

RNA decoys are small RNA molecules analogous to *cis*-acting element, which can compete with the corresponding endogenous sequences for *trans*-factors binding, thereby attenuating the authentic *cis-trans* interaction. As the interaction between *cis*-acting element and *trans*-acting factor is usually essential for viral replication, the mutation of the *trans*-acting factor that blocks its binding to RNA decoy also blocks its binding to the authentic target in viral RNA. Therefore, RNA decoys-based therapy can reduce the risk of escape mutants [220]. Except for the IFN-inducing activity, this study also indicated that the εRNA can function as a decoy RNA to interfere with the binding of HBV polymerase protein to pgRNA and to inhibit viral replication (Figures 3.13 and 3.14). Therefore, these findings may afford a new therapeutic modality in replace of conventional antiviral drugs that have been reported to have a risk to develop drug-resistance HBV mutations [139]. It was reported that overexpression of RNA decoys corresponding to stem-loop structures in the NS5B coding region of HCV which are driven by polymerase III can repress the HCV replication [221], and nucleolar-localized TAR (transactivation response) decoys has been shown to inhibit tat-activated HIV-1 transcription and replication [222,223]. All these findings give a promising expectation for successful development of nucleic acid medicine against HBV infection.

Taken together, the present study may provide a better approach to the strategy for development of nucleic acid medicine, and offer an attractive clinical option for the therapy against HBV infection. While various improvements may be required for the successful therapeutic application, including improvement of the transcription level, stability and liver-targeting ability of this εRNA expression vector, and optimization of the activity of innate immune response triggered by this expressed εRNA in liver. However, the large number of people suffering from chronic liver disease and the obvious limitations of current therapies make such efforts highly worthwhile.

References

1. Ganem, D., and Prince, A.M. Hepatitis B virus infection–natural history and clinical consequences. *N Engl J Med* **350**, 1118-1129 (2004).
2. Rehermann, B., and Nascimbeni, M. Immunology of hepatitis B virus and hepatitis C virus infection. *Nat Rev Immunol* **5**, 215-229 (2005).
3. Alter, H.J., and Blumberg, B.S. Further studies on a "new" human isoprecipitin system (Australia antigen). *Blood* **27**, 297-309 (1966).
4. Blumberg, B.S., Sutnick, A.I., and London, W.T. Australia antigen and hepatitis. *JAMA* **207**, 1895-1896 (1969).
5. Dane, D.S., Cameron, C.H., and Briggs, M. Virus-like particles in serum of patients with Australia-antigen-associated hepatitis. *Lancet* **1**, 695-698 (1970).
6. Kaplan, P.M., Greenman, R.L., Gerin, J.L., Purcell, R.H., and Robinson, W.S. DNA polymerase associated with human hepatitis B antigen. *J Virol* **12**,995-1005 (1973).
7. Robinson, W.S., Clayton, D.A., and Greenman, R.L. DNA of a human hepatitis B virus candidate. *J Virol* **14**, 384-391 (1974).
8. Charnay, P., Pourcel, C., Louise, A., Fritsch, A., and Tiollais, P. Cloning in Escherichia coli and physical structure of hepatitis B virion DNA. *Proc Natl Acad Sci U S A* **76**, 2222-2226 (1979).
9. Valenzuela, P., Gray, P., Quiroga, M., Zaldivar, J., Goodman, H.M., and Rutter, W.J. Nucleotide sequence of the gene coding for the major protein of hepatitis B virus surface antigen. *Nature* **280**, 815-819 (1979).
10. Pasek, M., Goto, T., Gilbert, W., Zink, B., Schaller, H., MacKay, P., Leadbetter, G., and Murray, K. Hepatitis B virus genes and their expression in E. coli. *Nature* **282**, 575-579 (1979).
11. Yan, H., Zhong, G., Xu, G., He, W., Jing, Z., Gao, Z., Huang, Y., Qi, Y., Peng, B., Wang, H., Fu, L., Song, M., Chen, P., Gao, W., Ren, B., Sun, Y., Cai, T., Feng, X., Sui, J., and Li, W. Sodium taurocholate cotransporting polypeptide is a functional receptor for human hepatitis B and D virus. *Elife* **1**, e00049 (2012).
12. Liang, T.J. Hepatitis B: the virus and disease. *Hepatology* **49**(Suppl 5), S13-21 (2009).
13. Doo, E.C., and Ghany, M.G. Hepatitis B virology for clinicians. *Clin Liver Dis* **14**, 397-408 (2010).

14. Baumert, T.F., Meredith, L., Ni, Y., Felmlee, D.J., Mckeating, J.A., and Urban, S. Entry of hepatitis B and C viruses–recent progress and future impact. *Curr Opin Virol* **4**, 58-65 (2014).
15. Block, T.M., Guo, H., and Guo, J.T. Molecular virology hepatitis B virus for clinicians. *Clin Liver Dis* **11**, 685-706 (2007).
16. Seeger, C., and Mason, W.S. Hepatitis B virus biology. *Microbiol Mol Biol Rev* **64**, 51-68 (2000).
17. Feitelson, M.A., Reis, H.M., Tufan, N.L., Sun, B., Pan, J., and Lian, Z. Putative roles of hepatitis B x antigen in the pathogenesis of chronic liver disease. *Cancer Lett.l* **286**, 69-79 (2009).
18. Gerlich, W.H. Medical virology of hepatitis B: how it began and where we are now. *Virol J* **10**, 239 (2013).
19. Ezzikouri, S., Ozawa, M., Kohara, M., Elmdaghri, N., Benjelloun S, and Tsukiyama-Kohara, K. Recent insights into hepatitis B virus- host interactions. *J Med Virol* **86**, 925-932 (2014).
20. Minor, M.M., and Slagle, B.L. Hepatitis B Virus HBx protein interactions with the ubiquitin proteasome system. *Viruses* **6**, 4683-4702 (2014).
21. Li, W., Goto, K., Matsubara, Y., Ito, S., Muroyama, R., Li, Q., and Kato, N. The characteristic changes in hepatitis B virus x region for hepatocellular carcinoma: a comprehensive analysis based on global data. *PLoS One* **10**, e0125555 (2015).
22. Lin, C.L., and Kao, J.H. Hepatitis B virus genotypes and variants. *Cold Spring Harb Perspect Med* **5**, a021436 (2015).
23. Mustafa, S. Hepatitis B virus genotypes: Global distribution and clinical importance. *World J Gastroenterol* **20**, 5427-5434 (2014).
24. Shi, W., Zhang, Z., Ling, C., Zheng, W., Zhu, C., Carr, M.J., and Higgins, D.G. Hepatitis B virus subgenotyping: history, effects of recombination, misclassifications, and corrections. *Infect Genet Evol* **16**, 355-361 (2013).
25. Schädler, S., Hildt, E. HBV life cycle: entry and morphogenesis. *Viruses* **1**, 185-209 (2009).
26. Nese, I., and Fehmi, T. Hepatitis B virus: biology and life cycle. *Viral Hepatitis Journal* **21**, 1-7 (2015).
27. Liu, N., Ji, L., Maguire, M.L., and Loeb, D.D. cis-Acting sequences that contribute

to the synthesis of relaxed-circular DNA of human hepatitis B virus. *J Virol* **78**, 642-649 (2004).

28. Gripon, P., Rumin, S., Urban, S, Le Seyec, J., Glaise, D., Cannie, I., Guyomard, C., Lucas, J., Trepo, C., and Guguen-Guillouzo, C. Infection of a human hepatoma cell line by hepatitis B virus. *Proc Natl Acad Sci U S A* **99**, 15655-15660 (2002).
29. Sells, M.A., Chen, M.L., and Acs, G. Production of hepatitis B virus particles in HepG2 cells transfected with cloned hepatitis B virus DNA. *Proc Natl Acad Sci U S A* **84**, 1005-1009 (1987).
30. Galle, P.R., Haglestein, J., and Kommerell, B. *In vitro* experimental infection of primary human heptocytes with hepatitis B virus. *Gastroenterology* **106**, 664-673 (1994).
31. Walter, E., Keist, R., Niederost, B., Pult, I., and Blum, H.E. Hepatitis B virus infection of tupaia hepatocytes *in vitro* and *in vivo*. *Hepatology* **24**, 1-5 (1996).
32. Hantz, O., Parent, R., Durantel, D., Gripon, P., Guguen-Guillouzo, C., and Zoulim, F. Persistence of the hepatitis B virus covalently closed circular DNA in HepaRG human hepatocyte-like cells. *J Gen Virol* **90**, 127-35 (2009).
33. Iwamoto, M., Watashi, K., Tsukuda, S., Aly, H.H., Fukasawa, M., Fujimoto, A., Suzuki, R., Aizaki, H., Ito, T., Koiwai, O., Kusuhara, H., and Wakita, T. Evaluation and identification of hepatitis B virus entry inhibitors using HepG2 cells overexpressing a membrane transporter NTCP. *Biochem Biophys Res Commun* **443**, 808-813 (2014).
34. Inuzuka, T., Takahashi, K., Chiba, T., and Marusawa, H. Mouse models of hepatitis B virus infection comprising host-virus immunologic interactions. *Pathogens* **3**, 377-89 (2014).
35. Barker, L.F., Chisari, F.V., McGrath, P.P., Dalgard, D.W., Kirschstein, R.L., Almeida, J.D., Edington, T.S., Sharp, D.G., and Peterson, M.R. Transmission of type B viral hepatitis tochimpanzees. *J Infect Dis* **127**, 648-662 (1973).
36. Walter, E., Keist, R., Niederost, B., Pult, I., and Blum, H.E. Hepatitis B virus infection of tupaia hepatocytes *in vitro* and in *vivo*. *Hepatology* **24**, 1-5 (1996).
37. Guidotti, L.G., Matzke, B., Schaller, H., and Chisari, F.V. High-level hepatitis B virus replication intransgenic mice. *J Virol* **69**, 6158–6169 (1995).
38. Yang, P.L., Althage, A., Chung, J., and Chisari, F.V. Hydrodynamic injection of viral DNA: A mousemodel of acute hepatitis B virus infection. *Proc Natl Acad Sci U*

S A **99**, 13825-13830 (2002).

39. Dion, S., Bourgine, M., Godon, O., Levillayer, F., and Michel, M.L. Adeno-associated virus-mediatedgene transfer leads to persistent hepatitis B virus replication in mice expressing HLA-A2 andHLA-DR1 molecules. *J Virol* **87**, 5554-5563 (2013).
40. Tateno, C., Yoshizane, Y., Saito, N., Kataoka, M., Utoh, R., Yamasaki, C., Tachibana, A., Soeno, Y., Asahina, K., Hino, H., Asahara, T., Yokoi, T., Furukawa, T., and Yoshizato, K. Near completely humanized liver in mice shows human-type metabolic responses to drugs. *Am J Pathol* **165**, 901-912 (2004).
41. Petersen, J., Dandri, M., Mier, W., Lutgehetmann, M., Volz, T., von Weizsacker, F., Haberkorn,U., Fischer, L., Pollok, J.M., Erbes, B., Seitz, S., and Urban, S. Prevention of hepatitis B virus infection *in vivo* byentry inhibitors derived from the large envelope protein. *Nat Biotechnol* **26**, 335-341 (2008).
42. Yatsuji, H., Noguchi, C., Hiraga, N., Mori, N., Tsuge, M., Imamura, M., Takahashi, S., Iwao, E., Fujimoto, Y., Ochi, H., Abe, H., Maekawa, T., Tateno, C., Yoshizato, K., Suzuki, F., Kumada, H., and Chayama, K. Emergence of a novel lamivudine-resistant hepatitis B virus variantwith a substitution outside the YMDD motif. *Antimicrob. Agents Chemother* **50**, 3867-3874 (2006).
43. Koyama, S., Ishii, K.J., Coban, C., and Akira, S. Innate immune response to viral infection. *Cytokine* **43**, 336-41 (2008).
44. Takeuchi, O., and Akira, S. Innate immunity to virus infection. *Immunol Rev* **227**, 75-86 (2009).
45. González-Navajas, J.M., Lee, J., David, M., and Raz, E. Immunomodulatory functions of type I interferons. *Nat Rev Immunol* **12**, 125-135 (2012).
46. Prokunina-Olsson, L., Muchmore, B., Tang, W., Pfeiffer, R.M., Park, H., Dickensheets, H., Hergott, D., Porter-Gill, P., Mumy, A., Kohaar, I., Chen, S., Brand, N., Tarway, M., Liu, L., Sheikh, F., Astemborski, J., Bonkovsky, H.L., Edlin, B.R., Howell, C.D., Morgan, T.R., Thomas, D.L., Rehermann, B., Donnelly, R.P., and O'Brien, T.R. A variant upstream of IFNL3 (IL28B) creating a new interferon gene IFNL4 is associated with impaired clearance of hepatitis C virus. *Nat Genet* **45**, 164-171 (2013).
47. Ank, N., West, H., Bartholdy, C., Eriksson, K., Thomsen, A.R., and Paludan, S.R. Lambda interferon (IFN-λ), a type III IFN, is induced by viruses and IFNs and

displays potent antiviral activity against select virus infections *in vivo*. *J Virol* **80**, 4501-4509 (2006).

48. Samuel, C.E. Antiviral actions of interferons. *Clin Microbiol Rev* **14**, 778-809 (2001).
49. Sadler, A.J., and Williams, B.R. Interferon-inducible antiviral effectors. *Nat Rev Immunol* **8**, 559-568 (2008).
50. Le Bon, A., and Tough, D.F. Links between innate and adaptive immunity via type I interferon. *Curr Opin Immunol* **14**, 432-436 (2002).
51. Broz, P., Monack, D.M. Newly described pattern recognition receptors team up against intracellular pathogens. *Nat Rev Immunol* **13**, 551-565 (2013).
52. Brubaker, S.W., Bonham, K.S., Zanoni, I., and Kagan, J.C. Innate immune pattern recognition: a cell biological perspective. *Annu Rev Immunol*. **33**, 257-290 (2015).
53. Mahla, R.S., Reddy, M.C., Prasad, D.V., and Kumar, H. Sweeten PAMPs: role of sugar complexed PAMPs in innate immunity and vaccine biology. *Front Immunol* **4**, 248 (2013).
54. Hardison, S.E., and Brown, G.D. C-type lectin receptors orchestrate antifungal immunity. *Nat Immunol* **13**, 817-822 (2012).
55. Sancho, D., and Reis e Sousa, C. Signaling by myeloid C-type lectin receptors in immunity and homeostasis. *Annu Rev Immunol*. **30**, 491-529 (2012).
56. Yoneyama, M., Onomoto, K., Jogi, M., Akaboshi, T., and Fujita, T. Viral RNA detection by RIG-I-like receptors. *Curr Opin Immunol* **32**, 48-53 (2015).
57. Schlee, M. Master sensors of pathogenic RNA-RIG-I like receptors. *Immunobiology* **218**, 1322-1335 (2013).
58. Chiu, Y.H., Macmillan, J.B., and Chen, Z.J. RNA polymerase III detects cytosolic DNA and induces type I interferons through the RIG-I pathway. *Cell* **138**, 576-591 (2009).
59. Kolakofsky, D., Kowalinski, E., and Cusack, S. A structure-based model of RIG-I activation. *RNA* **18**, 2118-2127 (2012).
60. Peisley, A., Wu, B., Xu, H., Chen, Z.J., and Hur, S. Structural basis for ubiquitin-mediated antiviral signal activation by RIG-I. *Nature* **509**, 110-114 (2014).
61. Jiang, X., Kinch, L.N., Brautigam, C.A., Chen, X., Du, F., Grishin, N.V., and Chen, Z.J. Ubiquitin-induced oligomerization of the RNA sensors RIG-I and MDA5 activates antiviral innate immune response. *Immunity* **36**, 959-973 (2012).

62. Zhu, Z., Zhang, X., Wang, G., and Zheng, H. The laboratory of genetics and physiology 2: emerging insights into the controversial functions of this RIG-I-like receptor. *Biomed Res Int* **2014**, 960190 (2014).
63. Ratsimandresey, R.A., Dorfleutner, A., and Stehlik, C. An update on PYRIN domain-containing pattern recognition receptors: from immunity to pathology. *Front Immunol* **4**, 440 (2013).
64. Morrone, S.R., Matyszewski, M., Yu, X., Delannoy, M., Egelman, E.H., and Sohn, J. Assembly-driven activation of the AIM2 foreign-dsDNA sensor provides a polymerization template for downstream ASC. *Nat Commun*. **6**, 7827 (2015).
65. Morrone, S.R., Wang, T., Constantoulakis, L.M., Hooy, R.M., Delannoy, M.J., and Sohn, J. Cooperative assembly of IFI16 filaments on dsDNA provides insights into host defense strategy. *Proc Natl Acad Sci U S A* **111**, E62-71 (2014).
66. Lu, A., Magupalli, V.G., Ruan, J., Yin, Q., Atianand, M.K., Vos, M.R., Schröder, G.F., Fitzgerald, K.A., Wu, H., and Egelman, E.H. Unified polymerization mechanism for the assembly of ASC-dependent inflammasomes. *Cell* **156**, 1193-1206 (2014).
67. Shaw, N., and Liu, Z.J. Role of the HIN domain in regulation of innate immune responses. *Mol Cell Biol* **34**, 2-15 (2014).
68. Duan, X., Ponomareva, L., Veeranki, S., Panchanathan, R., Dickerson, E., and Choubey, D. Differential roles for the interferon-inducible IFI16 and AIM2 innate immune sensors for cytosolic DNA in cellular senescence of human fibroblasts. *Mol Cancer Res* **9**, 589-602 (2011).
69. Corridoni, D., Arseneau, K.O., Cifone, M.G., and Cominelli, F. The dual role of nod-like receptors in mucosal innate immunity and chronic intestinal inflammation. *Front Immunol* **5**, 317 (2014).
70. Saxena, M., and Yeretssian, G. NOD-like receptors: master regulators of inflammation and cancer. *Front Immunol* **5**, 327 (2014).
71. Strober, W., Murray, P.J., Kitani, A., and Watanabe, T. Signalling pathways and molecular interactions of NOD1 and NOD2. *Nat Rev Immunol* **6**, 9-20 (2006).
72. Sabbah, A., Chang, T.H., Harnack, R., Frohlich, V., Tominaga, K., Dube, P.H., Xiang, Y., and Bose, S. Activation of innate immune antiviral responses by Nod2. *Nat Immunol* **10**, 1073-1080 (2009).
73. Vanaja, S.K., Rathinam, V.A., and Fitzgerald, K.A. Mechanisms of inflammasome

activation: recent advances and novel insights. *Trends Cell Biol* **25**, 308-315 (2015).

74. Takaoka, A., Wang, Z., Choi, M.K., Yanai, H., Negishi, H., Ban, T., Lu, Y., Miyagishi, M., Kodama, T., Honda, K., Ohba, Y., and Taniguchi, T. DAI (DLM-1/ZBP1) is a cytosolic DNA sensor and an activator of innate immune response. *Nature* **448**, 501-505 (2007).
75. Wang, Z., Choi, M.K., Ban, T., Yanai, H., Negishi, H., Lu, Y., Tamura, T., Takaoka, A., Nishikura, K., and Taniguchi, T. Regulation of innate immune responses by DAI (DLM-1/ZBP1) and other DNA-sensing molecules. *Proc Natl Acad Sci U S A* **105**, 5477-5482 (2008).
76. Rebsamen, M., Heinz, L.X., Meylan, E., Michallet, M.C., Schroder, K., Hofmann, K., Vazquez, J., Benedict, C.A., and Tschopp, J. DAI/ZBP1 recruits RIP1 and RIP3 through RIP homotypic interaction motifs to activate NF-kappaB. *EMBO Rep* **10**, 916-922 (2009).
77. Furr, S.R., Chauhan, V.S., Moerdyk-Schauwecker, M.J., and Marriott, I. A role for DNA-dependent activator of interferon regulatory factor in the recognition of herpes simplex virus type 1 by glial cells. *J Neuroinflammation* **8**, 99 (2011).
78. DeFilippis, V.R., Alvarado, D., Sali, T., Rothenburg, S., and Fruh, K. Human cytomegalovirus induces the interferon response via the DNA sensor ZBP1. *J Virol* **84**, 585-598 (2010).
79. Yang, P., An, H., Liu, X., Wen, M., Zheng, Y., Rui, Y., and Cao, X. The cytosolic nucleic acid sensor LRRFIP1 mediates the production of type I interferon via a beta-catenin-dependent pathway. *Nat Immunol* **11**, 487-494 (2010).
80. Parvatiyar, K., Zhang, Z., Teles, R.M., Ouyang, S., Jiang, Y., Iyer, S.S., Zaver, S.A., Schenk, M., Zeng, S., Zhong, W., Liu, Z.J., Modlin, R.L., Liu, Y.J., and Cheng, G. The helicase DDX41 recognizes the bacterial secondary messengers cyclic di-GMP and cyclic di-AMP to activate a type I interferon immune response. *Nat Immunol* **13**, 1155-1161 (2012).
81. Zhang, Z., Yuan, B., Bao, M., Lu, N., Kim, T., Liu, Y.J. The helicase DDX41 senses intracellular DNA mediated by the adaptor STING in dendritic cells. *Nat Immunol* **12**, 959-965 (2011).
82. Kim, T., Pazhoor, S., Bao, M., Zhang, Z., Hanabuchi, S., Facchinetti, V., Bover, L., Plumas, J., Chaperot, L., Qin, J., and Liu, Y.J. Aspartate-glutamate-alanine-histidine box motif (DEAH)/RNA helicase A helicases sense microbial DNA in human

plasmacytoid dendritic cells. *Proc Natl Acad Sci U S A* **107**, 15181-15186 (2010).

83. Sun, L., Wu, J., Du, F., Chen, X., and Chen, Z.J. Cyclic GMP-AMP synthase is a cytosolic DNA sensor that activates the type I interferon pathway. *Science* **339**, 786-791 (2013).
84. Wu, J., Sun, L., Chen, X., Du, F., Shi, H., Chen, C., and Chen, Z.J. Cyclic GMP-AMP is an endogenous second messenger in innate immune signaling by cytosolic DNA. *Science* **339**, 826-830 (2013).
85. Burdette, D.L., Monroe, K.M., Sotelo-Troha, K., Iwig, J.S., Eckert, B., Hyodo, M., Hayakawa, Y., and Vance, R.E. STING is a direct innate immune sensor of cyclic di-GMP. *Nature* **478**, 515-518 (2011).
86. Zhang, X., Shi, H., Wu, J., Zhang, X., Sun, L., Chen, C., and Chen, Z.J. Cyclic GMP-AMP containing mixed phosphdiester linkages is an endogenous high-affinity ligand for STING. *Mol Cell* **51**, 226-235 (2013).
87. Tamayo, R., Pratt, J.T., and Camilli, A. Roles of cyclic diguanylate in the regulation of bacterial pathogenesis. *Annu. Rev. Microbiol* **61**, 131-148 (2007).
88. Römling, U. Great times for small molecules: c-di-AMP, a second messenger candidate in Bacteria and Archaea. *Sci Signal* **1**, pe39 (2008).
89. Davies, B.W., Bogard, R.W., Young, T.S., and Mekalanos, J.J. Coordinated regulation of accessory genetic elements produces cyclic di-nucleotides for *V. cholerae* virulence. *Cell* **149**, 358-370 (2012).
90. Jin, L., Hill, K.K., Filak, H., Mogan, J., Knowles, H., Zhang, B., Perraud, A.L., Cambier, J.C., and Lenz, L.L. MPYS is required for IFN response factor 3 activation and type I IFN production in the response of cultured phagocytes to bacterial second messengers cyclic-di-AMP and cyclic-di-GMP. *J Immunol* **187**, 2595-2601 (2011).
91. Abe, T., and Barber, G.N. Cytosolic-DNA-mediated, STING-dependent proinflammatory gene induction necessitates canonical NF-κB activation through TBK1. *J Virol* **88**, 5328-5341 (2014).
92. He, X., Jia, H., Jing, Z., and Liu, D. Recognition of pathogen-associated nucleic acids by endosomal nucleic acid-sensing toll-like receptors. *Acta Biochim Biophys Sin* **45**, 241-258 (2013).
93. Lee, B.L., and Barton, G.M. Trafficking of endosomal Toll-like receptors. *Trends Cell Biol* **24**, 360-369 (2014).
94. Hemmi, H., Takeuchi, O., Kawai, T., Kaisho, T., Sato, S., Sanjo, H., Matsumoto, M.,

Hoshino, K., Wagner, H., Takeda, K., and Akira, S. A Toll-like receptor recognizes bacterial DNA. *Nature* **408**, 740-745 (2000).

95. Hornung, V., Ellegast, J., Kim, S., Brzózka, K., Jung, A., Kato, H., Poeck, H., Akira, S., Conzelmann, K.K., Schlee, M., Endres, S., and Hartmann, G. 5'-Triphosphate RNA is the ligand for RIG-I. *Science* **314**, 994-997 (2006).
96. Liddicoat, B.J., Piskol, R., Chalk, A.M., Ramaswami, G., Higuchi, M., Hartner, J.C., Li, J.B., Seeburg, P.H., and Walkley, C.R. RNA editing by ADAR1 prevents MDA5 sensing of endogenous dsRNA as nonself. *Science* **349**, 1115-1120 (2015).
97. Schuberth-Wagner, C., Ludwig, J., Bruder, A.K., Herzner, A.M., Zillinger, T., Goldeck, M., Schmidt, T., Schmid-Burgk, J.L., Kerber, R., Wolter, S., Stümpel, J.P., Roth, A., Bartok, E., Drosten, C., Coch, C., Hornung, V., Barchet, W., Kümmerer, B.M., Hartmann, G., and Schlee, M. A conserved histidine in the RNA Sensor RIG-I controls immune tolerance to N1-2'O-methylated self RNA. *Immunity* **43**, 41-51 (2015).
98. Yang, Y.G., Lindahl, T., and Barnes, D.E. Trex1 exonuclease degrades ssDNA to prevent chronic checkpoint activation and autoimmune disease. *Cell* **131**, 873-886 (2007).
99. Gao, D., Li, T., Li, X.D., Chen, X., Li, Q.Z., Wight-Carter, M., and Chen, Z.J. Activation of cyclic GMP-AMP synthase by self-DNA causes autoimmune diseases. *Proc Natl Acad Sci U S A* 201516465 [Epub ahead of print] (2015).
100. Simmons, R.A., Willberg, C.B., and Paul, K. Immune evasion by viruses. *eLS*. [doi: 10.1002/9780470015902.a0024790] (2013).
101. Pathak, H.B., Arnold, J.J., Wiegand, P.N., Hargittai, M.R., and Cameron, C.E. Picornavirus genome replication: assembly and organization of the VPg uridylylation ribonucleoprotein (initiation) complex. *J Biol Chem* **282**, 16202-16213 (2007).
102. Habjan, M., Andersson, I., Klingström, J., Schümann, M., Martin, A., Zimmermann, P., Wagner, V., Pichlmair, A., Schneider, U., Mühlberger, E., Mirazimi, A., and Weber, F. Processing of genome 5' termini as a strategy of negative-strand RNA viruses to avoid RIG-I-dependent interferon induction. *PLoS One* **3**, e2032 (2008).
103. Hastie, K.M., Kimberlin, C.R., Zandonatti, M.A., MacRae, I.J., and Saphire, E.O. Structure of the Lassa virus nucleoprotein reveals a dsRNA-specific 3′ to 5′ exonuclease activity essential for immune suppression. *Proc Natl Acad Sci U S A* **108**,

2396-2401 (2011).

104. Yan, N., Regalado-Magdos, A.D., Stiggelbout, B., Lee-Kirsch, M.A., and Lieberman, J. The cytosolic exonuclease TREX1 inhibits the innate immune response to human immunodeficiency virus type 1. *Nat Immunol* **11**, 1005-1013 (2010).

105. Papon, L., Oteiza, A., Imaizumi, T., Kato, H., Brocchi, E., Lawson, T.G., Akira, S., and Mechti, N. The viral RNA recognition sensor RIG-I is degraded during encephalomyocarditis virus (EMCV) infection. *Virology* **393**, 311-318 (2009).

106. Li, X.D., Sun, L., Seth, R.B., Pineda, G., and Chen, Z.J. Hepatitis C virus protease NS3/4A cleaves mitochondrial antiviral signaling protein off the mitochondria to evade innate immunity. *Proc Natl Acad Sci U S A* **102**, 17717-17722 (2005).

107. Bowie, A.G., and Unterholzner, L. Viral evasion and subversion of pattern-recognition receptor signaling. *Nat Rev Immunol* **8**, 911-922 (2008).

108. Hornef, M.W., Wick, M.J., Rhen, M., and Normark, S. Bacterial strategies for overcoming host innate and adaptive immune responses. *Nat. Immunol* **3**,1033-1040. (2002).

109. Andersen-Nissen, E., Smith, K.D., Strobe, K.L., Barrett, S.L., Cookson, B.T., Logan, S.M., and Aderem, A. Evasion of Toll-like receptor 5 by flagellated bacteria. *Proc Natl Acad Sci U S A* **102**, 9247-9252 (2005).

110. Wieland, S., Thimme, R., Purcell, R.H., and Chisari, F.V. Genomic analysis of the host response to hepatitis B virus infection. *Proc Natl Acad Sci U S A* **101**, 6669-6674 (2004).

111. Dunn, C., Peppa, D., Khanna, P., Nebbia, G., Jones, M., Brendish, N., Lascar, R.M., Brown, D., Gilson, R.J., Tedder, R.J., Dusheiko, G.M., Jacobs, M., Klenerman, P., and Maini, M.K. Temporal analysis of early immune responses in patients with acute hepatitis B virus infection. *Gastroenterology* **137**, 1289-1300 (2009).

112. World Health Organization. Hepatitis B: Fact Sheet. Geneva: World Health Organization, 2015. http://www.who.int/mediacentre/factsheets/fs204/en/

113. McClary, H., Koch, R., Chisari, F.V., and Guidotti, L.G. Relative sensitivity of hepatitis B virus and other hepatotropic viruses to the antiviral effects of cytokines. *J Virol* **74**, 2255-2264 (2000).

114. Stacey, A.R., Norris, P.J., Qin, L., Haygreen, E.A., Taylor, E., Heitman, J., Lebedeva, M., DeCamp, A., Li, D., Grove, D., Self, S.G., and Borrow, P. Induction of a striking systemic cytokine cascade prior to peak viremia in acute human

immunodeficiency virus type 1 infection, in contrast to more modest and delayed responses in acute hepatitis B and C virus infections. *J Virol* **83**, 3719-3733 (2009).

115. Hösel, M., Quasdorff, M., Wiegmann, K., Webb, D., Zedler, U., Broxtermann, M., Tedjokusumo, R., Esser, K., Arzberger, S., Kirschning, C.J., Langenkamp, A., Falk, C., Büning, H., Rose-John, S., and Protzer, U. Not interferon, but interleukin-6 controls early gene expression in hepatitis B virus infection. *Hepatology* **50**, 1773-1782 (2009).

116. Lütgehetmann, M., Bornscheuer, T., Volz, T., Allweiss, L., Bockmann, J.H., Pollok, J.M., Lohse, A.W., Petersen, J., and Dandri, M. Hepatitis B virus limits response of human hepatocytes to interferon-α in chimeric mice. *Gastroenterology* **140**, 2074-2083 (2011).

117. Hong, M., Sandalova, E., Low, D., Gehring, A.J., Fieni, S., Amadei, B., Urbani, S., Chong, Y.S., Guccione, E., and Bertoletti, A. Trained immunity in newborn infants of HBV-infected mothers. *Nat Commun* **6**, 6588 (2015).

118. Boltjes, A., Groothuismink, Z.M., van Oord, G.W., Janssen, H.L., Woltman, A.M., and Boonstra, A. Monocytes from chronic HBV patients react *in vitro* to HBsAg and TLR by producing cytokines irrespective of stage of disease. *PLoS One* **9**, e97006 (2014).

119. You, C.R., Lee, S.W., Jang, J.W., and Yoon, S.K. Update on hepatitis B virus infection. *World J. Gastroenterol* **20**, 13293-13305 (2014).

120. Chang, J., Guo, F., Zhao, X., and Guo, J.T. Therapeutic strategies for a functional cure of chronic hepatitis B virus infection. *Acta Pharmaceutica Sinica B* **4**, 248-257 (2014).

121. Leaman, D.W. Mechanism of interferon action. *Prog Mol Subcell Biol* **20**, 101-142 (1998).

122. Caselmann, W.H., Meyer, M., Scholz, S., Hofschneider, P.H., and Koshy, R. Type I interferons inhibit hepatitis B virus replication and induce hepatocellular gene expression in cultured liver cells. *J Infect Dis* **166**, 966-971 (1992).

123. Cavanaugh, V.J., Guidotti, L.G., and Chisari, F.V. Inhibition of hepatitis B virus replication during adenovirus and cytomegalovirus infections in transgenic mice. *J Virol* **72**, 2630-2637 (1998).

124. Nawa, T., Ishida, H., Tatsumi, T., Li, W., Shimizu, S., Kodama, T., Hikita, H., Hosui, A., Miyagi, T., Kanto, T., Hiramatsu, N., Hayashi, N., and Takehara, T.

Interferon-α suppresses hepatitis B virus enhancer II activity via the protein kinase C pathway. *Virology* **432**, 452-459 (2012).

125. Belloni, L., Allweiss, L., Guerrieri, F., Pediconi, N., Volz, T., Pollicino, T., Petersen, J., Raimondo, G., Dandri, M., and Levrero, M. IFN-α inhibits HBV transcription and replication in cell culture and in humanized mice by targeting the epigenetic regulation of the nuclear cccDNA minichromosome. *J Clin Invest* **122**, 529-537 (2012).

126. Xu, C., Guo, H., Pan, X.B., Mao, R., Yu, W., Xu, X., Wei, L., Chang, J., Block, T.M., and Guo, J.T. Interferons accelerate decay of replication-competent nucleocapsids of hepatitis B virus. *J Virol* **84**, 9332-9340 (2010).

127. Pei, R.J., Chen, X.W., and Lu, M.J. Control of hepatitis B virus replication by interferons and Toll-like receptor signaling pathways. *World J Gastroenterol* **20**, 11618-11629 (2014).

128. Lucifora, J., Xia, Y., Reisinger, F., Zhang, K., Stadler, D., Cheng, X., Sprinzl, M.F., Koppensteiner, H., Makowska, Z., Volz, T., Remouchamps, C., Chou, W.M., Thasler, W.E., Hüser, N., Durantel, D., Liang, T.J., Münk, C., Heim, M.H., Browning, J.L., Dejardin, E., Dandri, M., Schindler, M., Heikenwalder, M., and Protzer, U. Specific and nonhepatotoxic degradation of nuclear hepatitis B virus cccDNA. *Science* **343**, 1221-1228 (2014).

129. Rijckborst, V., and Janssen, H.L. The role of interferon in hepatitis B therapy. *Curr Hepat Rep* **9**, 231-238 (2010).

130. Guidotti, L.G., Ishikawa, T., Hobbs, M.V., Matzke, B., Schreiber, R., and Chisari, F.V. Intracellular inactivation of the hepatitis B virus by cytotoxic T lymphocytes. *Immunity* **4**, 25-36 (1996).

131. Pagliaccetti, N.E., Chu, E.N., Bolen, C.R., Kleinstein, S.H., and Robek, M.D. Lambda and alpha interferons inhibit hepatitis B virus replication through a common molecular mechanism but with different *in vivo* activities. *Virology* **401**, 197-206 (2010).

132. Sommereyns, C., Paul, S., Staeheli, P., and Michiels, T. IFN-lambda (IFN-λ) is expressed in a tissue-dependent fashion and primarily acts on epithelial cells *in vivo*. *PLoS Pathog* **4**, e1000017 (2008).

133. Voigt, E., Inankur, B., Baltes, A., and Yin, J. A quantitative infection assay for human type I, II, and III interferon antiviral activities. *Virol J* **10**, 224 (2013).

134. Craxi, A., and Cooksley, W.G. Pegylated interferons for chronic hepatitis B. *Antiviral Res* **60**, 87-89 (2003).
135. Kwon, H., and Lok, A.S. Hepatitis B therapy. *Nat Rev Gastroenterol Hepatol* **8**, 275-284 (2011).
136. Perrillo, R. Benefits and risks of interferon therapy for hepatitis B. *Hepatology* **49**, S103-111 (2009).
137. European Association For The Study Of The Liver. EASL clinical practice guidelines: Management of chronic hepatitis B virus infection. *J Hepatol* **57**, 167-185 (2012).
138. Chien, R.N., and Liaw, Y.F. Nucleos(t)ide analogues for hepatitis B virus: Strategies for long-term success. *Best Pract Res Clin Gastroenterol* **22**, 1081-1092 (2008).
139. Zoulim, F., and Locarnini, S. Hepatitis B virus resistance to nucleos(t)ide analogues. *J Virol* **137**, 1593-1608 (2009).
140. Hadziyannis, S.J. Update on hepatitis B virus infection: focus on treatment. *J Clin Transl Hepatol* **2**, 285-291 (2014).
141. Li, M.Y., Yuan, X.L., and Zhang, D.Z. Comparison of peg-interferon monotherapy to peg-interferon and nucleoside analogue combination therapy for hepatitis B: a meta-analysis of randomized controlled trials. *Zhonghua Gan Zang Bing Za Zhi* **20**, 442-447 (2012).
142. Wei, W., Wu, Q., Zhou, J., Kong, Y., and You, H.A. Better antiviral efficacy found in nucleos(t)ide analog (NA) combinations with interferon therapy than NA monotherapy for HBeAg positive chronic hepatitis B: A meta-analysis. *Int J Environ Res Public Health* **12**, 10039-10055 (2015).
143. Maepa, M.B., Roelofse, I., Ely, A., and Arbuthnot, P. Progress and prospects of anti-HBV gene therapy development. *Int J Mol Sci* **16**, 17589-17610 (2015).
144. Hasselblatt, P., Hockenjos, B., Thoma, C., Blum, H.E., and Offensperger, W.B. Translation of stablehepadnaviral mRNA cleavage fragments induced by the action of phosphorothioate-modifiedantisense oligodeoxynucleotides. *Nucleic Acids Res* **33**, 114-125 (2005).
145. DeVos, S.L., and Miller, T.M. Antisense oligonucleotides: treating neurodegeneration at the level of RNA. *Neurotherapeutics* **10**, 486-497 (2013).
146. Xia, C., Chen, Y.C., Gong, H., Zeng, W., Vu, G.P., Trang, P., Lu, S., Wu, J., and

Liu, F. Inhibition of hepatitis B virus gene expression and replication by ribonuclease P. *Mol Ther* 21, 995-1003 (2013).

147. Chen, Y., Cheng, G., and Mahato, R. RNAi for treating hepatitis B viral infection. *Pharm Res* 25, 72-86 (2008).

148. Sebestyen, M.G., Wong, S.C., Trubetskoy, V., Lewis, D.L., and Wooddell, C.I. Targeted *in vivo* delivery of siRNA and an endosome-releasing agent to hepatocytes. *Methods Mol Biol* **1218**, 163-186 (2015).

149. Weber, N.D., Stone, D., Sedlak, R.H., de Silva Feelixge, H.S., Roychoudhury, P., Schiffer, J.T., Aubert, M., and Jerome, K.R. AAV-mediated delivery of zinc finger nucleases targeting hepatitis B virus inhibits active replication. *PLoS One* **9**, e97579 (2014).

150. Chen, J., Zhang, W., Lin, J., Wang, F., Wu, M., Chen, C., Zheng, Y., Peng, X., Li, J., and Yuan, Z. An efficient antiviral strategy for targeting hepatitis B virus genome using transcription activator-like effector nucleases. *Mol Ther* **22**, 303-311 (2014).

151. Lin, S.R., Yang, H.C., Kuo, Y.T., Liu, C.J., Yang, T.Y., Sung, K.C., Lin, Y.Y., Wang, H.Y., Wang, C.C., Shen, Y.C., Wu, F.Y., Kao, J.H., Chen, D.S., and Chen, P.J. The CRISPR-cas9 system facilitates clearance of the intrahepatic HBV templates *in vivo*. *Mol Ther Nucleic Acids* **3**, e186 (2014).

152. Deres, K., Schroder, C.H., Paessens, A., Goldmann, S., Hacker, H.J., Weber, O., Kramer, T., Niewohner, U., Pleiss, U., Stoltefuss, J., Graef, E., Koletzki, D., Masantschek, R.N., Reimann, A., Jaeger, R., Gross, R., Beckermann, B., Schlemmer, K.H., Haebich, D., and Rubsamen-Waigmann, H. Inhibition of hepatitis B virus replication by drug-induced depletion of nucleocapsids. *Science* **299**, 893-896 (2003).

153. Butz, K., Denk, C., Fitscher, B., Crnkovic-Mertens, I., Ullmann, A., Schroder, C.H., and Hoppe-Seyler, F. Peptide aptamers targeting the hepatitis B virus core protein: a new class of molecules with antiviral activity. *Oncogene* **20**, 6579-6586 (2001).

154. Tomai, E., Butz, K., Lohrey, C., von Weizsacker, F., Zentgraf, H., and Hoppe-Seyler, F. Peptide aptamer-mediated inhibition of target proteins by sequestration into aggresomes. *J Biol Chem* **281**, 21345-21352 (2006).

155. Zhang, W., Ke, W., Wu, S.S., Gan, L., Zhou, R., Sun, C.Y., Long, Q.S., Jiang, W., and Xin, H.B. An adenovirus-delivered peptide aptamer C1-1 targeting the core protein of hepatitis B virus inhibits viral DNA replication and production *in vitro* and

in vivo. *Peptides* **30**, 1816-1821 (2009).

156. Sugiyama, M., Tanaka, Y., Kato, T., Orito, E., Ito, K., Acharya, S.K., Gish, R.G., Kramvis, A., Shimada, T., Izumi, N., Kaito, M., Miyakawa, Y., and Mizokami, M. Influence of hepatitis B virus genotypes on the intra- and extracellular expression of viral DNA and antigens. *Hepatology* **44**, 915-924 (2006).

157. Sakamoto, T., Tanaka, Y., Watanabe, T., Iijima, S., Kani, S., Sugiyama, M., Murakami, S., Matsuura, K., Kusakabe, A., Shinkai, N., Sugauchi, F., and Mizokami, M. Mechanism of the dependence of hepatitis B virus genotype G on co-infection with other genotypes for viral replication. *J Viral Hepat* **20**, e27-36 (2013).

158. Hayakawa, S., Shiratori, S., Yamato, H., Kameyama, T., Kitatsuji, C., Kashigi, F., Goto, S., Kameoka, S., Fujikura, D., Yamada, T., Mizutani, T., Kazumata, M., Sato, M., Tanaka, J., Asaka, M., Ohba, Y., Miyazaki, T., Imamura, M., and Takaoka, A. ZAPS is a potent stimulator of signaling mediated by the RNA helicase RIG-I during antiviral responses. *Nat Immunol* **12**, 37-44 (2011).

159. Tateno, C., Yoshizane, Y., Saito, N., Kataoka, M., Utoh, R., Yamasaki, C., Tachibana, A., Soeno, Y., Asahina, K., Hino, H., Asahara, T., Yokoi, T., Furukawa, T., and Yoshizato, K. Near completely humanized liver in mice shows human-type metabolic responses to drugs. *Am J Pathol* **165**, 901-912 (2004).

160. Kao, C., Zheng, M., and Rüdisser, S. A simple and efficient method to reduce nontemplated nucleotide addition at the 3 terminus of RNAs transcribed by T7 RNA polymerase. *RNA* **5**, 1268-1272 (1999).

161. Turelli, P., Mangeat, B., Jost, S., Vianin, S., and Trono, D. Inhibition of hepatitis B virus replication by APOBEC3G. *Science* **303**, 1829 (2004).

162. Fujiwara, K., Tanaka, Y., Paulon, E., Orito, E., Sugiyama, M., Ito, K., Ueda, R., Mizokami, M., and Naoumov, N.V. Novel type of hepatitis B virus mutation: replacement mutation involving a hepatocyte nuclear factor 1 binding site tandem repeat in chronic hepatitis B virus genotype E. *J Virol* **79**, 14404-14410 (2005).

163. Sato, Y., Hatakeyama, H., Sakurai, Y., Hyodo, M., Akita, H. and Harashima, H. A pH-sensitive cationic lipid facilitates the delivery of liposomal siRNA and gene silencing activity in *vitro* and *in vivo*. *J Control Release* **163**, 267-276 (2012).

164. Saito, T., Hirai, R., Loo, Y.M., Owen, D., Johnson, C.L., Sinha, S.C., Akira, S., Fujita, T., and Gale, M. Regulation of innate antiviral defenses through a shared

repressor domain in RIG-I and LGP2. *Proc Natl Acad Sci U S A* **104**, 582-587 (2007).

165. Junker-Niepmann, M., Bartenschlager, R., and Schaller, H. A short cis-acting sequence is required for hepatitis B virus pregenome encapsidation and sufficient for packaging of foreign RNA. *EMBO J* **9**, 3389-3396 (1990).

166. Cui, S., Eisenächer, K., Kirchhofer, A., Brzózka, K., Lammens, A., Lammens, K., Fujita, T., Conzelmann, K.K., Krug, A., and Hopfner, K.P. The C-terminal regulatory domain is the RNA 5'-triphosphate sensor of RIG-I. *Mol Cell* **29**, 169-179 (2008).

167. Saito, T., Owen, D.M., Jiang, F., Marcotrigiano, J., and Gale, M. Innate immunity induced by composition-dependent RIG-I recognition of hepatitis C virus RNA. *Nature* **454**, 523-527 (2008).

168. Sumpter, R., Loo, Y.M., Foy, E., Li, K., Yoneyama, M., Fujita, T., Lemon, S.M., and Gale, M. Regulating intracellular antiviral defense and permissiveness to hepatitis C virus RNA replication through a cellular RNA helicase, RIG-I. *J Virol* **79**, 2689-2699 (2005).

169. Takahasi, K., Yoneyama, M., Nishihori, T., Hirai, R., Kumeta, H., Narita, R., Gale, M., Inagaki, F., and Fujita, T. Nonself RNA-sensing mechanism of RIG-I helicase and activation of antiviral immune responses. *Mol Cell* **29**, 428-440 (2008).

170. Wei, C., Ni, C., Song, T., Liu, Y., Yang, X., Zheng, Z., Jia, Y., Yuan, Y., Guan, K., Xu, Y., Cheng, X., Zhang, Y., Wang, Y., Wen, C., Wu, Q., Shi, W., and Zhong, H. The hepatitis B virus X protein disrupts innate immunity by downregulating mitochondrial antiviral signaling protein. *J Immunol* **185**, 1158-1168 (2010).

171. Kumar, M., Jung, S.Y., Hodgson, A.J., Madden, C.R., Qin, J., and Slagle, B.L. Hepatitis B Virus regulatory HBx protein binds to adaptor protein IPS-1 and inhibits the activation of beta interferon. *J Virol*, **85**, 987-995 (2011).

172. Yu, S., Chen, J., Wu, M., Chen, H., Kato, N., and Yuan, Z. HepatitisB virus polymerase inhibits RIG-I- and Toll-like receptor 3-mediated beta interferon induction in human hepatocytes through interference with interferon regulatory factor 3 activation and dampening of the interaction between TBK1/ IKKepsilon and DDX3. *J Gen Virol* **91**, 2080-2090 (2010).

173. Wang, H., and Ryu, W.S. Hepatitis B virus polymerase blocks pattern recognition receptor signaling via interaction with DDX3: implications for immune evasion. *PLoS Pathog* **6**, e1000986 (2010).

174. Twu, J.S., Lee, C.H., Lin, P.M., and Schloemer, R.H. Hepatitis B virus suppresses expression of human beta-interferon. *Proc Natl Acad Sci U S A* **85**, 252-256 (1988).

175. Whitten, T.M., Quets, A.T., and Schloemer, R.H. Identification of the hepatitis B virus factor that inhibits expression of the beta interferon gene. *J Virol* **65**, 4699-4704 (1991).

176. Fernandez, M., Quiroga, J.A., and Carreno, V. Hepatitis B virus downregulates the human interferon-inducible MxA promoter through direct interaction of precore/core proteins. *J Gen Virol* **84**, 2073-2082 (2003).

177. Fernandez, M., Quiroga, J.A., Martin, J., Cotonat, T., Pardo, M., Horisberger, M.A., Carreno, V. Impaired interferon induction of human MxA protein in chronic hepatitis B virus infection. *J Med Virol* **51**, 332-337 (1997).

178. Chen, J., and Yuan, Z. Interplay between hepatitis B virus and the innate immune responses: implications for new therapeutic strategies. *Virol Sin* **29**, 17-24 (2014).

179. Visvanathan, K., Skinner, N.A., Thompson, A.J., Riordan, S.M., Sozzi, V., Edwards, R., Rodgers, S., Kurtovic, J., Chang, J., Lewin, S., Desmond, P., and Locarnini, S. Regulation of Toll-like receptor-2 expression in chronic hepatitis B by the precore protein. *Hepatology* **45**, 102-110 (2007).

180. Lang, T., Lo, C., Skinner, N., Locarnini, S., Visvanathan, K., and Mansell, A. The Hepatitis B e antigen (HBeAg) targets and suppresses activation of the Toll-like receptor signaling pathway. *J Hepatol* **55**, 762-769 (2011).

181. Revill, P., Yuen, L., Walsh, R., Perrault, M., Locarnini, S., and Kramvis, A. Bioinformatic analysis of the hepadnavirus e-antigen and its precursor identifies remarkable sequence conservation in all orthohepadnaviruses. *J Med Virol* **82**, 104-115 (2010).

182. Wilson, R., Warner, N., Ryan, K., Selleck, L., Colledge, D., Rodgers, S., Li, K., Revill, P., and Locarnini, S. The hepatitis B e antigen suppresses IL-1â-mediated NF-êB activation in hepatocytes. *J Viral Hepat* **18**, e499-507 (2011).

183. Xu, Y., Hu, Y., Shi, B., Zhang, X., Wang, J., Zhang, Z., Shen, F., Zhang, Q., Sun, S., and Yuan, Z. HBsAg inhibits TLR9-mediated activation and IFN-alpha production in plasmacytoid dendritic cells. *Mol Immunol* **46**, 2640-2646 (2009).

184. Vincent, I.E., Zannetti, C., Lucifora, J., Norder, H., Protzer, U., Hainaut, P., Zoulim, F., Tommasino, M., Trepo, C., Hasan, U., and Chemin, I. Hepatitis B virus impairs TLR9 expression and function in plasmacytoid dendritic cells. *PLoS One* **6**,

e26315 (2011).

185. Vanlandschoot, P., Van Houtte, F., Roobrouck, A., Farhoudi, A., Stelter, F., Peterson, D.L., Gomez-Gutierrez, J., Gavilanes, F., Leroux-Roels, G. LPS-binding protein and CD14-dependent attachment of hepatitis B surface antigen to monocytes is determined by the phospholipid moiety of the particles. *J Gen Virol* **83**, 2279-2289 (2002).

186. Vanlandschoot, P., Roobrouck, A., Van Houtte, F., and Leroux-Roels, G. Recombinant HBsAg, an apoptotic-like lipoprotein, interferes with the LPS-induced activation of ERK-1/2 and JNK-1/2 in monocytes. *Biochem Biophys Res Commu*n **297**, 486-491 (2002).

187. Cheng, J., Imanishi, H., Morisaki, H., Liu, W., Nakamura, H., Morisaki, T., and Hada, T. Recombinant HBsAg inhibits LPS-induced COX-2 expression and IL-18 production by interfering with the NF-κB pathway in a human monocytic cell line, THP-1. *J Hepatol* **43**, 465-471 (2005).

188. Onoguchi, K., Yoneyama, M., Takemura, A., Akira, S., Taniguchi, T., Namiki, H., and Fujita, T. Viral infections activate types I and III interferon genes through a common mechanism. *J Biol Chem* **282**, 7576-7581 (2007).

189. Iversen, M.B., Ank, N., Melchjorsen, J., and Paludan, S.R. Expression of type III IFN in the vaginal mucosa is mediated primarily by DCs and displays stronger dependence on NF-kB than type I IFNs. *J Virol* **84**, 4579-4586 (2010).

190. Odendall, C., Dixit, E., Stavru, F., Bierne, H., Franz, K.M., Durbin, A.F., Boulant, S., Gehrke, L., Cossart, P., and Kagan, J.C. Diverse intracellular pathogens activate type III interferon expression from peroxisomes. *Nat Immunol* **15**, 717-726 (2014).

191. Nakagawa, S., Hirata, Y., Kameyama, T., Tokunaga, Y., Nishito, Y., Hirabayashi, K., Yano, J., Ochiya, T., Tateno, C., Tanaka, Y., Mizokami, M., Tsukiyama-Kohara, K., Inoue, K., Yoshiba, M., Takaoka, A. and Kohara, M. Targeted induction of interferon-λ in humanized chimeric mouse liver abrogates hepatotropic virus infection. *PLoS One* **8**, e59611 (2013).

192. Park, H., Serti, E., Eke, O., Muchmore, B., Prokunina-Olsson, L., Capone, S., Folgori, A., and Rehermann, B. IL-29 is the dominant type III interferon produced by hepatocytes during acute hepatitis C virus infection. *Hepatology* **56**, 2060-2070 (2012).

193. Jewell, N.A., Cline, T., Mertz, S.E., Smirnov, S.V., Flaño, E., Schindler, C.,

Grieves, J.L., Durbin, R.K., Kotenko, S.V., and Durbin, J.E. Lambda interferon is the predominant interferon induced by influenza A virus infection in *vivo*. *J Virol* **84**, 11515-11522 (2010).

194. Okabayashi, T., Kojima, T., Masaki, T., Yokota, S., Imaizumi, T., Tsutsumi, H., Himi, T., Fujii, N., and Sawada, N. Type-III interferon, not type-I, is the predominant interferon induced by respiratory viruses in nasal epithelial cells. *Virus Res* **160**, 360-366 (2011).

195. Crotta, S., Davidson, S., Mahlakoiv, T., Desmet, C.J., Buckwalter, M.R., Albert, M.L., Staeheli, P., and Wack, A. Type I and type III interferons drive redundant amplification loops to induce a transcriptional signature in influenza-infected airway epithelia. *PLoS Pathog* **9**, e1003773 (2013).

196. Fox, J.M., Crabtree, J.M., Sage, L.K., Tompkins, S.M., and Tripp, R.A. Interferon lambda upregulates IDO1 expression in respiratory epithelial cells after influenza virus Infection. *J Interferon Cytokine Res* **35**, 554-562 (2015).

197. Jeong, J.K., Yoon, G.S., and Ryu, W.S. Evidence that the 5'-end cap structure is essential for encapsidation of hepatitis B virus pregenomic RNA. *J Virol* **74**, 5502-5508 (2000).

198. Baum, A., Sachidanandam, R., and García-Sastre, A. Preference of RIG-I for short viral RNA molecules in infected cells revealed by next-generation sequencing. *Proc Natl Acad Sci U S A* **107**, 16303-16308 (2010).

199. You, S., and Rice, C.M. 3' RNA elements in hepatitis C virus replication: kissing partners and long poly(U). *J Virol* **82**, 184-195 (2008).

200. Huang, L., Hwang, J., Sharma, S.D., Hargittai, M.R., Chen, Y., Arnold, J.J., Raney, K.D., and Cameron, C.E. Hepatitis C virus nonstructural protein 5A (NS5A) is an RNA-binding protein. *J Biol Chem* **280**, 36417-36428 (2005).

201. Moeller, A., Kirchdoerfer, R.N., Potter, C.S., Carragher, B., and Wilson, I.A. Organization of the influenza virus replication machinery. *Science* **338**, 1631-1634 (2012).

202. Weber, M., Sediri, H., Felgenhauer, U., Binzen, I., Bänfer, S., Jacob, R., Brunotte, L., García-Sastre, A., Schmid-Burgk, J.L., Schmidt, T., Hornung, V., Kochs, G., Schwemmle, M., Klenk, H.D., and Weber, F. Influenza virus adaptation PB2-627K modulates nucleocapsid inhibition by the pathogen sensor RIG-I. *Cell Host Microbe* **17**, 309-319 (2015).

203. Mogensen, K.E., Lewerenz, M., Reboul, J., Lutfalla, G., and Uzé, G. The type I interferon receptor: structure, function, and evolution of a family business. *J Interferon Cytokine Res* **19**, 1069-1098 (1999).

204. Ank, N., and Paludan, S.R. Type III IFNs: new layers of complexity in innate antiviral immunity. *Biofactors* **35**, 82-87 (2009).

205. Donnelly, R.P., Sheikh, F., Kotenko, S.V., and Dickensheets, H. The expanded family of class II cytokines that share the IL-10 receptor-2 (IL-10R2) chain. *J Leukoc Biol* **76**, 314-321 (2004).

206. Sheppard, P., Kindsvogel, W., Xu, W., Henderson, K., Schlutsmeyer, S., Whitmore, T. E., Kuestner, R., Garrigues, U., Birks, C., Roraback, J., Ostrander, C., Dong, D., Shin, J., Presnell, S., Fox, B., Haldeman, B., Cooper, E., Taft, D., Gilbert, T., Grant, F. J., Tackett, M., Krivan, W., McKnight, G., Clegg, C., Foster, D., and Klucher, K. M. IL-28, IL-29 and their class II cytokine receptor IL-28R. *Nat Immunol* **4**, 63-68 (2003).

207. Bolen, C.R., Ding, S., Robek, M.D., and Kleinstein, S.H. Dynamic expression profiling of type I and type III interferon-stimulated hepatocytes reveals a stable hierarchy of gene expression. *Hepatology* **59**, 1262-1272 (2014).

208. Pagliaccetti, N.E., and Robek, M.D. Interferon-lambda in the immune response to hepatitis B virus and hepatitis C virus. *J Interferon Cytokine Res* **30**, 585-590 (2010).

209. Wack, A., Terczyńska-Dyla, E., and Hartmann, R. Guarding the frontiers: the biology of type III interferons. *Nat Immunol* **16**, 802-809 (2015).

210. Miller, D., Klucher, K., and Freeman, J. Interferon lambda as a potential new therapeutic for hepatitis C. *Ann N Y Acad Sci* **1182**, 80-87 (2009).

211. Muir, A.J., Arora, S., Everson, G., Flisiak, R., George, J., Ghalib, R., Gordon, S.C., Gray, T., Greenbloom, S., Hassanein, T., Hillson, J., Horga, M.A., Jacobson, I.M., Jeffers, L., Kowdley, K.V., Lawitz, E., Lueth, S., Rodriguez-Torres, M., Rustgi, V., Shemanski, L., Shiffman, M.L., Srinivasan, S., Vargas, H.E., Vierling, J.M., Xu, D., Lopez-Talavera, J.C., Zeuzem, S., and EMERGE study group. A randomized phase 2b study of peginterferon lambda-1a for the treatment of chronic HCV infection. *J Hepatol* **61**, 1238-1246 (2014).

212. Revill, P., and Yuan, Z. New insights into how HBV manipulates the innate immune response to establish acute and persistent infection. *Antivir Ther* **18**, 1-15 (2013).

213. Ebert, G., Poeck, H., Lucifora, J., Baschuk, N., Esser, K., Esposito, I., Hartmann, G., Protzer, U. 5' triphosphorylated small interfering RNAs control replication of hepatitis B virus and induce an interferon response in human liver cells and mice. *Gastroenterology* **141**, 696-706 (2011).

214. Zhang, X., Kraft, A., Broering, R., Schlaak, J.F., Dittmer, U., and Lu, M. Preclinical development of TLR ligands as drugs for the treatment of chronic viral infections. *Expert Opin Drug Discov* **7**, 597-611 (2012).

215. Isogawa, M., Robek, M.D., Furuichi, Y., and Chisari, F.V. Toll-like receptor signaling inhibits hepatitis B virus replication *in vivo*. *J Virol* **79**, 7269-7272 (2005).

216. Zhang, X., Meng, Z., Qiu, S., Xu, Y., Yang, D., Schlaak, J.F., Roggendorf, M., and Lu, M. Lipopolysaccharide-induced innate immune responses in primary hepatocytes downregulates woodchuck hepatitis virus replication via interferon-independent pathways. *Cell Microbiol* **11**, 1624-1637 (2009).

217. Guo, F., Han, Y., Zhao, X., Wang, J., Liu, F., Xu, C., Wei, L., Jiang, J.D., Block, T.M., Guo, J.T., and Chang, J. STING agonists induce an innate antiviral immune response against hepatitis B virus. *Antimicrob Agents Chemothe* **59**, 1273-1281 (2015).

218. Lanford, R.E., Guerra, B., Chavez, D., Giavedoni, L., Hodara, V.L., Brasky, K.M., Fosdick, A., Frey, C.R., Zheng, J., Wolfgang, G., Halcomb, R.L., and Tumas, D.B. GS-9620, an oral agonist of Toll-like receptor-7, induces prolonged suppression of hepatitis B virus in chronically infected chimpanzees. *Gastroenterology* **144**, 1508-1517 (2013).

219. Gane, E.J., Lim, Y.S., Gordon, S.C., Visvanathan, K., Sicard, E., Fedorak, R.N., Roberts, S., Massetto, B., Ye, Z., Pflanz, S., Garrison, K.L., Gaggar, A., Mani Subramanian, G., McHutchison, J.G., Kottilil, S., Freilich, B., Coffin, C.S., Cheng, W., and Kim, Y.J. The oral toll-like receptor-7 agonist GS-9620 in patients with chronic hepatitis B virus infection. *J Hepatol* **63**, 320-328 (2015).

220. Jing, Z., and Toshio, H. Small RNA molecules as therapeutic agents for viral infectious diseases. *J Pharmacol Toxicol* **2**, 103-113 (2007).

221. Zhang, J., Yamada, O., Sakamoto, T., Yoshida, H., Araki, H., Murata, T., and Shimotohno, K. Inhibition of hepatitis C virus replication by pol III-directed overexpression of RNA decoys corresponding to stem-loop structures in the NS5B coding region. *Virology* **342**, 276-285 (2005).

222. Bohjanen, P.R., Liu, Y., and Garcia-Blanco, M.A. TAR RNA decoys inhibit tat-activated HIV-1 transcription after preinitiation complex formation. *Nucleic Acids Res* **25**, 4481-4486 (1997).

223. Michienzi, A., Li, S., Zaia, J.A., and Rossi, J.J. A nucleolar TAR decoy inhibitor of HIV-1 replication. *Proc Natl Acad Sci U S A* **99**, 14047-14052 (2002).

Acknowledgements

Firstly, I would like to thank my supervisor Professor Akinori Takaoka. Thanks for giving me the opportunity to participate in this great research area, and also thanks for his guidance, great support and kind advice throughout this research. I learnt from him a great deal, not only his exceptional scientific knowledge but also his extraordinary human qualities of kindness, hearty, humour and understanding. Additionally, I would also like to thank my sub-adviser Professors Yasuyuki Fujita and Mutsumi Takagi for their kind, availability and constructive suggestions, which were determinant for the accomplishment of my doctoral study.

I am very much thankful and grateful to Dr. Seiichi Sato for the great support not only on research but also my life in Hokkaido. I learnt a great deal from working with him, not only professional experimental skills, but also communication skills, problem-solving and decision-making skills, as well as Japanese culture. Thank you also for the constructive comments during the writing of the thesis.

Thanks to all the collaboration partners of this work, T. Kameyama, T. Hayashi, Y. Sakurai, Y. Sato, H. Akita, and H. Harashima from Hokkaido University; S. Murakami, T. Watanabe, S. Iijima, S. Tsutsumi, and Y. Tanaka from Nagoya City University; K. Watashi, and T. Wakita from National Institute of Infectious Diseases, Tokyo; C. M. Rice (The Rockefeller University), Y. Ishida (PhoenixBio Co., Ltd. Japan), and M. Kohara (Tokyo Metropolitan Institute of Medical Science),

My sincere thanks also goes to M. Hijikata and K. Shimotohno (Kyoto University) for providing HuS-E/2 cell line, N. Sakamoto (Hokkaido University) for Huh-7.5.1/Rep-Feo-1b cells, A. Miyawaki (RIKEN) for pCAGGS-YFP vector, T. Fujita (Kyoto University) for the luciferase reporter plasmid p-55C1BLuc, A. Takada (Hokkaido University) for VSV, H. Kida (Hokkaido University) for NDV, H. Ishizu and T. Hirose (Hokkaido University) for technical advice on RIP assay.

I also need to thank all the members from Division of Signaling in Cancer and Immunology for their kind help and support, you create such a good research environment and friendly atmosphere in the laboratory. There was a lot of scientific discussion in the laboratory, which improve my research and knowledge.

I gratefully acknowledge the financial support provided by China Scholarship Council to undertake my doctoral study. I also heartily thank Hokkaido University for

waiving all of my tuition fees and giving me this opportunity to study in Japan.

I express my greatest gratitude to my parents and grandparents for their unconditional love, support and prayers. There are no words sufficient to express my gratitude. I thank my lovely son, for his sweet smile and understanding. Finally, a special thanks to my wife for her patience, kindness, supportive love, and so many other things I conveniently fail to remember. Thank you very much for taking care of our son, and sharing the housework during the most difficult time of thesis writing.